Journal of Long-Term Effects of Medical Implants

Subrata Saha, PhD, Editor-in-Chief

Research Professor & Director of Musculoskeletal Research
Department of Orthopaedic Surgery & Rehabilitation Medicine

Research Professor
Department of Neurosurgery

Research Professor
Department of Physiology & Pharmacology
SUNY Downstate Medical Center

450 Clarkson Avenue - Box 30
Brooklyn, NY 11203 USA
subrata.saha@downstate.edu

begell house, inc.
publishers
www.begellhouse.com

Journal of Long-Term Effects of Medical Implants (ISSN 1050-6934) is published quarterly and owned by Begell House, Inc., 50 Cross Highway, Redding CT 06896, telephone (203) 938-1300. US subscription rate for 2010 is $1072.00. Add $10.00 per issue for foreign airmail shipping and handling fees to all orders shipped outside the United States or Canada. Subscriptions are payable in advance. Subscriptions are entered on an annual basis, i.e., January to December. For immediate service and charge card sales, call (203) 938-1300 Monday through Friday 9 am–5 pm EST. Fax orders to (203) 938-1304. Send written orders to Subscriptions Department, Begell House, Inc., 50 Cross Highway, Redding CT 06896.

Journal of Long-Term Effects of Medical Implants is indexed and included in *Index Medicus*®/Medline; is covered in Current Contents/ Clinical Medicine, the Research Alert™ service, and the Biomedical Engineering Citation Index™; is abstracted and indexed in Metal Abstracts, Aluminum Industry Abstracts, Alerts, Engineered Materials Abstracts, Current Awareness in Biological Sciences, The Engineering Index, and COMPENDEX; and indexed in EMBASE/Excerpta Medica.

Printed January 31, 2011

JOURNAL OF LONG-TERM EFFECTS OF MEDICAL IMPLANTS

Thomas J. Gampper, MD
Vice Chairman of Department of Plastic Surgery, Assoc. Professor of Plastic Surgery, Department of Plastic Surgery
University of Virginia Health System
Charlottesville, VA 22908
tjg6f@virginia.edu

William L. Hickerson, MD
Clinical Professor of Surgery, Medical College of Georgia
3623 J. Dewey Gray Circle, Suite 309
Augusta, GA 30909
bhickerson@mac.com

John N. K. Hsiang, MD, PhD
Department of Neurological Surgery,
Virginia Mason Medical Center, Seattle, WA 98101
john.hsiang@vmmc.org

Mary Anne Hudson, RN, BSN
Public Health Nurse
Coos County Public Health Department
1975 McPherson St. #1, North Bend, OR 97459
anne@wingusa.org

William Paul Irvin, Jr., MD
Associate Professor, Division of Gynecologic Oncology
Department of Obstetrics and Gynecology
University of Virginia Health System
Charlottesville, VA 22908
wpi9d@hscmail.mcc.virginia.eduIrving

Marina S. Kurian, MD
Assistant Director of Surgical Education
Lenox Hill Hospital
130 East 77th Street, Black Hall, 13th Floor
New York, NY 10021
mkurian@lenoxhill.net

Scott E. Langenburg, MD, FACS
Assist. Professor Pediatric Surgery, Director of Trauma; Director, Computer-Assisted Robotic-Enhanced Surgery
Children's Hospital of Michigan
3901 Beaubien Blvd., Detroit, MI 48201
slangenb@dmc.org

Michael A.K. Liebschner, PhD
Associate Professor, Department of Neurosurgery
Baylor College of Medicine
Houston, Texas 77030
Liebschner@bcm.edu

Kant Y. Lin, MD
Associate Professor of Plastic Surgery,
Chief of Division of Craniofacial Surgery, Department of Plastic Surgery and Pediatrics
University of Virginia Health System
Charlottesville, VA 22908
Kyl5s@virginia.edu

William B. Long, III, MD
Medical Director Trauma Specialists, LLP
Legacy Emanuel Hospital
2801 N. Gantenbein Avenue MOB 130
Portland, OR 97227
wlong@lhs.org

Joseph K. McLaughlin, PhD
Professor of Medicine, President
Vanderbilt Medical School, Int. Epidemiology Institute
1455 Research Blvd., Suite 550, Rockville, MD 20850-3127
jkm@intepi.org

Vladimir Mironov, MD, PhD
Director, Shared Tissue Engineering Laboratory
Department of Cell Biology and Anatomy
Medical University of South Carolina
173 Ashley Avenue, Suite 601
Charleston SC 29425
mironovv@musc.edu

Joseph A. Molnar, MD, PhD
Assistant Professor, Department of Plastic and Reconstructive Surgery, Wake Forest University
Medical Center Blvd.
Winston-Salem, NC 27157
jmolnar@wfubmc.edu

Kenric M. Murayama, MD
Professor of Surgery Chief, Department of Surgery
Penn Presbyterian Medical Center, Chief of Surgery
University of Pennsylvania
51 N. 39th Street, W266, Philadelphia, PA 19104
kenric.murayama@uphs.upenn.edu

Adrian Park, MD
Campbell and Jeanette Plugge Professor of Surgery
Vice Chair, Department of Surgery
Head Division of General Surgery
University of Maryland Medical Center
22 S. Greene Street, Rm S4B14
Baltimore, MD 21201-1595
apark@smail.umaryland.edu

Dix Phillip Poppas, MD, F.A.A.P., F.A.C.S.
Professor & Chief, Institute for Pediatric Urology
Richard Rodgers Family Professor of Pediatric Urology
New York Presbyterian Hospital
Weill Medical College of Cornell University
525 East 68th Street, Box 94, New York, NY 10065
dpoppas@med.cornell.edu

Vijay J. Rasquinha, MD
Associate Professor of Orthopaedic Surgery
Department of Orthopaedic Surgery and Rehabilitation Medicine, Director, Adult Reconstruction Service
SUNY Downstate Medical Center
450 Clarkson Avenue, Box 30
Brooklyn, New York 11203
vijay.rasquinha@downstate.edu

William J. Rea, MD
Founder, Environmental Health Center, Dallas
8345 Walnut Hill Lane, Suite 220
Dallas TX 75231
wjr@ehcd.com

George T. Rodeheaver, PhD
Edlich Research Professor of Plastic Surgery
University of Virginia Health Center
P.O. Box 801351, Charlottesville, VA 22908-1351
gtr3s@virginia.edu

Eduardo A. Salvati, MD
Clinical Professor Orthopædic Surgery, Director of Hip and Knee Service, Hospital for Special Surgery
Weill Medical College of Cornell University
535 East 70th Street, New York, NY 10021
salvatie@hss.edu

Robert G. Sawyer, MD
Associate Professor of Surgery, Charles O. Strickler Transplant Center, Director, Surgical Nutrition Service
University of Virginia Health System
Charlottesville, VA 22908
rws2k@virginia.edu

Bruce D. Schirmer, MD
Stephen H. Watts Prof. of Surgery, Dept. of Surgery
Director of Minimally Invasive Surgery
University of Virginia Health System
Charlottesville, VA 22908
bs@virginia.edu

William D. Spotnitz, MD
Professor of Surgery; Director of the Surgical Therapeutic Advancement Center
University of Virginia Health System
PO Box 801370
Charlottesville, VA 22908-1370
wspotnitz@bellsouth.net
www.hsc.virginia.edu/stac

John F. Sweeney, MD
Associate Professor of Surgery, Chief, Minimally Invasive Surgery, Michael E. DeBakey Department of Surgery
Baylor College of Medicine
6550 Fannin, Suite 1661
Houston TX 77030
jsweeney@bcm.tmc.edu

Dean M. Toriumi, MD
Professor of Facial Plastic and Reconstructive Surgery, Department of Otolaryngology/Head and Neck Surgery
University of Illinois at Chicago
College of Medicine
1855 W. Taylor Street
Suite 2.42 (M/C 648)
Chicago, IL 60612
dtoriumi@uic.edu

Alfred J. Tria, Jr., MD
Clinical Professor of Orthopædic Surgery,
Robert Wood Johnson Medical School,
Orthopedic Center of New Jersey
1527 State Highway 27, Suite 1300
Somerset, NJ 08873
atriajrmd@aol.com

Gil Triplett, DDS, PhD
Regents Professor and Chairman
Department of Oral and Maxillofacial Surgery
Texas A&M University, Baylor College of Dentistry
3302 Gaston Avenue
Dallas, TX 75246
gtriplett@tambcd.edu

Jafar Vossoughi, PhD
Editor-in-Chief,
International Journal of Medical Implants and Devices
3616 Martins Diary Circle
Olney, MD 29832
vossoughi@verizon.net

W. R. Walsh, Ph.D.
Director, Surgical and Orthopedic Research Laboratories, Prince of Wales Clinical School
Prince of Wales Hospital
Randwick NSW 2031 Australia

Kathryne L. Winters
Website Manager and Information Specialist
Trauma Specialists, LLP, Legacy Emanuel Hospital, Portland Oregon
1917 NE 97th St.
Vancouver, WA 98665
kathrynelwinters@gmail.com

Feng Zhang, MD, PhD
Associate Professor, Division of Plastic Surgery;
Director, Microsurgery Laboratory
University of Mississippi Medical Center
2500 North State Street
Jackson, MS 39216-4505
fzhang@surgery.umsmed.edu

Robert D. Zura, MD
Assistant Professor of Orthopedic Surgery
Duke University Medical Center
Division of Orthopedic Surgery
Box 3205, Durham, NC 27710
bobzura@hotmail.com

SCOPE, OBJECTIVES, AND EDITORIAL POLICY OF JOURNAL

MEDICAL IMPLANTS are being used in every organ of the human body. Ideally, medical implants must have biomechanical properties comparable to those of autogenous tissues without any adverse effects. In each anatomic site, studies of the long-term effects of medical implants must be undertaken to determine accurately the safety and performance of the implants. Today, implant surgery has become an interdisciplinary undertaking involving a number of skilled and gifted specialists. For example, successful cochlear implants will involve audiologists, audiological physicians, speech and language therapists, otolaryngologists, nurses, neuro-otologists, teachers of the deaf, hearing therapists, cochlear implant manufacturers, and others involved with hearing-impaired and deaf individuals. A similar list of specialists can be identified for each implant site, from dentistry to cardiovascular surgery. Consequently, scholarly work from all disciplines involved in implants is welcome.

Realizing the interdisciplinary components of successful implant programs, we have considerably expanded the number of members of the Editorial Board. These gifted scholars are recognized as leaders in the field of implants. Each member has been listed with careful identification of academic title, institution, and mailing addresses. Because the ultimate success of implants depends on daily interactive communication, the email addresses of each Editorial Board member has been listed.

The ability to predict the long-term in vivo performance of medical implants is of vital interest. The extrapolation of in vitro data to the in vivo environment remains largely unproven. Among the major challenges are our limited ability to simulate the complexities of the biological milieu; the current lack of reliable computer modeling of in vivo performance characteristics of implants; and difficulties in evaluating the synergistic contributions of materials, design features, and therapeutic drug regimens.

The aims of the *Journal of Long-Term Effects of Medical Implants* are a better understanding of the mechanisms of failure of preclinically tested medical implants during long-term in vivo service life, both in appropriate animal models and in humans; and establishing an effective linkage between preclinical and clinical studies. Of particular interest are original, critical analyses of data of retrieved implants, interpretive discussions of data based on invasive and noninvasive procedures, and computer modeling of in vivo performance. Also of interest are articles on healthcare technology assessment involving implants and their social impact and economic consequences. We are adding a new dimension to our Journal, which includes health education as well as accident and disease prevention and cure. The Journal will also publish guest editorials, letters to the Editor, and book reviews. All articles are subject to peer review by at least two referees.

Subrata Saha, PhD
Editor-in-Chief

JOURNAL OF LONG-TERM EFFECTS OF MEDICAL IMPLANTS
INSTRUCTIONS TO AUTHORS

GENERAL INSTRUCTIONS: Manuscripts should be submitted through the Begell House Online Submission Program by registering on the site (http://submission.begellhouse.com/). More detailed instructions can be found on the submission site.

SUBMISSION INSTRUCTIONS: If you are a first time user of our Submission Program, please click on the ***New User*** icon located on the left sidebar of the Submission home page. Please complete the registration form and submit by clicking the ***Register*** link. Your completed form will be reviewed and your username and password will be emailed to you within 24 hours.

If you have previously registered please click on the ***Login*** icon located on the left sidebar and continue to submit your article.

PREPARATION OF MANUSCRIPTS:

(1) Write in clear, concise English. Authors are responsible for all aspects of manuscript preparation. Extensive changes to the manuscript will not be undertaken by the Editor or during the production process.

(a) **Non-English Speaking Authors.** Authors in non-English speaking countries are requested to find persons who are fully conversant and competent in English writing and also familiar with medical terminology to edit manuscripts before submitting them to the editor. Referrals for authorized U.S. translation services are available at www.submission.begellhouse.com.

(2) Original submitted manuscript should be provided in pdf format. After acceptance of your manuscript for publication in one of our journals, please provide your manuscript as follows: double spaced with 1" margins all around with the page size set for letter (8½" x 11"). Times Roman is the preferred typeface for manuscripts. Acceptable formats for text files are Microsoft Word or LaTex. All pages should be numbered consecutively. Manuscripts should begin with title information and end with pages containing references, tables, and figure legends. Figures must be submitted in either a separate file containing all figures or individual figure files. All figures must be labeled (example: 1, 2, 3, etc) clearly for proper placement within the text. Figures can be submitted in the following formats: word, tiff, jpeg, or eps.

(3) All manuscripts must include the following:

Author Information: Senior authors full name, affiliation, and e-mail address. Corresponding authors complete mailing address and e-mail address. Additional author's affiliation and email address.

Abstract: All manuscripts must have an abstract not to exceed 200 words.

Key Words: All manuscripts should have a list of key (indexing) terms. Three to ten key words or terms not in the title will assist indexers in cross-indexing your article.

Body: The body of the article presents details of the review. It should be divided into several sections identified by headings and subheadings according to the following scheme:

I. PRINCIPAL HEADING

A. First Subheading

1. Second Subheading

a. Third Subheading

Italic or boldface type should be clearly indicated and Greek or unusual characters should be written plainly or explained by annotations. Simple fractional expressions should be written with a slant line rather than stacked, so that only a single line of type if required in the text.

TABLES: Tables should be used only when they can present information more effectively than can be done in running text. Avoid any arrangement that unduly increases the depth of a table, column heads should be as brief as possible, use abbreviations liberally. Lines of data should not be numbered nor run numbers given unless those numbers are needed for reference in the text.

ILLUSTRATIONS: Figures should be numbered in series, and all legends should be typed double spaced and placed at the end of the text file. All figures should be called out in the text in numerical order. Figures should be supplied in a separate file or in individual files. Symbols used in figures (open or closed circles, triangles, squares, etc) and lettering of labels should be sized for optimum reproduction but should not exceed the size of the journal pages (size requirements can be obtained by emailing erica@begellhouse.com). Color reproduction of figures is possible at the author's expense, rates will be provided upon request.

COPYRIGHTED MATERIAL: Authors who make use of artwork already published, or verbatim quotations of text amounting to more than a few words, are required by copyright law to ask the owner of the copyright (usually the publisher) for permission. Assign proper credit in the caption (the publisher granting permission may specify wording). Send copies of permissions clearly marked to indicate the relevant figure or table. If authors use material from their own published work, permission must be obtained from the publisher. **ALL PERMISSIONS MUST BE INCLUDED WITH THE FINAL DRAFT OF YOUR ARTICLE.**

FORMULAS AND EQUATIONS: Displayed equations should be incorporated in the text and should be numbered using Arabic numerals (in parentheses) in sequence. In the text, they should be referred to as, e.g., Eq. (12). At the beginning of a sentence, the word Equation(s) should be written out. Equations should be part of the word-processing document, using software component such as Equation Editor or MathType. All symbols should be identified in the text at first mention. Symbols that denote mathematical variables should be in italics. A clear distinction should be made between the characters "I," "l" (el) and "1" (one); "o," "O," and "0" (zero); "w" and "ω" (omega); "v" and "ν" (nu), etc. Please observe correct spacing

— e.g., 25°C (not 25° C or 25 °C). For numerical values of measurable quantities, show no more digits than are significant. The use of powers of ten is recommended, e.g., 1.23 x 10^5 instead of 123,000. Use decimal points, not commas.

EMPIRICAL AND STRUCTURAL FORMULAS AND MATHEMATICAL AND CHEMICAL EQUATIONS should be arranged to fill the width of a single or double column. Subscripts and superscripts (i.e., exponents), such as +, -, =, <, or >, (ex: $10^2 + 11^4$, 125 – 47) should be spaced but the components of mathematical products should not be spaced.

ORGANIC STRUCTURAL FORMULAS should be submitted as copy suitable for direct photographic reproduction. Do not use structures when a simple formula will suffice. Do not use multiple lines unnecessarily. In order to avoid errors, carefully arrange and execute all formula matter, paying special attention to correctness of symbols; location of subscripts, superscripts and electric charges; and the placing and close join-up of single and multiple bond lines. Originals should be grouped at the end of the manuscript with other figures.

UNITS AND QUANTITIES Units should be in accordance with the Systeme International d'Unites (SI http://www.physics.nist.gov/cuu/Units/units.html). Symbols for physical quantities should be those recommended by IUPAC, IUPAP, or ASTM.

REFERENCES References follow ***Vancouver Style***, which is available in all reference management software. Detailed instructions to set up ***Vancouver Style References*** can be found on the ***NLM*** site http://www.nlm.nih.gov/bsd/uniform_requirements.html. Cite references in the text in numerical order using superscript numerals, placed closed-up (no space) after punctuation. References to classified documents and reports or unpublished material not generally available to the scientific public should not be used. Journal abbreviations should be consistent with ***Index Medicus*** *(please check for appropriate* journal abbreviations at http://www2.bg.am.poznan.pl/czasopisma/medicus.php?lang=eng). Format references exactly as follows:

Journal Articles

NOTE: Previously the first six authors were followed by et al., however, NLM now lists all authors.

Agarwal S, Rao A. Modulation of chromatin structure regulates cytokine gene expression during T-cell differentiation. Immunity. 1998 Dec 25;9(6):765-75.

Books and Other Monographs

Editor(s), compiler(s) as author

Gilstrap LC 3rd, Cunningham FG, VanDorsten JP, editors. Operative obstetrics. 2nd ed. New York: McGraw-Hill; 2002.

Author(s) and editor(s)

Breedlove GK, Schorfheide AM. Adolescent pregnancy. 2nd ed. Wieczorek RR, editor. White Plains (NY): March of Dimes Education Services; 2001.

Chapter in a book

Meltzer PS, Kallioniemi A, Trent JM. Chromosome alterations in human solid tumors. In: Vogelstein B, Kinzler KW, editors. The genetic basis of human cancer. New York: McGraw-Hill; 2002. p. 93-113.

Conference Proceedings

Harnden P, Joffe JK, Jones WG, editors. Germ cell tumours V. Proceedings of the 5th Germ Cell Tumour Conference; 2001 Sep 13-15; Leeds, UK. New York: Springer; 2002.

Conference paper

Christensen S, Oppacher F. An analysis of Koza's computational effort statistic for genetic programming. In: Foster JA, Lutton E, Miller J, Ryan C, Tettamanzi AG, editors. Genetic programming. EuroGP 2002: Proceedings of the 5th European Conference on Genetic Programming; 2002 Apr 3-5; Kinsdale, Ireland. Berlin: Springer; 2002. p. 182-91.

Dissertation

Borkowski MM. Infant sleep and feeding: a telephone survey of Hispanic Americans [dissertation]. Mount Pleasant (MI): Central Michigan University; 2002.

Transmittal Form must be filled out for each article submitted. The transmittal form includes the following information: article title, short title for running heads, keywords (no more then 10 keywords), and all author names (include affiliation and e-mail addresses). Corresponding authors must include their complete mailing address, e-mail address, telephone number, and fax number. This form is provided on the Begell House Submission site, only when you are submitting your final files.

Copyright Release are available on the submission website only when your final manuscript is submitted. Original copyright forms must be completely filled out, signed, and submitted with your final manuscript. To avoid delays in processing your article, please upload a copy of your signed copyright form with your final manuscript.

Statement: Each manuscript must be accompanied by a statement that the article has not been published elsewhere and that it has not been simultaneously submitted for publication elsewhere. The original drawings and photos should be retained by the author until the conclusion of the review process. The original typed manuscript should also be retained by the author.

OFFPRINTS An order form for offprints, copies of issues, subscriptions, and orders for color figures will be sent to the corresponding author with the author proofs. Authors who wish to purchase any of the above should fill out the order form and return it with their author corrections. Corresponding authors are asked to provide their co-authors with the above information. Corresponding authors will receive a complimentary copy of the issue in which the article appears. If corresponding authors do not receive their complimentary copy of the journal, within 3 months after receiving their page proofs, they should notify Begell House immediately. Begell House will not honor claims for missing complimentary copies after the year in which the article is published.

JOURNAL OF LONG-TERM EFFECTS OF MEDICAL IMPLANTS

Volume 20 / Issue 1 2010

CONTENTS

Journal of Long-Term Effects of Medical Implants, 20(1): 1–12 (2010)

Side Effects of Chemotherapy in Musculoskeletal Oncology

Andreas F. Mavrogenis,[1] Panayiotis J. Papagelopoulos,[2] Matteo Romantini,[1] Andrea Angelini,[1] & Pietro Ruggieri[1]*

[1]Istituto Ortopedico Rizzoli, Department of Orthopaedics, University of Bologna, Bologna, Italy; [2]First Department of Orthopaedics, Athens University Medical School, Athens, Greece

*Address all correspondence to Pietro Ruggieri, MD, PhD, Department of Orthopedics, University of Bologna, Istituto Ortopedico Rizzoli, Via Pupilli, 1, 40136, Bologna (BO) Italy; Tel.: +390516366460; Fax: 0039/051/63.66.540; pietro.ruggieri@ior.it..

ABSTRACT: With recent advances in medical and orthopedic oncology, radiation therapy and single- or multiple-agent perioperative chemotherapy are currently applied as an essential part of the multidisciplinary treatment to improve disease-free and overall survival of patients with primary and metastatic bone and soft tissue tumors. However, these treatments have led to unwanted complications. A better understanding of the effects of various antineoplastic agents on bone, soft tissue, and organs may provide the basis for the more efficacious use of antiproliferative drugs when fracture healing or allograft incorporation is required. This knowledge may also provide a rationale for concurrent treatment with drugs that protect against or compensate for adverse effects in osseous repair resulting from chemotherapy.

KEY WORDS: chemotherapy; complications

I. INTRODUCTION

With recent advances in medical and orthopedic oncology, radiation therapy and single- or multiple-agent perioperative chemotherapy are currently applied as an essential part of the multidisciplinary treatment to improve disease-free and overall survival of patients with primary and metastatic bone and soft tissue tumors,[1-3] but have led to unwanted complications.[4-7] Each organ has a unique radiation and drug dose-volume response pattern, and different complications may occur, each of which depend on the dose distribution within a given treatment plan.[8] In addition, the combination of chemotherapy with radiation therapy makes normal tissues sensitized to radiation, and this may cause more complications.[4]

In this article, we present the side effects of chemotherapy in wound, bone, and various organs in order to provide the physician with the most current information to assist in choosing the best method of combined or primary treatment, and to predict which patients are at risk for complications for improved preoperative planning, prevention of morbidity, and better surveillance.

II. CHEMOTHERAPY-INDUCED WOUND-HEALING SIDE EFFECTS

The effect of certain chemotherapeutic agents on bone and wound healing is difficult to assess in cancer patients because of the short-term survival and the combination with adjuvant treatment.[9-14] However, experimental studies in animals have shown that perioperative chemotherapy significantly impairs wound healing.[15-17] Most of these studies indicate that the dosage level, time of drug administration relative to the surgical operation, and time at which wound-strength measurements are made are important param-

1050-6934/10 $35.00

eters in the determination of the effects of antineoplastic agents on wound healing. An experimental study in mice[15] evaluating the effects of different antineoplastic agents on wound healing noted decreased wound strength at 3 d postoperatively but not on d 7 or 21 after the administration of vincristine and methotrexate. Actinomycin D interfered with early phases of wound healing, but showed less effect on later phases. Bleomycin had no effect on wound strength at d 3 or 21, but prevented an increase in wound strength from d 3 to 7; administration of 1,3-bis (2-choroethyl)-1-nitrosurea decreased wound strength at all time points after surgery, whereas 5-fluorouracil was not found to have any significant effect at any time.[15] The presence of a large tumor mass had no direct effect on wound strength, nor did it modify the effect of cyclophosphamide on wound strength.[15]

In a similar study,[16] the administration of therapeutic levels of cyclophosphamide as a single dose or as a daily treatment for 5 d during the perioperative period resulted in a significant decrease in the strength of surgical wounds in mice 21 d postoperatively. The administration of a single dose of 200 mg/kg cyclophosphamide either at the time of surgery, up to 4 d prior to surgery, or postoperatively impaired 21-d wound strength; the most extensive depression was observed when the drug was given 1 or 2 d after surgery. Earlier stages of wound healing (d 3 or 7) were not found to be sensitive to cyclophosphamide.[16] Doxorubicin in the therapeutic dosage range for mice did not significantly impair wound healing. Combination treatment with cyclophosphamide and doxorubicin at the time of surgery impaired 21-d wound strength to a greater degree than that observed with either agent alone, but did not significantly affect wound strength 3 or 7 d after surgery.[16] Rats treated with doxorubicin prior to or on the day of surgery demonstrated decreased wound-breaking strength in incisional wounds at all intervals after operation.[18] Decreased amounts of collagen and DNA and less cellularity were noted in wound chambers from rats treated in the same manner. In both the incisional wound and wound chamber models, rats treated with doxorubicin 7 d after the surgery showed a less dramatic healing impairment. No difference in collagen types was noted between chambers from the doxorubicin-treated and untreated rats.[18] Perioperative administration of doxorubicin impaired wound healing in all tested regimens depending on the interval between drug administration and surgery.[14,19,20] Doxorubicin administered up to 21 d after the surgery caused an impairment in wound healing that was manifested up to 2 weeks after doxorubicin administration; doxorubicin administered 28 d after surgery induced no demonstrable impairment in wound-breaking strength. In addition, doxorubicin did not decrease the breaking strength of a wound after a certain degree of strength had been obtained.[14,19,20]

Studies in animals using antineoplastic agents such as doxorubicin, nitrogen mustard, cyclophosphamide, and methotrexate have shown a dose-dependent impairment of wound healing.[14] Extrapolation of these doses to regimens employed in humans is very difficult. Information regarding complications of chemotherapeutic agents in wound healing in humans is only available from adjuvant clinical studies. Increased frequency of complications from nitrogen mustard, thiotepa, or cyclophosphamide have not been reported, even when these agents were given in the immediate perioperative period. Increased wound complications have been reported with 5-fluorouracil when a 60 mg/kg dose was administered 7 d after surgery, but not when this was begun 14 d after surgery.[14]

The results of the above-mentioned studies stress the need for continued attention to wound complications reported in adjuvant clinical studies, and suggest that delayed administration of chemotherapy until at least 7 d after surgery may result in minimal impairment of wound healing.

III. CHEMOTHERAPY-INDUCED GROWTH SIDE EFFECTS

Chemotherapy-induced side effects in children, primarily systemic, may result in serious problems. Pediatric patients frequently have very different side-effect profiles compared with adults when exposed to similar doses. Systemic growth and development

retardation occurs during treatment, yet the growth rate accelerates and reaches normal limits after the cessation of chemotherapy, a phenomenon called "catchup growth."[5] The epiphysis is the most sensitive portion of the skeleton to radiation and chemotherapy.[21,22] Slippage of the capital femoral and the proximal humeral epiphysis has been identified in patients undergoing combined chemotherapy and radiation therapy treatment.[21,23,24] Histologic changes including swelling, fragmentation, and degeneration of chondrocytes may be seen in skeletally immature patients who have received radiation doses as low as 3 Gy.[25] Delayed changes include cartilage degeneration and bone atrophy secondary to vascular injury and direct cellular damage to osteocytes, short stature in relation to radiated area, deformity, and pelvis asymmetry.[26] Growth disturbances are greater with higher radiation doses, in those irradiated at a young age, and in bones with the greatest growth potential.[26]

IV. CHEMOTHERAPY-INDUCED SIDE EFFECTS ON BONE METABOLISM

Little is known regarding the direct systemic effects of antineoplastic drugs on bone biology.[27-31] In the treatment of childhood leukemia, methotrexate has been reported to cause osteoporosis, bone pain, and spontaneous fractures that are refractory to union, despite adequate orthopedic management.[29,31] Few experimental studies have analyzed the effect of chemotherapeutic agents on bone metabolism.[32,33] Short-term administration of methotrexate and doxorubicin was shown to cause a 26.9% and 11.5% reduction in net trabecular bone volume, respectively, and both drugs significantly and profoundly diminished bone-formation rates by nearly 60%.[32] The toxic effect on osteoblasts was reflected in the reduced volume and thickness of osteoid without affecting the total numbers of osteoblasts and the percentage of trabecular surface covered by bone-forming cells.[32]

The difference in mineral apposition rate of cancellous bone showed that although the effect of temporary chemotherapy on bone may have minor effects on normal turnover and is a reversible effect, it causes disturbance in bone-mass accumulation,[32,33] and later this may increase the risk for pathological fractures and osteoporosis. The effect of combined doxorubicin, cisplatin, and ifosfamide chemotherapy in normal bone turnover has been evaluated in a safe and clinically relevant canine model of multidrug perioperative chemotherapy that simulates current cancer treatment.[33] The bone specimens were analyzed using microradiography, bone histomorphometry, and torsional testing. Results were compared with canines that underwent a similar surgical protocol without chemotherapy, and showed no differences in mechanical properties after 22 weeks of chemotherapy. The porosity, osteonal activity, and mineral apposition rate of the cortical bone were unaffected. A difference in the porosity of the perimeter in cancellous bone was not observed; however, the mineral apposition rate was significantly reduced.[33]

V. CHEMOTHERAPY-INDUCED FRACTURES

High-dose (≥50 Gy), postoperative radiation therapy and periosteal stripping during resection of soft-tissue sarcomas, in addition to adjuvant chemotherapy, female gender, tumor location in the anterior thigh compartment, positive tumor margins, age older than 55 years, and radiation to the entire circumference of bone, have been reported to be significant risk factors for chemoradiation-induced fractures.[4,34-37] Concurrent chemotherapy increases the toxicity of radiation.[38] All fractures occur within the radiation field; most lower extremity fractures that have been reported following radiation therapy occur in the proximal femur.[4,34-37] Any variable that is associated with lower bone mass, such as female sex and osteoporosis, likely places the patient at higher risk for a fracture.[4,37,39-42] Pretreatment measurement of bone density is required for these patients to evaluate the risk of fracture.[42,43] Although the overall fracture rate may not be so high that prophylactic fixation is warranted, and although prophylactic nailing adds additional time to often lengthy procedures and potential morbidity,[4,44] patients with several risk factors should be considered for prophylactic fixation.[36,39-41,45] In ad-

dition, patients who sustain a fracture in a high-dose radiation field should be closely evaluated for subsequent fractures.[4]

VI. CHEMOTHERAPY-INDUCED SIDE EFFECTS ON FRACTURE HEALING

Pathological fractures subsequent to bone metastases are a frequent complication of malignant disease and are particularly disabling when weight-bearing bones are involved. In addition to the effects of chemotherapy on intact bone, other clinically relevant concerns include fracture healing, bone ingrowth in porous-coated replacement prostheses, and bone-allograft incorporation during periods of chemotherapy.[46-49]

The mechanical properties and the anatomical and histological changes of the fracture-healing process, including the effect of cytostatic drugs on mucopolysaccharides and collagen metabolism, have been extensively studied.[20,46,50-55] Biochemical and histochemical methods have been introduced but mainly concern the inorganic constituent of bone.[50] The importance of organic constituency in bone healing was first indicated by Nilsonne,[51] who stated that "fracture non-union is not the result of primary disturbance in the mineral process, but rather a change in the organic matrix which diminishes or prevents its calcifiability." A negative influence of cytostatic drugs on the process of formation and evolution of bone callus, abnormal patterns of ossification, and inhibition of the postnatal growth of long bones in white mice have been reported.[54] Others have reported the delayed effect of cyclophosphamide on bone-fracture healing after osteotomy, as shown by a reduction in the hydroxyproline content, diminution of calcium and phosphate deposition on the fracture callus that inhibit collagen formation, and delayed mineralization.[55] Moreover, the inhibition of collagen was decreased when cyclophosphamide treatment was discontinued prior to osteotomy.[55] In a study using bone grafts, methotrexate showed increased osteoclastic activity and inhibition of interior osteoclastic activity without affecting the periphery of the bone tissue.[46]

In oncological reconstructive surgery, bone healing occurs coincidentally with the administration of chemotherapy. A series of osteoinductive proteins (bone morphogenetic proteins or BMPs) has been described and shown to enhance bone formation in animal models. In one study,[56] the effect of chemotherapy on bone healing enhanced by rhBMP-2 was evaluated in a critical-sized bone-defect rabbit model. Histological and radiological analysis showed that chemotherapy affected both the quantity and the quality of the bone enhanced by rhBMP-2. These results suggest that the effect of chemotherapy on bone formation could be related to inhibition of a specific pathway stimulated by rhBMP-2.[56]

VII. CHEMOTHERAPY-INDUCED SIDE EFFECTS ON BONE INGROWTH

Chemotherapeutic agents have negative effects on bone-graft incorporation and bone ingrowth into porous-coated prostheses.[49,57] Young et al.[49] studied the effect of preoperative and postoperative cisplatin chemotherapy on the biologic fixation of porous-coated prostheses using autologous corticocancellous bone graft. Although bone ingrowth into the prosthesis was not affected, electron microscopic, histomorphometric, and radiologic analyses showed a clear difference in the formation of new bone around the prosthesis. Preoperative chemotherapy did not alter the formation of new bone, but specimens from animals treated with cisplatin postoperatively showed significantly less new bone formation.[49] Another study[57] showed that extracortical bone grafting is an effective modality for implant fixation even under intensive chemotherapy. In this study, the authors performed a unilateral resection of a 6-cm segment of the femoral diaphysis and reconstruction with a porous-coated segmental prosthesis in eight mixed-breed dogs under perioperative chemotherapy with doxorubicin, cisplatin, and ifosfamide. Eight strips of autogenous cortical bone were evenly placed around the junctions between the femur and the prosthetic surface. Autogenous cancellous bone was placed under and between the strips of cortical bone. Two cycles of

the chemotherapy were given preoperatively and three cycles postoperatively. The animals were followed for 12 weeks, with sequential assessments of weight-bearing and radiographic evaluation. Combination chemotherapy with doxorubicin, cisplatin, and ifosfamide showed a significant negative effect on new bone formation, as seen by a reduction of callus size and a lower ultimate strength of extracortical fixation.[57] However, the onlay corticocancellous grafting method provided better biologic fixation of the prosthesis compared with fixation without any bone grafting under non-chemotherapy conditions.[33]

VIII. CHEMOTHERAPY-INDUCED SIDE EFFECTS ON ALLOGRAFT INCORPORATION

Although there is limited clinical evidence suggesting a high rate of allograft-associated complications, the use of massive allografts in reconstructive procedures following limb-salvage surgery should be avoided in patients receiving chemotherapy.[32,58-60] These complications include failure of union, delayed or inadequate incorporation leading to graft fragmentation and collapse, and increased incidence of deep wound infection. Cortical bone allografts are known to incorporate more slowly and incompletely than autografts. Segmental allografts are nonviable, nonvascularized structures that possess some osteoinductive potential and provide for osteoconduction by serving as a scaffold for bone ingrowth. Freezing and immunogenicity of the allograft have been noted to impair the rate and the extent of revascularization, as well as new bone formation. These effects are apparent by 4 weeks after implantation of the allograft.[61,62] Zart et al.[63] studied the effects of cisplatin on the incorporation of fresh cortical bone homografts and frozen cortical bone allografts in animals, and found that revascularization and host-graft union was poor in the cisplatin-treated groups by 2 months, but by 4 months vessel ingrowth in fresh homografts approached control values. Frozen allografts remained poorly revascularized after 4 months. The authors concluded that cortical bone allografts incorporate more slowly and incompletely than homografts, and that this handicap was exacerbated by the administration of cisplatin.[63]

IX. CHEMOTHERAPY-INDUCED SARCOMAS

Malignancies secondary to chemotherapy occur within the first 5 years after treatment, usually in the form of acute non-lymphoid leukemia, especially due to the use of increasing doses of topoisomerase-II inhibitors, anthracyclines, or alkylating agents.[5] The probability of leukemia after chemotherapy in children has been shown to be 1% to 2%.[6,64]

X. CHEMOTHERAPY-INDUCED CENTRAL NERVOUS SYSTEM SIDE EFFECTS

Chemotherapy-induced central nervous system (CNS) side effects can be acute or delayed.[7,65] These side effects have been attributed to toxic effects in the parenchyma and CNS progenitor cells at therapeutic doses and to an increase of blood-brain barrier permeability of chemotherapeutic agents.[66,67] Headache and seizures occur with almost every chemotherapeutic agent. Causes of seizures include direct toxic effects, indirect changes linked to hyperhydration, metabolic changes such as renal toxicity after cisplatin administration, or inappropriate antidiuretic hormone secretion with encephalopathy after vincristine or ifosfamide administration.[68,69] Cerebellar syndrome is likely to occur after high-dose cytarabine and fluorouracil.[65] Stroke is rare but can take several forms. Venous sinus thrombosis can complicate the use of asparaginase via depletion of hemostatic factors, but this complication can be prevented and treated with antithrombin concentrates.[70] Mitomycin can trigger thrombotic microangiopathy,[71] and anti-vascular endothelial growth factor drugs can cause cerebral hemorrhage and arterial infarction.[72] Fatal leukoencephalopathy has been reported in four adult patients who received a combination of carmustine, cyclophosphamide, cisplatin, melphalan, cytarabine, and etoposide for non-CNS tumors.[73] Reversible posterior leukoencephalopathy syndrome is associated with an increasing number of anticancer drugs.[74-77] The underlying mechanism is unknown, but could in-

volve vasogenic edema.[74] Intrathecal chemotherapy with methotrexate, cytarabine, and its liposomal formulation, depocyte, can produce aseptic meningitis and, very rarely, transverse myelopathy that can usually be prevented with concomitant corticosteroids.[78] Chemotherapy-induced histopathological lesions consisting of demyelination, axonal loss, gliosis, focal areas of necrosis, and macrophage infiltration have been documented in humans after accidental administration of methotrexate through a misplaced Ommaya reservoir[79] and in animals given cisplatin.[80]

Cognitive dysfunction has been reported after chemotherapy alone for lymphomas, usually when high-dose methotrexate is combined with other drugs. Additionally, cognitive dysfunction is sometimes associated with intrathecal or intraventricular chemotherapy or after intensive chemotherapy with thiotepa, busulfan, and cyclophosphamide. A group of changes initially called "chemobrain" or "chemo fog syndrome," referring to persistent post-chemotherapy cognitive changes that are independent of depression, anxiety, or fatigue, have been reported in cancer survivors. Global impairment in attention, memory, and executive functions has been reported in 15% to 50% of adult survivors of solid tumor after chemotherapy.[81]

XI. CHEMOTHERAPY-INDUCED SPINAL CORD SIDE EFFECTS

Chemotherapy increases the toxicity of radiation therapy in the spinal cord.[82] Radiation-induced spinal cord injury can be acute (during radiation), early-delayed (up to 6 months), or late-delayed (more than 6 months to several years post-radiation).[83] Early-delayed tumor pseudoprogression occurs within 6 weeks to 3 months after therapy due to early-onset radionecrosis or chemonecrosis, and mimics tumor recurrence both clinically and on standard magnetic resonance imaging (MRI). The syndrome has been reported mainly after combined radiochemotherapy.[7,84,85] Tumor pseudoprogression improves over a few weeks to months with supportive care and steroids. However, in the absence of pathognomonic MRI features, pseudoprogression might need surgical treatment.[7] Late-delayed myelopathy has occurred after safe radiation doses in combination with high-dose or intensive chemotherapy.[86,87]

XII. CHEMOTHERAPY-INDUCED PERIPHERAL NERVE SIDE EFFECTS

Brachial plexopathy and peripheral nerve injury leading to progressive muscle denervation and atrophy are more common after radiation therapy.[88,89] The risk of delayed brachial plexopathy is increased when large radiation fields are used, when patients receive two separate courses of subthreshold radiation therapy, or with concomitant chemotherapy.[90] The exact pathophysiology of plexopathy is unclear. Extensive fibrosis within and surrounding nerve trunks of the plexus, with demyelination and loss of axons and microvascular injury, are consistently present at surgery or autopsy.[82,91] Unlike brachial plexus metastasis, patients do not experience Horner's syndrome and/or early, severe pain.[91] MRI and electromyography are usually diagnostic.[91,92] Treatment options are not satisfactory: surgical neurolysis, dorsal root entry zone lesions, chemical sympathectomy, and warfarin administration have all been reported, with variable success.[93-95]

XIII. CHEMOTHERAPY-INDUCED HEPATIC SIDE EFFECTS

Acute or subacute hepatobiliary toxicity is recognized with varying frequency following radiation, multiple chemotherapies, or hematopoietic stem-cell transplantation in cancer survivors.[96-98] Additionally, hepatobiliary toxicity and cirrhosis are associated with transfusion-acquired chronic viral hepatitis, transfusion-associated iron overload, cholestatic disease from total parenteral nutrition, or venoocclusive hepatic disease.[98,99] The risk of hepatic injury increases with radiation dose, hepatic volume, younger age at treatment, prior partial hepatectomy, and concomitant chemotherapy. The latency period for manifestation of liver dysfunction after chemotherapy is unknown. The chemotherapy agents with established acute and emerging

chronic hepatotoxic potential include thiopurines, antimetabolite agents such as 6-mercaptopurine, 6-thioguanine, methotrexate, and, rarely, dactinomycin in children treated for Wilms' tumor and rhabdomyosarcoma.[96,98,100-104] Although the majority of children with veno-occlusive hepatic disease from thiopurine chemotherapy recover, a subset of patients have progressive fibrosis leading to portal hypertension.[100,105,106] The risk of fibrosis or cirrhosis after daily oral methotrexate is more than 2-fold greater than intermittent parenteral administration in some childhood leukemia treatment protocols.[107] Acute and subacute methotrexate-induced hepatic injury is characterized by transient elevations of serum transaminases or alkaline phosphatase; interestingly, biochemical changes are not consistently correlated with severity of hepatic injury.[108] Methotrexate-induced fibrosis usually regresses or stabilizes after discontinuation, and rarely produces end-stage liver disease in the absence of other antimetabolite therapy or comorbidities.[98,108] Late liver dysfunction manifests as persistent hepatomegaly, splenomegaly, and thrombocytopenia.[105,108]

XIV. OTHER CHEMOTHERAPY-INDUCED SIDE EFFECTS

Toxic mucositis induced by radiation therapy and chemotherapy and vascular erosion of mucosal vessels or major vessels in the field of radiation are rare but life-threatening complications after primary or adjuvant radiation therapy and chemotherapy. Vascular erosion should be treated with emergent surgical ligature and/or embolization.[109]

XV. CONCLUSIONS

A better understanding of the effects of various chemotherapeutic agents on soft tissue and bone healing is required. Delays in the administration of preoperative and postoperative chemotherapy for up to 3 weeks are recommended to allow patients time to recover from the side effects of chemotherapy agents. Further studies may provide the basis for more efficacious use regarding timing and dosage of anticancer drugs, especially when bone healing or allograft incorporation is required. This knowledge may provide physicians with a rationale for concurrent treatment using drugs that protect against or compensate for the chemotherapy-induced side effects in bone, soft tissue, and organs. Predicting which patients are at risk for complications will allow for improved preoperative planning, prevention of morbidity, and better surveillance.

REFERENCES

1. Chan KW, Knowling M, Beauchamp CP. Perioperative chemotherapy for primary sarcoma of bone. Can J Surg. 1989;32:43-6.
2. Jaffe N, Frei E III, Watts H, Traggis D. High-dose methotrexate in osteogenic sarcoma: A 5-year experience. Cancer Treat Rep. 1978;62:259-64.
3. Sutow WW, Gehan EA, Dyment PG, Vietti T, Miale T. Multidrug adjuvant chemotherapy for osteosarcoma: interim report of the southwest oncology group studies. Cancer Treat Rep. 1978;62:265-9.
4. Cannon CP, Ballo MT, Zagars GK, Mirza AN, Lin PP, Lewis VO, Yasko AW, Benjamin RS, Pisters PWT. Complications of combined modality treatment of primary lower extremity soft-tissue sarcomas. Cancer. 2006;107:2455-61.
5. Ozger H, Bulbul M, Eralp L. Complications of limb salvage surgery in childhood tumors and recommended solutions. Strat Traum Limb Recon. 2010;5:11-5.
6. Hundsdoerfer P, Albrecht M, Rühl U, Fengler R, Kulozik AE, Henze G. Long-term outcome after polychemotherapy and intensive local radiation therapy of high-grade osteosarcoma. Eur J Cancer. 2009;45: 2447-51.
7. Soussain C, Ricard D, Fike JR, Mazeron J-J, Psimaras D, Delattre J-Y. CNS complications of radiotherapy and chemotherapy. Lancet. 2009;374:1639-51.
8. Hopewell JW, Trott KR. Volume effects in radiobiology as applied to radiotherapy. Radiother Oncol. 2000;56:283-8.
9. Aisner J, Morris D, Elias EG, Wiernik PH. Mastectomy as an adjuvant to chemotherapy

for locally advanced or metastatic breast cancer. Arch Surg. 1982;117:882-7.
10. Bertermann O, Marcove RC, Rosen G. Effect of intensive adjuvant chemotherapy on wound healing in 69 patients with osteogenic sarcomas of the lower extremities. Recent Results Cancer Res. 1985;98:135-41.
11. Enneking WF, Eady JL, Burchard H. Autogenous cortical bone grafts in reconstruction of segmental skeletal defects. J Bone Joint Surg Am. 1980;62:1039-58.
12. Graves G, Gaaf JH. Effects of chemotherapy on the healing of surgical wounds. Clin Bull Memorial Sloane Kettering Cancer Centre. 1980;10:4.
13. McDonald DJ, Capanna R, Gherlinzoni F, Bacci G, Ferruzzi A, Casadei R, Ferraro A, Cazzola A, Campanacci M. Influence of chemotherapy on perioperative complications in limb salvage for bone tumors. Cancer. 1990;65:1509-16.
14. Shamberger RC, Devereux DF, Brennan MF. The effect of chemotherapeutic agents on wound healing. Int Adv Surg Oncol. 1981;4:15-81.
15. Cohen SC, Gabelnick HL, Johnson RK, Goldin A. Effects of antineoplastic agents on wound healing in mice. Surgery. 1975;78: 238-44.
16. Cohen SC, Gabelnick HL, Johnson RK, Goldin A. Effects of cyclophosphamide and adriamycin on the healing of surgical wounds in mice. Cancer. 1975;36:1277-81.
17. Devereux DF, Thibault L, Boretos J, Brennan MF. The quantitative and qualitative impairment of wound healing by adriamycin. Cancer. 1979;43:932-8.
18. Lawrence WT, Norton JA, Harvey AK, Gorschboth CM, Talbot TL, Grotendorst GR. Doxorubicin-induced impairment of wound healing in rats. J Nat Cancer Inst. 1986;76:119-26.
19. Lawrence WT, Talbot TL, Norton JA. Preoperative or postoperative doxorubicin hydrochloride (adriamycin): which is better for wound healing? Surgery. 1986;100:9-13.
20. Khoo DBA. The effect of chemotherapy on soft tissue and bone healing in the rabbit model. Ann Acad Med. 1992;21:217-21.
21. Mitchell MJ, Logan MP. Radiation-induced changes in bone. Radiographics. 1998;18:1125-36.
22. Krasin MJ, Xiong X, Wu S, Merchant TE. The effects of external beam irradiation on the growth of flat bones in children: Modeling a dose-volume effect. Int J Radiat Biol Phys. 2005;62:1458-63.
23. Edeiken BS, Libshitz HI, Cohen MA. Slipped proximal humeral epiphysis: a complication of radiotherapy to the shoulder in children. Skeletal Radiol. 1982;9:123-5.
24. Libshitz HI, Edeiken BS. Radiotherapy changes of the pediatric hip. AJR Am J Roentgenol. 1981;137:585-8.
25. Dalinka MK, Mazzeo VP. Complications of radiation therapy. Cmit Rev Diagn Imaging. 1985;23:235-67.
26. Dawson WB. Growth impairment following radiotherapy in childhood. Clin Radiol. 1968;19:241-56.
27. Alho A, Karaharju EO, Korkala O, Laasonen EM, Holmström T, Müller C. Allogeneic grafts for bone tumor: 21 cases of osteoarticular and segmental grafts. Acta Orthop Scand. 1989;60:143-53.
28. Prosnitz LR, Lawson JP, Friedlaender GE, Farber LR, Pezzimenti JF. Avascular necrosis of bone in Hodgkin's disease patients treated with combined modality therapy. Cancer. 1981;47:2793-7.
29. Ragab AH, Frech RS, Vietti TJ. Osteoporotic fractures secondary to methotrexate therapy of acute leukemia in remission. Cancer. 1970;25:580-5.
30. Robins PR, Jowsey J. Effect of mithramycin on normal and abnormal bone turnover. J Lab and Clin Med. 1973;82:576-86.
31. Stanislavjevic S, Babcock AL. Fractures in children treated with methotrexate for leukemia. Clin Orthop Relat Res. 1977;125: 139-44.
32. Friedlaender GE, Tross RB, Doganis AC, Kirkwood JM, Baron R. Effects of chemotherapeutic agents on bone. I. Short-term methotrexate and doxorubicin (adriamycin) treatment in a rat mode. J Bone Joint Surg Am. 1984;4:602-7.
33. Virolainen P, Inoue N, Nagao M, Frassica FJ,

Chao EY. The effect of a doxorubicin, cisplatin and ifosfamide combination chemotherapy on bone turnover. Anticancer Res. 2002;22:1971-5.
34. Blomlie V, Rofstad EK, Talle K, Sundfør K, Winderen M, Lien HH. Incidence of radiation-induced insufficiency fractures of the female pelvis: evaluation with MR imaging. AJR Am J Roentgenol. 1996;167(5): 1205-10.
35. Shapeero LG, De Visschere PJL, Verstraete KL, Poffyn B, Forsyth R, Sys G, Uyttendaele D. Post-treatment complications of soft tissue tumours. Eur J Radiol. 2009;69: 209-221.
36. Gortzak Y, Lockwood GA, Mahendra A, Wang Y, Chung PWM, Catton CN, O'Sullivan B, Deheshi BM, Wunder JS, Ferguson PC. Prediction of pathologic fracture risk of the femur after combined modality treatment of soft tissue sarcoma of the thigh. Cancer. 2010;116:1553-9.
37. Schmeler KM, Jhingran A, Iyer RB, Sun CC, Eifel PJ, Soliman PT, Ramirez PT, Frumovitz M, Bodurka DC, Sood AK. Pelvic fractures after radiotherapy for cervical cancer. Implications for survivors. Cancer. 2010;116: 625-30.
38. Jenkins PJ, Montefiore DJ, Arnott SJ. Hip complications following chemoradiotherapy. Clin Oncol (R Coll Radiol). 1995;7:123-6.
39. Helmstedter CS, Goebel M, Zlotecki R, Scarborough MT. Pathologic fractures after surgery and radiation for soft tissue tumors. Clin Orthop Relat Res. 2001;389:165-72.
40. Holt GE, Griffin AM, Pintilie M, Wunder JS, Catton C, O'Sullivan B, Bell RS. Fractures following radiotherapy and limb-salvage surgery for lower extremity soft-tissue sarcomas: A comparison of high-dose and low-dose radiotherapy. J Bone Joint Surg Am. 2005;87:315-9.
41. Lin PP, Schupak KD, Boland PJ, Brennan MF, Healey JH. Pathologic femoral fracture after periosteal excision and radiation for the treatment of soft tissue sarcoma. Cancer. 1998;82:2356-65.
42. Baxter NN, Habermann EB, Tepper JE, Durham SB, Virnig BA. Risk of pelvic fractures in older women following pelvic irradiation. JAMA. 2005;294:2587-93.
43. Grangier C, Garcia J, Howarth NR, May M, Rossier P. Role of MRI in the diagnosis of insufficiency fractures of the sacrum and acetabular roof. Skeletal Radiol. 1997;26:517-24.
44. O'Sullivan B, Davis A, Turcotte R, Bell R, Catton C, Chabot P, Wunder J, Kandel R, Goddard K, Sadura A, Pater J, Zee B. Preoperative versus postoperative radiotherapy in soft-tissue sarcoma of the limbs: a randomised trial. Lancet. 2002;359:2235-41.
45. Lin PP, Boland PJ, Healey JH. Treatment of femoral fractures after irradiation. Clin Orthop Relat Res. 1998;352:168-78.
46. Burchardt H, Glowczewskie, FP Jr, Enneking WF. The effect of adriamycin and methotrexate on the repair of segmental cortical autografts in dogs. J Bone Joint Surg Am. 1983;65:103-8.
47. Friedlaender GE, Goodman A, Hausman M, Troiano N. The effects of methotrexate and radiation therapy on histologic aspects of fracture healing. Trans Orthop Res Soc. 1983;8:224.
48. Hajj A, Mnaynmeh W, Ghandur-Mnaymneh L, Latta L. The effects of methotrexate on the healing of rats femora. Trans Orthop Res Soc. 1981;6:79.
49. Young DR, Shih LY, Rock MG, Frassica FJ, Virolainen P, Chao EY. Effect of cisplatin chemotherapy on extracortical tissue formation in canine diaphyseal segmental replacement. J Orthop Res. 1997;15:773-80.
50. Penttinen R. Biochemical studies on fracture healing rat. Acta Chir Scand. 1972; 432:1-32.
51. Nilsonne U. The distribution of mineral salts in nonunion of fractures. Acta Orthop Scand. 1961;31:81-9.
52. Hansen TM, Prause JU, Lorenzen I. Effect of different cyclophosphamide treatment schedules on collagen and collagenolytic activity in granulation tissue. Acta Pharmacol Toxicol. 1978;42:219-25.
53. Udupa KN, Prasad GC. Chemical and histochemical studies on the organic constituents in fracture repair in rats. J Bone Joint Surg Br. 1963;45:770-9.

54. Sanyal AK, Singh S. Abnormal patterns of ossification in foot bones of rat fetuses induced cyclophosphamide. Anal Anz. 1974;136:1-9.
55. Sommer-Tsilenis EH, Saner HD, Kruse HP. Delaying effect of cyclophospamide on bone fracture healing. Chemical analyses of rat femora. Arch Orthop Trauma Surg. 1983;101:89-93.
56. Morcuende JA, Gomez P, Stack J, Oji G, Martin J, Fredericks DC, Buckwalter JA. Effect of chemotherapy on segmental bone healing enhanced by rhBMP-2. Iowa Orthop J. 2004;24:36-42.
57. Virolainen P, Inoue N, Nagao M, Frassica FJ, Chao EY. The effect of multidrug chemotherapy on bone graft augmented prosthesis fixation. J Orthop Res. 2005;23:795-801.
58. Delloye C, de Nayer P, Allington N, Munting E, Coutelier L, Vincent A. Massive bone allografts in large skeletal defects after tumor surgery: a clinical and microradiographic evalution. Arch Orthop Trauma Surg. 1988;107:31-41.
59. Ortiz-Cruz E, Gebhardt MC, Jennings LC, Springfield DS, Mankin HJ. The results of transplantation of intercalary allografts after resection of tumors. A long-term follow up study. J Bone Joint Surg Am. 1997;79: 97-106.
60. Shinohara N, Yokoyama K, Chuman H. Massive bone allografts in large bone defects after tumor surgery: A clinical long-term study. Gan To Kagaku Ryoho. 1989;16: 1820-6.
61. Stevenson S, Fredericks RW, Zart DJ, Li XQ, Bensusan J, Davy D, Klein L, Goldberg VM. The interaction and effects of freezing and histocompatibility on the incorporation of allogeneic cortical grafts in rats. Trans Orthop Res Soc. 1989;14:269.
62. Stevenson S, Fredericks RW, Li XQ, Zart DJ, Bensusan J, Davy D, Klein L, Goldberg VM. Together, the host bed and the properties of the graft determine the outcome of graft incorporation. Trans Orthop Res Soc. 1989;14:463.
63. Zart DJ, Miya L, Wolff DA, Makley JT, Stevenson S. The effects of cisplatin on the incorporation of fresh syngeneic and frozen allogeneic cortical bone grafts. J Orthop Res. 1993;11:240-9.
64. Bernstein M, Kovar H, Paulussen M. Ewing's sarcoma family of tumors: current management. Oncologist. 2006;11:503-19.
65. Verstappen C, Heimans J, Hoekman K, Postma T. Neurotoxic complications of chemotherapy in patients with cancer: clinical signs and optimal management. Drugs. 2003;63:1549-63.
66. Dietrich J, Han R, Yang Y, Mayer-Pröschel M, Noble M. CNS progenitor cells and oligodendrocytes are targets of chemotherapeutic agents in vitro and in vivo. J Biol. 2006;5:22.
67. Sugimoto S, Yamamoto YL, Nagahiro S, Diksic M. Permeability change and brain tissue damage after intracarotid administration of cisplatin studied by double-tracer autoradiography in rats. J Neurooncol. 1995;24:229-40.
68. Eberly AL, Anderson GD, Bubalo JS, McCune JS. Optimal prevention of seizures induced by high-dose busulfan. Pharmacotherapy. 2008;28:1502-10.
69. Patel PN. Methylene blue for management of ifosfamide-induced encephalopathy. Ann Pharmacother. 2006;40:299-303.
70. Hunault-Berger M, Chevallier P, Delain M, Bulabois CE, Bologna S, Bernard M, Lafon I, Cornillon J, Maakaroun A, Tizon A, Padrazzi B, Ifrah N, Gruel Y; GOELAMS (Groupe Ouest-Est des Leucémies Aiguës et Maladies du Sang). Changes in antithrombin and fibrinogen levels during induction chemotherapy with l-asparaginase in adult patients with acute lymphoblastic leukemia or lymphoblastic lymphoma. Use of supportive coagulation therapy and clinical outcome: the capelal study. Haematologica. 2008;93:1488-94.
71. Zakarija A, Bennett C. Drug-induced thrombotic microangiopathy. Semin Thromb Hemost. 2005;31:681-90.
72. Kamba T, McDonald DM. Mechanisms of adverse eff ects of anti-VEGF therapy for cancer. Br J Cancer. 2007;96:1788-95.
73. Moore-Maxwell CA, Datto MB, Hulette CM. Chemotherapy-induced toxic leukoencephalopathy causes a wide range of symp-

toms: a series of four autopsies. Mod Pathol. 2004;17:241-7.
74. Rajasekhar A, George TJJ. Gemcitabine-induced reversible posterior leukoencephalopathy syndrome: a case report and review of the literature. Oncologist. 2007;12:1332-35.
75. Martin G, Bellido L, Cruz JJ. Reversible posterior leukoencephalopathy syndrome induced by sunitinib. J Clin Oncol. 2007;25:3559.
76. Kastrup O, Diener HC. TNF-antagonist etanercept induced reversible posterior leukoencephalopathy syndrome. J Neurol. 2008;255:452-53.
77. Onujiogu N, Lengyel E, Yamada SD. Reversible posterior leukoencephalopathy syndrome following intravenous paclitaxel and intraperitoneal cisplatin chemotherapy for fallopian tube cancer. Gynecol Oncol. 2008;111:537-39.
78. Graus F. Acute meningospinal syndromes: acute myelopathy and radiculopathy. In: Hildebrandt J, editor. Neurological adverse reactions to anticancer drugs. Berlin: Springer; 1990. p. 87-92.
79. Perry A, Schmidt RE. Cancer therapy-associated CNS neuropathology: an update and review of the literature. Acta Neuropathol. 2006;111:197-212.
80. Troy L, McFarland K, Littman-Power S, Kelly BJ, Walpole ET, Wyld D, Thomson D. Cisplatin-based therapy: a neurological and neuropsychological review. Psychooncology. 2000;9:29-39.
81. Sierra del Rio M, Rousseau A, Soussain C, Ricard D, Hoang-Xuan K. Primary CNS lymphoma in immunocompetent patients. Oncologist. 2009;14: 526-39.
82. Dropcho EJ. Neurotoxicity of Radiation Therapy. Neurol Clin. 2010;28:217-34.
83. Sheline G. Radiation therapy of brain tumors. Cancer. 1977;39:873-81.
84. Correa DD, DeAngelis LM, Shi W, Thaler H, Glass A, Abrey LE. Cognitive functions in survivors of primary central nervous system lymphoma. Neurology. 2004;62:548-55.
85. Brandes AA, Tosoni A, Spagnolli F, Frezza G, Leonardi M, Calbucci F, Franceschi E. Disease progression or pseudoprogression after concomitant radiochemotherapy treatment: pitfalls in neurooncology. Neuro Oncol. 2008;10: 361-7.
86. Seddon BM, Cassoni AM, Galloway MJ, Rees JH, Whelan JS. Fatal radiation myelopathy after high-dose busulfan and melphalan chemotherapy and radiotherapy for Ewing's sarcoma. Clin Oncol (R Coll Radiol). 2005 Aug;17(5):385-90.
87. Gatcombe H, Lawson J, Phuphanich S, Crocker I. Treatment related myelitis in Hodgkin's lymphoma following stem cell transplant, chemotherapy and radiation. J Neurooncol. 2006;79:293-8.
88. Merimsky O, Soyfer V, Kovner F, Bickels J, Issakov J, Flusser G, Meller I, Ofer O, Kollender Y. Limb sparing approach: adjuvant radiation therapy in adults with intermediate or high-grade limb soft tissue sarcoma. Radiother Oncol. 2005;77:295-300.
89. Livi L, Antoni R, Paiar F, Bastiani P, Beltrami G, Caldora P, Capanna R, De Biase P, Detti B, Fondelli S, Meldolesi E, Pertici M, Polli C, Simontacchi G, Biti G. Late treatment-related complications in 214 patients with extremity soft-tissue sarcoma treated by surgery and postoperative radiation therapy. Am J Surg. 2006;191:230-4.
90. Olsen NK, Pfeiffer P, Johannsen L, Schrøder H, Rose C. Radiation-induced brachial plexopathy: neurological follow-up in 161 recurrence-free breast cancer patients. Int J Radiat Oncol Biol Phys. 1993;26:43-9.
91. Harper CM, Thomas JE, Cascino TL, Litchy WJ. Distinction between neoplastic and radiation-induced brachial plexopathy, with emphasis on the role of EMG. Neurology. 1989;39:502-6.
92. Thyagarajan D, Cascino T, Harms G. Magnetic resonance imaging in brachial plexopathy of cancer. Neurology. 1995;45:421-7.
93. Teixeira MJ, Fonoff ET, Montenegro MC. Dorsal root entry zone lesions for treatment of pain related to radiation-induced plexopathy. Spine. 2007;32:E316-9.
94. Fathers E, Thrush D, Huson SM, Norman A. Radiation-induced brachial plexopathy in women treated for carcinoma of the breast. Clin Rehabil. 2002;16:160-5.

95. Dubuisson AS, Kline DG, Weinshel SS. Posterior subscapular approach to the brachial plexus: report of 102 patients. J Neurosurg. 1993;79:319-30.
96. Floyd J, Mirza I, Sachs B, Perry MC. Hepatotoxicity of chemotherapy. Semin Oncol. 2006;33:50-67.
97. Rodriguez-Frias EA, Lee WM. Cancer chemotherapy II: Atypical hepatic injuries. Clin Liver Dis. 2007;11:663-76, viii.
98. Castellino S, Muir A, Shah A, Shope S, McMullen K, Ruble K, Barber A, Davidoff A, Hudson MM. Hepato-biliary late effects in survivors of childhood and adolescent cancer: a report from the Children's Oncology Group. Pediatr Blood Cancer. 2010;54: 663-9.
99. Socie G, Stone JV, Wingard JR, Weisdorf D, Henslee-Downey PJ, Bredeson C, Cahn JY, Passweg JR, Rowlings PA, Schouten HC, Kolb HJ, Klein JP. Long-term survival and late deaths after allogeneic bone marrow transplantation. Late Effects Working Committee of the International Bone Marrow Transplant Registry. N Engl J Med. 1999;341:14-21.
100. Piel B, Vaidya S, Lancaster D, Taj M, Pritchard-Jones K. Chronic hepatotoxicity following 6-thioguanine therapy for childhood acute lymphoblastic leukaemia. Br J Haematol. 2004;125:410-2.
101. Sulis ML, Bessmertny O, Granowetter L, Weiner M, Kelly KM. Veno-occlusive disease in pediatric patients receiving actinomycin D and vincristine only for the treatment of rhabdomyosarcoma. J Pediatr Hematol Oncol. 2004;26:843-6.
102. Greten TF, Manns MP, Reinisch I, Kaatsch P. Hepatocellular carcinoma occurring after successful treatment of childhood cancer with high dose chemotherapy and radiation. Gut. 2005;54:732.
103. Bassal M, Mertens AC, Taylor L, Neglia JP, Greffe BS, Hammond S, Ronckers CM, Friedman DL, Stovall M, Yasui YY, Robison LL, Meadows AT, Kadan-Lottick NS. Risk of selected subsequent carcinomas in survivors of childhood cancer: A report from the Childhood Cancer Survivor Study. J Clin Oncol. 2006;24:476-83.
104. Lennard L, Richards S, Cartwright CS, Mitchell C, Lilleyman JS, Vora A; UK MRC/NCRI Childhood Leukaemia Working Party. The thiopurine methyltransferase genetic polymorphism is associated with thioguanine-related veno-occlusive disease of the liver in children with acute lymphoblastic leukemia. Clin Pharmacol Ther. 2006;80:375-83.
105. Broxson EH, Dole M,Wong R, Laya BF, Stork L. Portal hypertension develops in a subset of children with standard risk acute lymphoblastic leukemia treated with oral 6-thioguanine during maintenance therapy. Pediatr Blood Cancer. 2005;44:226-31.
106. De Bruyne R, Portmann B, Samyn M, Bansal S, Knisely A, Mieli-Vergani G, Dhawan A. Chronic liver disease related to 6-thioguanine in children with acute lymphoblastic leukaemia. J Hepatol. 2006;44:407-10.
107. Hutter RV, Shipkey FH, Tan CT, Murphy ML, Chowdhury M. Hepatic fibrosis in children with acute leukemia: A complication of therapy. Cancer. 1960;13:288-307.
108. Parker D, Bate CM, Craft AW, Graham-Pole J, Malpas JS, Stansfeld AG. Liver damage in children with acute leukaemia and non-Hodgkin's lymphoma on oral maintenance chemotherapy. Cancer Chemother Pharmacol. 1980;4:121-7.
109. Greve J, Bas M, Schuler P, Turowski B, Scheckenbach K, Budach W, Bölke E, Bergmann C, Lang S, Arweiler-Harbeck D, Lehnerdt G, Mattheis S, Bier H, Hoffmann TK. Acute arterial hemorrhage following radiotherapy of oropharyngeal squamous cell carcinoma. Strahlenther Onkol. 2010;186(5): 269-73.

Journal of Long-Term Effects of Medical Implants, 20(1): 13–21 (2010)

Right Ventricular Outflow Tract Pacing: An Alternative, Safe, and Effective Pacing Site

Okan Erdogan & Burak Hunuk*

Department of Cardiology, School of Medicine, Marmara University, Istanbul, Turkey

*Address all correspondence to Okan Erdogan, MD, Mimar Sinan Sitesi L6D D. 35 Atakoy, Istanbul Turkey; Tel.: 90-212-5606793; Fax: 90-212-5727905; okanerdogan@yahoo.com.

ABSTRACT: The right ventricular apex (RVA) has traditionally been preferred for the insertion of permanent cardiac pacemaker leads because of vast experience with their use, their ease of implantation, and the stability of passive fixation leads in the RVA trabeculae. However, prolonged RVA pacing is associated with progressive left ventricular dysfunction due to dysynchronous ventricular activation, and often results in substantial functional, hemodynamic, electrical, and structural changes, as previously demonstrated in many studies. Only in recent years has interest in the use of alternate pacing sites developed. The right ventricular outflow tract (RVOT) is now the preferred site of pacing because of potential advantages such as ease of application, better hemodynamics, synchronous activation, fewer myocardial perfusion defects, and a narrower QRS complex compared with RVA pacing. This review article comprehensively discusses this novel technique in terms of its beneficial effects, long-term safety, and performance measures compared with RVA pacing, and as an alternative method for biventricular pacing.

KEY WORDS: pacing; right ventricular outflow tract; hemodynamics; cardiac resynchronization; myocardial perfusion; pacing site

I. INTRODUCTION

In patients treated with permanent cardiac pacemakers, the ventricular electrode is traditionally placed in the right ventricular apex (RVA), because this location provides ease of implantation, safety, and a low possibility of dislocation of pacemaker leads. Apical pacing activates ventricles in a non-physiological way, just opposite to the normal activation axis from the base to the apex. In recent years, it has been recognized that RVA pacing changes the ventricular activation sequence, causing ventricular dyssynchrony, and thus increases the risk of new onset left ventricular dysfunction, ventricular dilatation, myocardial perfusion defects, atrial fibrillation, asymmetric septal hypertrophy, and death in permanent cardiac pacemaker patients without any structural heart defects.[1-6]

To overcome the detrimental effects caused by asynchronous activation, enhance the hemodynamic contribution, and improve patient quality of life, alternative pacing techniques such as biventricular application and the optimization of atrioventricular delay have been attempted.[7-8] In addition, with the development of screw-in leads (active electrodes), it became possible to reliably activate different areas in the right ventricle. These leads can safely be screwed in anywhere in the right ventricle where acceptable threshold values are obtained. To overcome the non-physiological aspects of RVA pacing, and in order to maintain a normal physiological synchronized activation, the right ventricular outflow tract (RVOT) has recently become an anatomical area of interest, leading to numerous clinical and experimental studies.[9-17] With this novel pacing site adjacent to the septal bundles and conduction system, it is assumed that more

synchronous ventricular activation will be achieved, cardiac output will be increased, and the imbalance caused by RVA pacing in the microvascular circulation will be improved.[10-17] The present review article comprehensively discusses this relatively novel technique in terms of its application techniques and clinical aspects compared with RVA, and as an alternative method for biventricular pacing.

II. RVOT LEAD IMPLANTATION TECHNIQUE

According to our experience, RVOT lead implantation requires a bit more skill than the currently used apical technique, and therefore the physician's experience is an important concern. The preparation of the patient for the procedure, subclavian vein puncture, or vena cephalica "cut down" are all performed in a standard fashion. Screw-in leads must be used for implantation in the ventricle. Many medical companies produce various sizes and shapes of leads for this purpose. To obtain optimal lead position, a 12-lead electrocardiogram (ECG) should be applied before the procedure. The distal tip of the stylet is shaped as follows: first, a generous curve is created using the distal 5 to 6 cm of the wire, and then the terminal 2 cm is bent to create a "swan neck" deformity similar to the design suggested by Vlay.[18,19] However, to reliably position the leads on the right ventricular septum, a posterior angulation is essential. After the stylet is put in the lead, it is sent to the right ventricle through the sheet. The lead shaped by the stylet easily goes through the tricuspid valve and is advanced into the RVOT.

Fluoroscopic views may be obtained in postero-anterior or left-anterior-oblique positions. At our center, we generally prefer the postero-anterior view for the procedure itself and evaluating the position of the leads in the right- and left-anterior-oblique views (angles 40–45 degrees). With the help of fluoroscopic views, the tip of the lead is advanced to the level of the pulmonary valve. On that level, the lead is gently pulled back inferiorly until its tip touches to the interventricular septum, and then the stylet is slightly pulled back from the tip of the lead. It must be ensured that the tip of the lead touches the septum or anterior wall of the RVOT. The most appropriate anatomical position is placing the lead pointing posterolaterally in the RVOT and generally in the second intercostal space.

At that stage, with the help of an analyzer, a lead stimulation test is performed externally and paced QRS complexes and maximal positive deflections are obtained on the inferior derivations on surface ECG. The optimal lead positions are not only determined anatomically but also electrocardiographically. After optimal values are confirmed and if the leads are stable, the leads are screwed on the septal or anterior wall of the RVOT, the stylet is withdrawn, and the leads checked to make sure that they are not moving in their positions. The threshold values are measured, and if they are all appropriate, the lead is connected to the generator and the procedure is finished.[12,14,17-19] In some patients, because of the easy excitability of the RVOT, frequent ventricular arrhythmias (ventricular tachycardias and fibrillation) may occur. An external defibrillator must be kept nearby for life-threatening arrhythmias.

III. CLINICAL TRIALS AND APPLICATIONS OF RVOT PACING

Barin et al.[14] first demonstrated the efficacy and safety of positioning a lead on the RVOT, and Karpawich[15] showed direct stimulation of the His-Purkinje system. The hemodynamic superiority of RVOT pacing over apical pacing was reported by De Cock et al. in 1992.[10] After these initial reports, some striking results were reported from various centers about RVOT pacing applications. Giudici et al.[11] drew much attention with their study on 89 patients that found a significant augmentation in cardiac output acutely with RVOT pacing. In a study of 33 patients with RVOT pacemakers, Barin et al.[13] stated that the complication rates, threshold values, and applicability of RVOT pacing were similar to those of apical pacing. However, the anatomical differences in the optimal pacing site on RVOT brought out some discrepancies in the results of different trials. It was technically not always

possible to implant the lead just on the His bundle or nearby His, so terminologically different anatomical terms were then expressed. These different terms are high septal, RVOT or right ventricular inflow, and infundibular pacing sites, but all share a common feature of being away from the apical region. Guidici et al.[12] defined right ventricular inflow, infundibulum, and outflow tract septal pacing regions by accentuating a need for an anatomical classification for optimal pacing on the septal region. Generally, infundibular and outflow tract septal pacing regions exhibited left bundle branch block and a vertical axis, while inflow septal pacing ECG exhibited a normal axis and normal QRS deflections. In order to efficiently set forth these regions and guide the clinician, there is also an anatomical map that is more convenient and easier to understand.

The RVOT is considered not only as a septum but also as an anterior free wall. The higher septal region does not have an actual adjacency to the left ventricle, so the lower septal region is the real septal region with an actual adjacency to the left ventricle. Therefore, stimulating the lower regions of septum is more significant because it is the real septum and is adjacent to conduction pathways.[20,21] However, in trials on RVOT pacing, the leads are implanted wherever appropriate on the anterior free wall or septum, and these regions can be more clearly distinguished with left anterior oblique fluoroscopic projections. When the lead is implanted on the upper or lower regions, right anterior oblique fluoroscopic projection is preferred.[20,21] It is not appropriate to claim that the hemodynamic contribution is only related to the position of the lead, especially when we consider other possible factors. Shortening of the QRS time may occur independently from the lead position and may affect ventricular function in different ways. Results of studies have supported the hypothesis that as an indicator of left ventricular activation time, QRS time is inversely related to left ventricular function.[13] In an editorial comment,[9] it was emphasized that the pacing region of the right ventricle could not be the only determinant of hemodynamic and functional performance of RVOT pacing. Nevertheless, providing a synchronous activation RVOT application theoretically seems logical. It is important to effectively position the lead while fixing it in order to prevent it from moving away from the appropriate pacing region, and to pay attention to the stability of the lead. We did not observe any complications or lead problems in a study involving 16 patients implanted with leads in the RVOT region.[17] While performing the procedure, we recommend obtaining unfiltered intra-cardiac recordings and investigating the presence of an injury current.

Apical pacing causes regional myocardial perfusion defects because of its asynchronous activation. These myocardial perfusion defects, which are determined by myocardial perfusion scintigraphy, occur because of an imbalance in the coronary blood flow in the microvascular bed, probably caused by the asynchronous activation.[2,16,22] However, this relationship cannot always be explained by such asynchronization. In a case report, we found an inferolateral perfusion defect in a patient with normal coronary arteries and chronic exposure to RVOT pacing.[16] However, RVOT pacing resulted in significantly lower rates of perfusion defects and better global left ventricular function compared with RVA pacing.[2] There are also some studies stressing that RVA causes abnormal myocardial histology, thinning of the ventricular walls, and asymmetrical hypertrophy.[23] Long-term apical pacing causes deterioration in left ventricular function in patients with both preserved and reduced left ventricular functions.[2,24]

De Cock et al.[25] published a meta-analysis comparing apical pacing applications hemodynamically by selecting nine trials using quantitative review techniques. This meta-analysis involved 217 patients and showed that RVOT pacing achieved better hemodynamic contribution compared with apical pacing. The RVOT technique was therefore recommended, especially in the patient subsets with bradyarrhythmias and left ventricular dysfunction.[25] Buckhingam et al.[26] found that stimulation of apical and RVOT regions led to an increased dP/dT ratio, although this was not statistically significant. Similarly, Victor et al.[27] found no difference in improvement of the functional capacity

and hemodynamic parameters between the apical and RVOT pacing groups. These conflicting results may be explained by the following problems. First of all, there was no long-term follow-up in the majority of the published studies. There might also have been some technical differences between the left ventricle measurements and patient selections or some kind of bias might have occurred. Also, it is technically impossible to implant the leads every time on the exact location in the RVOT. In some studies, higher septal regions and in others mid-septal regions were preferred. Factors such as adjacency to the His bundle and shortening of QRS time may also be the source of different results. Finally, it is still unknown whether the beneficial effects observed in the acute period will persist in the long term.

The ideal point for pacer placement in the RVOT appears to be the mid-septum, because the high septal region is farther away from the His bundle. Stimulations from the mid-septum showed narrower QRS complexes resembling the stimulus deriving from the His bundle.[28] Stimulating the His bundle directly may be a wise approach, especially in patients with a normal infra-His conduction system. QRS time achieved by the RVOT stimulation is affected by the native QRS time. RVOT pacing uses His-Purkinje bundles if the conduction system is normal, and therefore the QRS complex gets narrower. Thus, it is assumed that patients with an abnormal conduction system theoretically benefit less than the other patient subsets.[29] Placing the leads near the His bundle, or adjacent to it, seems to be logical, but the procedural technique is cumbersome and success of the intervention is poor.

It is hard to foresee the success of a continuous and reliable pacing. During both early and late follow-up, the thresholds are very high because of the natural structure of the His bundle, and this unfortunately may lead to premature depletion of the battery. Both early and late efficacy and safety results are still lacking.[30-32] The first study about direct His pacing was published by Deshmukh et al.[32] The study involved 54 patients with dilated cardiomyopathy and atrial fibrillation with narrow QRS complexes. With direct His bundle pacing, the patients' dP/dT ratios and ejection fractions increased, functional capacities and cardiopulmonary exercise parameters improved, and QRS complexes got narrower. Very high threshold values, increased acute lead complications, long implantation times, and lack of long-term efficacy and safety data limit the extensive use of this technique.

One of the most important studies comparing RVOT and RVA pacing to date was performed by Stambler et al.[33] In this study, they conducted a randomized, crossover trial to determine whether quality of life was better after 3 months of RVOT than after RVA pacing in 103 pacemaker recipients with congestive heart failure, left ventricular systolic dysfunction (left ventricular ejection fraction ≤ 40%), and chronic atrial fibrillation. All of the patients' functional capacities were World Health Organization class II and III, and they were all symptomatic heart failure patients. Patients underwent implantation of a standard dual-chamber, permanent cardiac pacemaker, along with two bipolar, active-fixation pacing leads. One lead was placed at the RVA and one lead was implanted in the RVOT. Quality of life was assessed by the Medical Outcomes Study short-form health survey (SF-36) questionnaire and performed after 3 months of ventricular pacing from each right ventricular site (RVOT vs. RVA). At the end of the study, it was determined that RVOT and dual-site right ventricular pacing shortened QRS duration, but after 3 months did not consistently improve quality of life or other clinical outcomes compared with RVA pacing. Nonetheless, the 3-month follow-up period was the most important component of that study. Finally, it should be kept in mind that this study was carried out in a specific subset of patients followed for a limited time period. In a recent study, the long-term effect of permanent RVA versus RVOT pacing on the all-cause and cardiovascular mortality was compared.[34] A total of 122 consecutive patients (70 men, 69 ± 11 years) with standard pacing indications were randomized to RVA (n = 66) or RVOT (n = 56) ventricular lead placement. After a 10-year follow-up period, the mortality data were summarized on the basis of

an intention-to-treat analysis. During long-term follow-up, 31 patients from the RVA group died, compared with 24 patients in the RVOT group (hazard ratio [HR], 0.96; 95% confidence interval [CI], 0.57–1.65; $P = 0.89$). There were 10 cardiovascular deaths in the RVA group and 12 in the RVOT group (HR, 1.04; 95% CI, 0.45–2.41; $P = 0.93$). There were no differences in all-cause or cardiovascular mortality between the pacing sites after adjustment for age, gender, arterial hypertension, atrial fibrillation, New York Heart Association class, and left ventricular end-diastolic diameter.

In another recent study, it was investigated whether RVOT pacing was superior to RVA pacing in terms of ventricular synchrony, cardiac function, and remodeling in patients with normal cardiac function.[35] A total of 96 consecutive patients with high or third-degree atrial ventricular block were enrolled and randomized into two groups: the RVOT group (n = 48) and the RVA group (n = 48). There were no significant differences with respect to the mean myocardial systolic and early diastolic velocities, left ventricular ejection fraction, or left ventricular end-diastolic and systolic volume in the two groups at 12 months of follow-up. It was concluded that although RVOT pacing caused more synchronous left ventricular contraction compared with RVA pacing, it had no benefit over RVA pacing in terms of preventing cardiac remodeling and preserving left ventricular systolic function after 12 months in patients with normal cardiac function.

In patients with advanced heart failure and widened QRS complexes, some positive results have emerged about relieving symptoms with left ventricular epicardial electrodes implanted in the coronary sinus tributaries and biventricular cardiac stimulation achieved by simultaneous RVA and left ventricular pacing, also called cardiac resynchronization therapy.[36,37] However, despite the proposed current indication criteria, approximately 35% of patients do not benefit or deteriorate from the biventricular pacing approach. Because of inappropriate venous anatomy, high threshold values, or phrenic nerve stimulation, it is not always possible to implant biventricular pacemakers in every patient with the appropriate indications. Additionally, it is an expensive and difficult technique, and the learning curve and duration of the operation are fairly long. Therefore, as an alternative to this system, some investigators have published case reports about simultaneous stimulation of the RVOT and RVA. In one case report, patients in whom there were technical difficulties in placing epicardial leads to the left ventricle had leads placed to the RVOT and RVA instead. With a 50-ms delay, RVOT and RVA were both stimulated simultaneously. By the end of the study, significant clinical improvement was observed.[38] In another case report, a heart failure patient with a cardiac resynchronization therapy device was followed up, and after 17 months the battery became depleted because of the high capture threshold of the left ventricular lead. Therefore, in view of the high capture threshold, dual-site right ventricular pacing was selected in that patient. Another active fixation endocardial pacing lead was positioned on the high septum of the right ventricle near the RVOT. With simultaneous apical/RVOT bifocal right ventricular stimulation, similar clinical efficacy was observed at 12 weeks of follow-up.[39] In another observational, single-center study, implantation of a bifocal right ventricular lead system was reported because lateral left-ventricular placement for a biventricular pacemaker could not be achieved. A total of six patients underwent implantation of a bifocal right-ventricular lead system with two active fixation leads, one placed septally at the apex and the other in the high-septal RVOT. A biventricular stimulation system was implanted in 44 patients. All patients were followed up for 12 months, and the two groups were compared. At the end of the follow-up, both groups experienced a similar improvement in functional capacity, electrocardiographic and hemodynamic parameters, increase in 6-min walking distance, and a decreased need for hospitalizations.[40] In an ongoing randomized, single-blind, crossover study of atrial synchronized bi-right ventricular pacing in patients in New York Heart Association heart failure functional class III, a left ventricular ejection fraction under 35%, left bundle branch block, and QRS complexes 120 ms or above, the investigators compared the electrical

and handling characteristics, as well as the complications of pacing at the RVA with passive versus RVOT with active fixation leads.[41] At the end of the study, ease and success rate of lead implantation was similar in both positions. Sensing values were significantly higher at the apex than at the RVOT. The average R-wave amplitude among published reports is between 10 and 16 mV, with no significant difference between RVOT and RVA, in populations of patients who were not in heart failure. In conclusion, marked differences were observed between leads positioned at the RVOT versus the RVA. This is partially explained by differences in lead design, with lower impedance and higher stimulation thresholds at the RVOT. The higher R-waves amplitude at the RVA than at the RVOT was unexplained.[41]

In an intriguing study, over a 5-year period, 112 patients (89 male/23 female, mean age 65 years) underwent RVOT placement of permanent active-fixation transvenous pacing/defibrillating leads. At the time of the implantation, both pacing and defibrillation thresholds were determined to be between the normal limits in the short- and long-term follow-up visits. At the end of the study, it was concluded that RVOT pacing-defibrillation lead implantation was safe, efficacious, and potentially attractive because preliminary evidence suggested that it might not have been associated with the adverse hemodynamic effects of pacing at the RVA.[42]

There have also been studies investigating the lead performance of RVOT pacing. In a previous study, we sought to investigate long-term safety and change in pacing parameters of right ventricular RVOT pacing.[43] This prospectively designed, controlled clinical study comprised patients in two groups, the RVOT group (n = 16) and the RVA group (n = 16), who were selected from patients with permanent pacemakers who were routinely followed up at our pacemaker clinic. The mean duration of follow-up was 38.3 ± 18 months for RVOT and 30.4 ± 20 months for RVA ($P = 0.255$). Impedance values, pacing thresholds, and R-wave amplitudes measured at implant and last pacemaker check did not significantly differ between the RVOT and the RVA pacing groups. There was no lead dislodgment or any other procedure-related complications during follow-up. In a recent study by Medi et al.,[44] a total of 100 patients with ventricular lead placement on the RVOT septum undergoing pacemaker implantation for bradycardia indications were retrospectively analyzed. Long-term (1-year) follow-up was obtained in 92 patients. At the end of the study, lead performance at the RVOT septal position was stable in the long term. Ventricular electrical parameters were acceptable, with stable long-term stimulation thresholds, sensing, and impedance for all lead types. There were no cases of high pacing thresholds or inadequate sensing. Therefore, the long-term performance of leads placed on the RVOT septum was comparable to those placed at other traditional sites.

IV. CONCLUSIONS

In the light of emerging data, RVOT pacing is going to become more widespread in the near future as an alternative method in pacemaker procedures. Even though conflicting results have been published so far about the effectiveness of this technique, RVOT pacing seems to be more advantageous than apical pacing in terms of hemodynamic improvement and clinical aspects. Furthermore, this technique can also be applied as an alternative to biventricular pacing by simultaneous bifocal right ventricular pacing in suitable heart failure patients. However, in order to reliably use this relatively new technique, larger, multi-center, randomized, controlled clinical trials are needed to assess the long-term benefits and safety measures.

REFERENCES

1. Van Oosterhout MF, Prinzen FW, Arts T, Schreuder JJ, Vanagt WY, Cleutjens JP, Reneman RS. Asynchronous electrical activation induces inhomogeneous hypertrophy of the left ventricular wall. Circulation. 1998 Aug 11;98(6):588-95.
2. Tse HF, Yu C, Wong KK, Tsang V, Leung YL, Ho WY, Lau CP. Functional abnormalities in patients with permanent right ventricular pac-

ing: the effect of sites of electrical stimulation. J Am Coll Cardiol. 2002 Oct 16;40(8):1451-8.
3. Sweeney MO, Hellkamp AS, Ellenbogen KA, Greenspon AJ, Freedman RA, Lee KL, Lamas GA; MOde Selection Trial Investigators. Adverse effect of ventricular pacing on heart failure and atrial fibrillation among patients with normal baseline QRS duration in a clinical trial of pacemaker therapy for sinus node dysfunction. Circulation. 2003 Jun 17;107(23): 2932-7.
4. Tantengco MV, Thomas RL, Karpawich PP. Left ventricular dysfunction after long term right ventricular apical pacing in the young. J Am Coll Cardiol. 2001 Jun 15;37(8):2093-100.
5. Wilkoff BL, Cook JR, Epstein AE, Greene HL, Hallstrom AP, Hsia H, Kutalek SP, Sharma A. Dual chamber pacing or ventricular backup pacing in patients with an implantable defibrillator: the Dual chamber and VVI implantable defibrillator (DAVID) trial. JAMA. 2002 Dec 25;288(24):3159-61.
6. Thambo JB, Bordachar P, Garrigue S, Lafitte S, Sanders P, Reuter S, Girardot R, Crepin D, Reant P, Roudaut R, Jaïs P, Haïssaguerre M, Clementy J, Jimenez M. Detrimental ventricular remodeling in patients with congenital complete heart block and chronic right ventricular apical pacing. Circulation. 2004 Dec 21;110(25):3766-72.
7. Maron BJ, Nishimura RA, Mc Kenna WJ, Rakowski H, Josephson ME, Kieval RS. Assessment of permanent dual chamber pacing as a treatment for drug refractory symptomatic patients with obstructive hypertrophic cardiomyopathy. A randomized, double-blind, crossover study (M-Pathy). Circulation. 1999 Jun 8;99(22):2927-33.
8. Dupuis JM, Kobeissi A, Vitali L, Gaggini G, Merheb M, Rouleau F, Leftheriotis G, Ritter P, Victor J. Programming optimal atrioventricular delay in dual chamber pacing using peak endocardial acceleration: comparison with a standard echocardiographic procedure. Pacing Clin Electrophysiol. 2003 Jan;26(1 Pt 2):210-3.
9. Gold MR. Optimization of ventricular pacing: Where should we implant the leads? J Am Coll Cardiol. 1999 Feb;33(2):324-6.
10. DeCock CC, Meyer A, Kamp O. Assessment of left ventricular function in relation to electrode position: Effects of right ventricular outflow tract pacing [abstract]. Pacing Clin Electrophysiol. 1992 Apr;15(4):511.
11. Giudici MC, Thornburg GA, Buck DL, Coyne EP, Walton MC, Paul DL, Sutton J. Comparison of right ventricular outflow tract and apical lead permanent pacing on cardiac output. Am J Cardiol. 1997 Jan 15;79(2):209-12.
12. Giudici MC, Karpawich PP. Alternative site pacing: It's time to define terms. Pacing Clin Electrophysiol. 1999 Apr;22(4 Pt 1):551-3.
13. Schwaab B, Fröhlig G, Alexander C, Kindermann M, Hellwig N, Schwerdt H, Kirsch CM, Schieffer H. Influence of right ventricular stimulation site on left ventricular function in atrial synchronous ventricular pacing. J Am Coll Cardiol. 1999 Feb;33(2):317-23.
14. Barin ES, Jones SM, Ward DE, Camm AJ, Nathan AW. The right ventricular outflow tract as an alternative permanent pacing site: Long term follow-up. Pacing Clin Electrophysiol. 1991 Jan;14(1):3-6.
15. Karpawich PP, Justice CD, Chang CH, Gause CY, Kuhns LR. Septal ventricular pacing in the immature canine heart: A new perspective. Am Heart J. 1991 Mar;121(3 Pt 1):827-33.
16. Erdogan O, Altun A, Durmus-Altun G, Ozbay G. Inferolateral myocardial perfusion defect caused by right ventricular outflow tract pacing. Pacing Clin Electrophysiol. 2004 Jun;27(6 Pt 1):808-11.
17. Erdogan O, Altun A, Ozbay G. The effect of right ventricular outflow tract and apical pacing sites on electrocardiographic parameters in patients with permanent pacemakers. Arch Turk Soc Cardiol. 2004 Apr;32(3):152-7.
18. Vlay SC. Right ventricular outflow tract pacing: practical and beneficial. A 9-year experience of 460 consecutive implants. Pacing Clin Electrophysiol. 2006 Oct;29(10):1055-62.
19. Mond HG. The road to right ventricular septal pacing: techniques and tools. Pacing Clin Electrophysiol. 2010 Jul;33(7):888-98
20. Lieberman R, Grenz D, Mond HG, Gammage MD. Selective site pacing: defining and reaching the selected site. Pacing Clin Electrophysiol. 2004 Jun;27(6 Pt 2):883-6.

21. McGavigan AD, Mond HG. Selective site ventricular pacing. Curr Opin Cardiol. 2006 Jan;21(1):7-14.
22. Simantirakis EN, Prassopoulos VK, Chrysostomakis SI, Kochiadakis GE, Koukouraki SI, Lekakis JP, Karkavitsas NS, Vardas PE. Effects of asynchronous ventricular activation on myocardial adrenergic innervation in patients with permanent dual chamber pacemakers: an I-123 metaiodobenzylguanidine cardiac scintigraphic study. Eur Heart J. 2001 Feb;22(4):323-32.
23. Prinzen FW, Cheriex EC, Delhaas T, van Oosterhout MF, Arts T, Wellens HJ, Reneman RS. Asymmetric thickness of the left ventricular wall resulting from asynchronous electric activation: A study in dogs with ventricular pacing and in patients with left bundle branch block. Am Heart J. 1995 Nov;130(5):1045-53.
24. Blanc JJ, Etienne Y, Gilard M, Mansourati J, Munier S, Boschat J. Evaluation of different ventricular pacing sites in patients with severe heart failure: Results of an acute hemodynamic study. Circulation. 1997 Nov 18;96(10): 3273-7.
25. De Cock CC, Giudici MC, Twisk JW. Comparison of the haemodynamic effects of right ventricular outflow-tract pacing with right ventricular apex pacing. Europace. 2003 Jul;5(3):275-8.
26. Buckingham TA, Candinas R, Attenhofer C, Van Hoeven H, Hug R, Hess O, Jenni R, Amann FW. Systolic and diastolic function with alternate and combined site pacing in the right ventricle. Pacing Clin Electrophysiol. 1998 May;21(5):1077-84.
27. Victor F, Leclercq C, Mabo P, Pavin D, Deviller A, de Place C, Pezard P, Victor J, Daubert C. Optimal right ventricular pacing site in chronically implanted patients: Prospective randomized crossover comparison of apical and outflow tract pacing. J Am Coll Cardiol. 1999 Feb;33(2):311-6.
28. Riedlebauchova L, Kautzner J, Hatala R, Buckingham TA. Is right ventricular outflow tract pacing an alternative to left ventricular / biventricular pacing? Pacing Clin Electrophysiol. 2004 Jun;27(6 Pt 2):871-7.
29. Giudici MC, Barold SS, Moeller AL, Meierbachtol CJ, Paul DL, Walton MC. Influence of native conduction status on clinical results with right ventricular outflow tract pacing. Am J Cardiol. 2003 Jan 15;91(2):240-2.
30. Mabo P, Scherlag B, Munsif A, Otomo K, Lazzara R. A technique for stable His bundle recording and pacing: electrophysiologic and hemodynamic correlates. Pacing Clin Electrophysiol. 1995 Oct;18(10):1894-901.
31. Deshmukh P, Casavant DA, Romanyshyn M, Anderson K. Permanent direct His bundle pacing : a novel approach to cardiac pacing in patients with normal His-Purkinje activation. Circulation. 2000 Feb 29;101(8):869-77.
32. Deshmukh P, Romanyshyn M. Direct His bundle pacing: present and future. Pacing Clin Electrophysiol. 2004 Jun;27(6 Pt 2):862-70.
33. Stambler BS, Ellenbogen K, Zhang X, Porter TR, Xie F, Malik R, Small R, Burke M, Kaplan A, Nair L, Belz M, Fuenzalida C, Gold M, Love C, Sharma A, Silverman R, Sogade F, Van Natta B, Wilkoff BL. Right ventricular outflow versus apical pacing in pacemaker patients with congestive heart failure and atrial fibrillation. J Cardiovasc Electrophysiol. 2003 Nov;14(11):1180-6.
34. Dabrowska-Kugacka A, Lewicka-Nowak E, Tybura S, Wilczek R, Staniewicz J, Zagozdzon P, Faran A, Kozłowski D, Raczak G, Swiatecka G. Survival analysis in patients with preserved left ventricular function and standard indications for permanent cardiac pacing randomized to right ventricular apical or septal outflow tract pacing. Circ J. 2009 Oct;73(10):1812-9.
35. Gong X, Su Y, Pan W, Cui J, Liu S, Shu X. Is right ventricular outflow tract pacing superior to right ventricular apex pacing in patients with normal cardiac function? Clin Cardiol. 2009 Dec;32(12):695-9.
36. Linde C, Leclercq C, Rex S, Garrigue S, Lavergne T, Cazeau S, McKenna W, Fitzgerald M, Deharo JC, Alonso C, Walker S, Braunschweig F, Bailleul C, Daubert JC. Long-term benefits of biventricular pacing in congestive heart failure: Results from the Multisite Stimulation in Cardiomyopathy (MUSTIC) study. J Am Coll Cardiol. 2002 Jul 3;40(1):111-8.
37. Young JB, Abraham WT, Smith AL, Leon AR, Lieberman R, Wilkoff B, Canby RC, Schroeder JS, Liem LB, Hall S, Wheelan K. Com-

bined cardiac resynchronization and implantable cardioversion defibrillation in advanced chronic heart failure: The MIRACLE-ICD Trial. JAMA. 2003 May 28;289(20):2685-94.
38. Vlay SC. Alternatives when coronary sinus pacing is not possible. Pacing Clin Electrophysiol. 2003 Jan;26(1 Pt 1):4-7.
39. Sai Satish O, Yeh K, Wen M, Wang C. Cardiac resynchronization therapy versus dual site right ventricular pacing in a patient with permanent pacemaker and congestive heart failure. Europace. 2005 Jan;7(4):380-4.
40. O' Donnell V, Nadurata V, Hamer A, Kertes B, Mohammed W. Bifocal right ventricular cardiac resynchronization therapies in patients with unsuccessful percutaneous lateral left ventricular venous access. Pacing Clin Electrophysiol. 2005 Jan;28 Suppl 1:S27-30.
41. Res JC, Bokern MJ, Vos DH. Characteristics of bifocal pacing: Right ventricular apex versus outflow tract. An interim analysis. Pacing Clin Electrophysiol. 2005 Jan;28 Suppl 1:S36-8.
42. Giudici MC, Barold SS, Paul DD, Schrumpf PF, Van Why KJ, Orias DW. Right ventricular outflow tract placement of defibrillation leads: 5-year experience. Pacing Clin Electrophysiol. 2004 Apr;27(4):443-6.
43. Erdoğan O, Aktöz M, Altun A. Long-term safety and efficacy of right ventricular outflow tract pacing in patients with permanent pacemakers. Anadolu Kardiyol Derg. 2008 Oct;8(5):350-3.
44. Medi C, Mond HG. Right ventricular outflow tract septal pacing: long-term follow-up of ventricular lead performance. Pacing Clin Electrophysiol. 2009 Feb;32(2):172-6.

JOURNAL OF LONG-TERM EFFECTS OF MEDICAL IMPLANTS

Special Section:
Retrieval Analysis of Implanted Medical Devices
Guest Editor:
William M. Mihalko

Journal of Long-Term Effects of Medical Implants, 20(1): 25–26 (2010)

Preface: Retrieval Analysis of Implanted Medical Devices

Each year millions of patients improve their quality of life through surgical procedures that involve implanted medical devices. As the rising cost of health care continues to be debated within our country, it is clear that we must be certain that Americans are receiving the best, most cost effective health care treatments. Advances in medical technology continue to be a large part of the rising cost of health care, and the decision to provide the increased cost of care due to new technology must be determined from evidence-based studies.

The Food and Drug Administration this past year issued an internal report where they stated that science-based reviews must be strived for and that the agency must first provide safe devices for patients while making sure not to impede the advancement and innovation of technology in the medical field. With the focus on both cost and innovation, it is clear that everything must be done to make certain that the devices we utilize in medicine are safe and that they are given a pathway to be improved on using science and lessons learned from device retrieval studies. Retrieval analysis studies of medical devices have been utilized for decades to learn lessons from failed devices removed at the time of revision or repeated procedures, as well as from those that functioned well for the life of a patient and were obtained at necropsy.

The value of implant retrieval analysis in orthopaedic surgery has been well recognized in advancing implant longevity. If we use the example of total hip and knee arthroplasty, we know that analysis of devices has provided insight into wear, corrosion, design characteristics, and material issues that have advanced the design and longevity of these devices. Prosthetic implants retrieved at revision surgery (for implant failure) or devices retrieved postmortem from patients with clinically successful reconstructions provide a unique set of specimens that can be studied to evaluate the effect of the implant on the host environment and vice versa. In this issue, there are two articles that try to determine commonalities of patellar polyethylene buttons from total knee arthroplasty, with one obtained from necropsy retrievals and the other from implants obtained at time of revision surgery. A systematic analysis of retrieved components, in combination with histologic, radiographic, and clinical data, can provide valuable insights into the mechanisms of failure of the biomaterials and implant designs used in joint replacement applications. If computer modeling can be added to properly predict wear patterns and kinematics of the joint, then the first steps toward intraoperative computer assistance for optimal functionality and implant longevity may be realized. This type of analysis can be seen in this issue's article that utilizes a 3D dynamic TKA model to show how the kinematics and contact stresses change after wear of the polyethylene insert (Williams et al.).

The first retrieval observations were performed for failures of implants during their subsequent revision surgeries. While these studies gave valuable insight into the failure modes of early designs and biomaterials, it was not until the 1980s when donor-related studies were organized. At that time, usually the establishment of a retrieval program within a practice of orthopaedic surgeons allowed for the analysis of a series of patients who had a specific implant utilized at the time of surgery. There are few retrieval programs that encompass a large variety of implants, and many times those laboratories only receive the implant itself without the surrounding joint and musculoskeletal tissues. It has been evident from past

studies that several significantly important modes of wear and or implant failure have been reported that have allowed changes in the field of hip and knee arthroplasty to further the design-related and surgical-related techniques in the field. We must continue to update our investigative techniques of these devices, and this issue also has reports from London, Ontario, investigators evaluating new techniques to evaluate the wear of polyethylene components.

Ultimately, it is the patient and the improvement in their quality of life that benefit from retrieval analysis studies. It is imperative that the field of medicine continue these kinds of studies to investigate newer, more modern implant designs and surgical techniques since the in vitro testing and the computer modeling techniques cannot always predict the in vivo wear or failure mechanisms that may have a negative impact on the longevity or functional result for the patient.

William M. Mihalko, MD Ph.D.
University of Tennessee, Campbell Clinic Orthopedics
Chief Scientific Officer, InMotion Orthopaedic Research Center

Journal of Long-Term Effects of Medical Implants, 20(1): 27–34 (2010)

Technique to Quantify Subsurface Cracks in Retrieved Polyethylene Components Using Micro-CT

Matthew G. Teeter,[1,2,] Xunhua Yuan,[1,2] Douglas D. R. Naudie,[3] & David W. Holdsworth[1,2,3]*

[1]Imaging Research Laboratories, Robarts Research Institute, London, ON, Candad; [2]Department of Medical Biophysics, The University of Western Ontario, London, ON, Canada; [3]Division of Orthopaedic Surgery, The University of Western Ontario, London, ON, Canada

*Address all correspondence to Matthew Teeter, Imaging Research Laboratories, Robarts Research Institute, P.O. Box 5015, 100 Perth Drive, London, ON, N6A 5K8 Canada; Tel.: 519-931-5777; Fax: 519-931-5713; mteeter@imaging.robarts.ca.

ABSTRACT: No current method to study delamination and subsurface cracking in polyethylene joint replacement components provides accurate, nondestructive, and quantitative measurements. A technique to study damage both at and below the surface could be of great benefit. We report the development of a micro-CT technique to nondestructively examine and quantify subsurface cracking in retrieved polyethylene tibial inserts. Five severely delaminated inserts and two never-implanted inserts were obtained from our institution's implant retrieval library and scanned with micro-CT. The insert subsurface was examined for cracks, and their location and widths were measured using a digital line tool. Subsurface cracks were readily apparent only in the images of the delaminated inserts. Cracks ran horizontally, just below the articular and back-side surfaces, and vertically at the center and lateral edges of the inserts and at the tibial post. Cracks ranged from 0.12 to 6.01 mm below the surface, with widths of 0.06–0.97 mm. Micro-CT can nondestructively visualize and quantify subsurface cracks. This is an enhancement to its previously reported use to quantify surface deviations from wear. Micro-CT is well suited for longitudinal pin-on-disk and wear simulator trials, in addition to studies of retrieved components.

KEY WORDS: total knee replacement, polyethylene wear, delamination, implant retrieval, micro–computed tomography, subsurface crack

I. INTRODUCTION

The mechanisms of polyethylene wear in total joint components can be divided into adhesive and abrasive wear, leading to surface damage and osteolysis, and fatigue wear, leading to delamination and subsurface cracking.[1–4] Fluctuating stresses and sliding motions are thought to be responsible for the subsurface failure of the polyethylene, and can be accelerated by oxidation and certain material processing techniques.[2,4] Innovations in design and materials have led to components with greater resistance to delamination and cracking.[1] Recently, the potential use of highly cross-linked polyethylene in total knee arthroplasty has become controversial, due to certain decreases in its mechanical properties (versus conventional polyethylene) that might increase fatigue failure and delamination.[5–7]

No current method to study delamination and subsurface cracking in polyethylene joint replacement components provides accurate, nondestructive and quantitative measurements. Delamination in total knee replacements is often first observed by examining the surface of a tibial insert for discoloration, using the naked eye or a microscope.[5,8] However, this does not detect the smallest regions of delamination, specifically the initial subsurface cracking. After the material has sloughed off, the surface

changes may be measured by coordinate measuring machines (CMMs).[9] As a contact measurement technique, CMM cannot quantify cracks below the insert surface, and its accuracy depends on the tip size of its probe. Subsurface cracks from fatigue can be quantified using scanning electron microscopy (SEM), but only in a manner that is destructive to the specimen and may destroy some of the smallest cracks.[4,10] Nondestructive imaging of subsurface cracks has been attempted with ultrasound and scanning acoustic tomography (SAT).[4,11] Unfortunately, the ultrasonic techniques provide only low-resolution images and limited quantitative information regarding the subsurface cracks, with no information on surface damage, limiting its practical application. Although these various methods have been successfully used to yield a certain degree of insight into delamination and subsurface cracking, a nondestructive and fully quantitative method to study polyethylene damage both at and below the insert surface would be of great benefit.

Recently, micro–computed tomography (micro-CT) has been implemented to evaluate surface damage in components from knee, hip, and spinal disc replacement.[12–16] Typically, the micro-CT images are reconstructed to analyze the 3D geometry and volume of the component. Micro-CT nondestructively projects X-rays through the components,[17] rather than probing the surface as in CMM or laser scanning.[18–20] Therefore, details of the component's subsurface are also obtained, potentially revealing valuable information on subsurface fatigue wear.

We report the development of a micro-CT technique to nondestructively examine and quantify subsurface cracking in retrieved polyethylene tibial inserts. We evaluated two questions: Are subsurface cracks visible in reconstructed micro-CT images of the inserts? If so, can the location and extent of the subsurface cracks be quantified?

II. METHODS

Five severely delaminated inserts were obtained from our institution's implant retrieval library. Inserts with obvious, extensive delamination were selected because they would be the most likely to have subsurface cracking. Two never-implanted inserts, which would not be expected to have any deviations in their subsurface structure, were also obtained. The five delaminated inserts included one AMK (DePuy Inc., Warsaw, Indiana), one Genesis I (Smith & Nephew Inc., Memphis, Tennessee), one Miller-Galante I (Zimmer Inc., Warsaw, Indiana), one Kinemax, and one Duracon (Stryker Inc., Kalamazoo, Michigan). The lengths of implantations were 15 years for the AMK and Kinemax, 12 years for the Miller-Galante, 11 years for the Duracon, and 10 years for the Genesis I. All had obvious delamination across the articular surfaces (Fig. 1). The surface of the polyethylene was relatively intact for the Kinemax and Duracon, but the majority of the surfaces of the AMK, Genesis I, and Miller-Galante I were removed. The new, never-implanted inserts included one AMK and one Genesis II (Smith & Nephew, Memphis, Tennessee).

Each insert was scanned with a dedicated laboratory micro-CT scanner (eXplore Vision 120, GE Healthcare, London, Ontario) in a previously described fashion.[12,13,16] The delaminated inserts were laid flat in the scanner bed within a radiotranslucent polystyrene foam holder. This orientation maximized the viewing angle for the scanner to visualize any subsurface cracks that were present. Two scans were performed per insert, each covering slightly more than half of the insert. The scans were then stitched together automatically to restore the complete insert geometry, using software built into the scanner console. All scans were obtained using an isotropic resolution of 50 μm, with image acquisition over 1200 views, and 10 frames averaged per view at an exposure time of 16 ms per frame. The X-ray tube voltage was 90 kV with a current of 40 mA. The scans were reconstructed at the full 50 μm isotropic resolution.

The reconstructed scan images were analyzed with dedicated micro-CT software (MicroView v2.2, GE Healthcare, London, Ontario). A threshold (to separate the insert from the surroundings) was determined automatically for each reconstructed scan by the software. Windowing was adjusted to aid visualization. For each insert, projections were

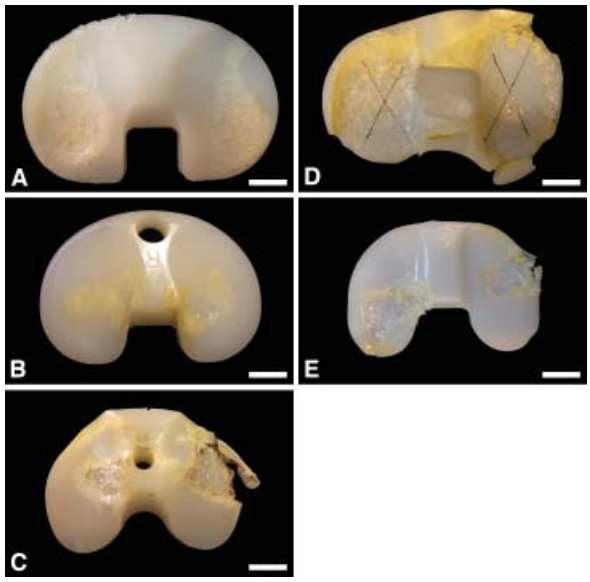

FIGURE 1. Photographs of the five retrieved inserts with obvious delamination on their surfaces: (A) Kinemax; (B) Duracon; (C) AMK; (D) Genesis I; (E) Miller-Galante. Scale bars are 10 mm.

visualized for each slice in the *X*, *Y*, and *Z* planes (Fig. 2). The presence of subsurface cracks and their locations were noted, and screen captures were obtained. For a subset of slices where cracks were present, the digital line tool within the software was used to measure the minimum and maximum crack widths, as well as distance from the articular or back-side surface. In one case, an advanced region of interest (ROI) tool was used to manually segment one of the cracks. Isosurface rendering was performed to create a 3D volume of the crack, and of the insert surface. The two volumes were exported in VTK format and visualized with an open source visualization utility (ParaView, Kitware Inc.,

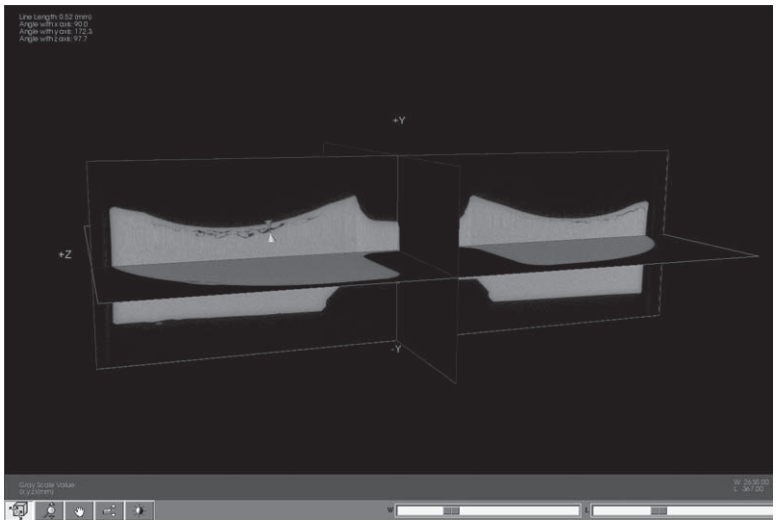

FIGURE 2. Dedicated analysis software allows 3D visualization and localization of the subsurface cracks, and measurements using a digital line tool.

Clifton Park, New York). The insert surface was set at half opacity, allowing the 3D crack volume to be visualized within the insert. The delaminated insert volumes were also imported into a volume graphics application (VGStudio Max Version 2.0, Volume Graphics GmbH, Heidelberg, Germany). A threshold was again selected with those values corresponding to the insert volume set as opaque and other values set as transparent. This created a full-thickness rendering of the insert that enhanced the visualization of the subsurface cracks.

III. RESULTS

Subsurface cracks were readily apparent in the 2D planar images of the delaminated inserts. The cracks predominantly ran horizontally, just below the articular surface of the inserts (Fig. 3). The cracks tended to expand from narrow openings to larger gaps, running at mostly the same depth just below the surface with some expansions to further down within the surface. Vertical cracks were also found at the center of one insert (Fig. 3B), at the lateral edge of the articular surface (Fig. 3D), and in the tibial post of the Genesis I. In one case, a horizontal crack was seen just below the back-side surface of the insert (Fig. 4). Unlike the cracks below the articular surface, there were no obvious surface changes that suggested the presence of the crack below the back-side surface (Fig. 4A). In some cases, small regions of greater X-ray attenuation (i.e., denser material) appeared at the outermost edges of the cracks (Fig. 5). The subsurface of the never-implanted inserts was uniform and devoid of cracks.

The location (measured as depth from surface) and width of the cracks were easily determined using the viewing software's linear measurement tool. For cracks beneath the articular surface, depths ranged from 0.12 to 6.01 mm, with crack widths ranging from 0.06 to 0.97 mm. The crack above the back-side surface was 0.23–0.44 mm in width and was 0.26–1.95 mm from the back-side surface. The 3D rendering of the cracks and insert surface assisted in visualizing and localizing the location and extent of the crack propagation (Fig. 6).

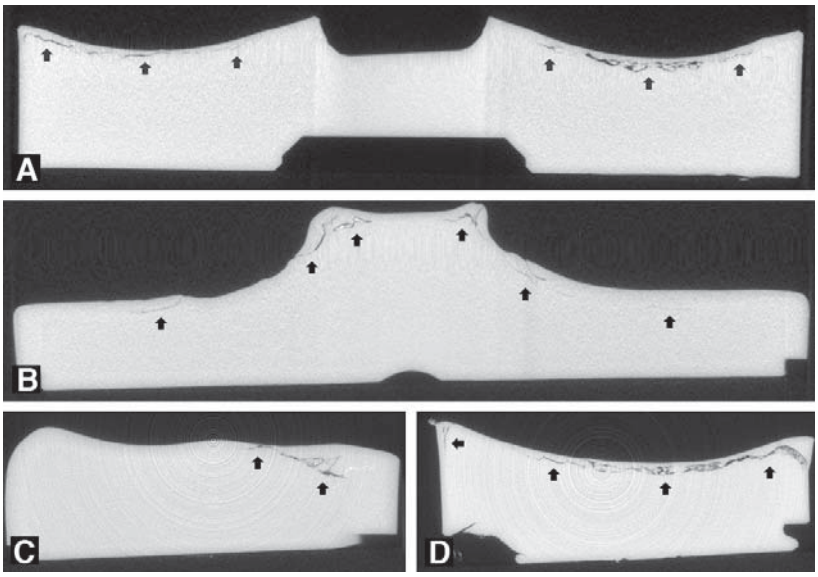

FIGURE 3. Two-dimensional planar views of the delaminated inserts with subsurface cracking (arrows): (A) Cracks are visible beneath both the left and right side of the articular surface; (B) Cracks are visible in the middle of the insert in addition to below the articular surface; (C) Side view demonstrating cracks below the articular surface of the insert; (D) Side view demonstrating cracking below the articular surface and at the lateral edge of the insert.

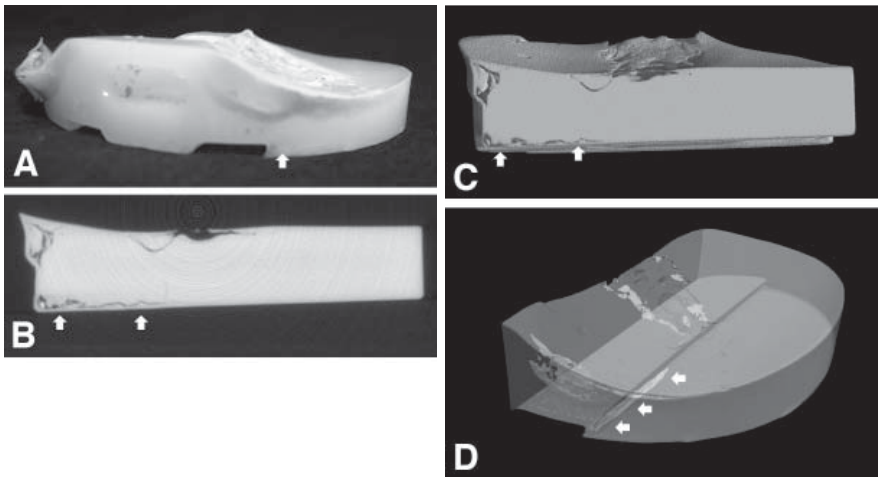

FIGURE 4. Image of a crack beneath the back-side surface of the retrieved insert (AMK): (A) Photograph of the insert, with an arrow denoting the approximate location of the slice visualized with micro-CT; (B) Two-dimensional planar image through the insert, demonstrating cracks below the back-side surface (arrows), articular surface, and rear of the insert; (C) Three-dimensional volume rendered image at approximately the same plane as (B), demonstrating the same cracks below the back-side surface (arrows), articular surface, and rear of the insert; (D) Cropped volume rendering of the insert surface (at half opacity) and the crack at the back-side surface (arrows), demonstrating the volume of the crack.

IV. DISCUSSION

Subsurface cracking was readily visualized in the 2D planar images and 3D rendering of the inserts obtained with micro-CT. The extent of this subsurface cracking was not apparent from examination of the insert surface, and therefore could not have been observed with stereomicroscopy or CMM. In one case, a crack below the back-side surface was found without any significant changes to the overlying surface. Interestingly, denser regions appeared at the edges of some of the cracks, signifying that the polyethylene was compressed at these locations. This could be a sign of the initial formation of the cracks, suggesting micro-CT might be able to track the propagation of the subsurface cracking over time. All of these observations were performed in a nondestructive fashion, which is a significant advantage over SEM, for which the specimen must be physically segmented.[4,10] The nondestructive nature

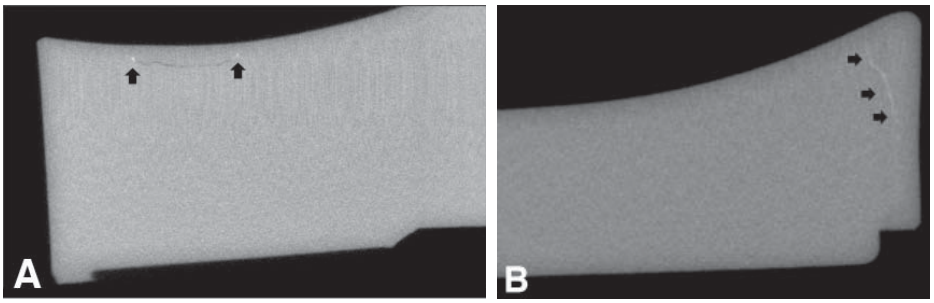

FIGURE 5. Regions with greater intensity (corresponding to a denser material) were found at the edges of some of the subsurface cracks (arrows): (A) Small regions of higher intensity at each end of a crack; (B) Larger region of high intensity running vertically.

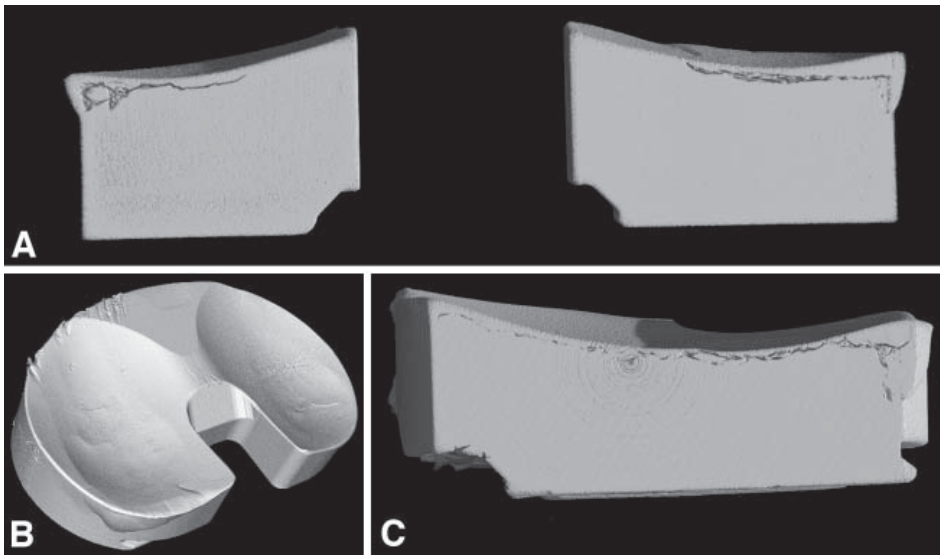

FIGURE 6. Three-dimensional renderings aid in the visualization of the insert surface and subsurface: (A) Subsurface cracks are visible medially and laterally in an anterior-posterior view of the insert; (B) Three-dimensional rendering of the insert surface; (C) Subsurface cracks are visible in a lateral view of the insert.

of micro-CT enables the examination of subsurface cracks across multiple time points in a pin-on-disk or wear simulator study. The ultrasonographic methods might have also visualized the cracks nondestructively, but at a much poorer resolution, and such methods would not enable additional analysis of the insert surface damage.[4,11] Quantification of surface deviations is possible with micro-CT, through surface rendering of the worn insert and comparison to an unworn reference.[12,13,16] Micro-CT also provides a much higher resolution than previously reported ultrasound techniques (50 μm versus 300 μm), allowing a clear and easily interpretable visualization of the subsurface cracks.

Beyond visualization of the subsurface cracks, the dimensions of the cracks and their depth from the insert surface were also quantified. Similar measurements are possible with SEM, but only after destructively segmenting the component.[4,10] In the study using a basic ultrasound technique, cracks were not quantified, but percent area covered by the cracks was measured in the study using SAT.[4,11] In contrast, linear measurements of the crack width and depth from surface were reported here. Both methods are valuable; however, we believe the ability of micro-CT to further measure surface deviations in addition to the subsurface cracking is a significant advantage. The time for examination using the micro-CT technique is also advantageous, requiring less than 30 min of actual user intervention per insert when measuring both subsurface cracking and 3D surface deviation. The majority of the examination is automated, including the CT scanning, image reconstruction, geometry coregistration, and calculation of the surface deviations. These automated processes currently require approximately 2–3 h, but are limited only by computational power. Therefore, as the hardware technology improves, less time will be required to conduct the technique.

As a preliminary study of the feasibility of visualizing and quantifying subsurface cracking with micro-CT, this work is associated with some limitations. First, only a few inserts were examined, with fairly obvious and extensive delamination. We believe this sample is appropriate for a development study; only a single retrieved insert was used in testing the use of ultrasound for studying

subsurface cracking.[11] Second, the measurements of the subsurface cracks within the inserts were not compared to another technique such as SEM. While this would have helped validate the measurements of the cracks, ensuring the same cracks are measured in both techniques is challenging, and results in destruction of the insert.[4] Finally, the retrieved inserts that were examined can be classified as historical polyethylene, and are known to be more susceptible to delamination and subsurface cracking than newer inserts manufactured with modern sterilization techniques.[21] Such inserts were specifically chosen because subsurface cracks were more likely to be present, facilitating the development of the technique.

In summary, micro-CT was successfully used to nondestructively visualize and quantify subsurface cracks due to fatigue wear and delamination in retrieved tibial inserts. Since micro-CT is nondestructive, additional tests may be performed on the components after scanning, or it allows the components to be scanned at multiple time points during a pin-on-disk or wear simulator study. Other wear measurement techniques cannot directly visualize the cracks, or are destructive, or do not also quantify surface deviation in addition to the subsurface cracking. Micro-CT is suitable for evaluating all types of polyethylene used in joint replacement, including hip, knee, and spinal arthroplasty.[12–16] This new use for micro-CT expands the completeness of the technique, enabling quantification of both surface and subsurface damage in all types of polyethylene-based arthroplasty components from in vitro and ex vivo sources.[12,13,16]

ACKNOWLEDGMENTS

The authors thank Kory Charron and Daniel Lorusso for their assistance. This study was funded by a grant from the Canadian Institutes of Health Research (No. MOP-89852). MGT received support from a Frederick Banting and Charles Best Canada Graduate Scholarship from the Canadian Institutes of Health Research and is supported in part by the Joint Motion Program—A CIHR Training Program in Musculoskeletal Health Research and Leadership. DWH holds the Dr. Sandy Kirkley Chair for Musculoskeletal Research at the Schulich School of Medicine and Dentistry. The department in which DDN is affiliated received institutional research support from Smith & Nephew and Zimmer.

REFERENCES

1. McKellop HA. The lexicon of polyethylene wear in artificial joints. Biomaterials. 2007 Dec;28(34):5049–57.
2. McGloughlin TM, Kavanagh AG. Wear of ultra-high molecular weight polyethylene (UHMWPE) in total knee prostheses: a review of key influences. Proc Inst Mech Eng H. 2000;214(4):349–59.
3. Fisher J, Jennings LM, Galvin AL, Jin ZM, Stone MH, Ingham E. 2009 Knee Society Presidential Guest Lecture: Polyethylene wear in total knees. Clin Orthop Relat Res. 2010 Jan;468(1):12–8.
4. Todo S, Tomita N, Kitakura T, Yamano Y. Effect of sliding locus on subsurface crack formation in ultra-high-molecular-weight polyethylene knee component. Biomed Mater Eng. 1999;9(1):13–20.
5. Popoola OO, Yao JQ, Johnson TS, Blanchard CR. Wear, delamination, and fatigue resistance of melt-annealed highly crosslinked UHMWPE cruciate-retaining knee inserts under activities of daily living. J Orthop Res. 2010 Sep;28(9):1120–6.
6. Rodriguez JA. Cross-linked polyethylene in total knee arthroplasty: in opposition. J Arthroplasty. 2008 Oct;23(7 Suppl):31–4.
7. Willie BM, Foot LJ, Prall MW, Bloebaum RD. Surface damage analysis of retrieved highly crosslinked polyethylene tibial components after short-term implantation. J Biomed Mater Res B. 2008 Apr;85(1):114–24.
8. Puloski SK, McCalden RW, MacDonald SJ, Rorabeck CH, Bourne RB. Tibial post wear in posterior stabilized total knee arthroplasty. An unrecognized source of polyethylene debris. J Bone Joint Surg Am. 2001;83-A(3):390–7.
9. Wannomae KK, Christensen SD, Micheli BR, Rowell SL, Schroeder DW, Muratoglu OK.

Delamination and adhesive wear behavior of alpha-tocopherol-stabilized irradiated ultra-high-molecular-weight polyethylene. J Arthroplasty. 2010 Jun;25(4):635–43.
10. Oral E, Christensen SD, Malhi AS, Wannomae KK, Muratoglu OK. Wear resistance and mechanical properties of highly cross-linked, ultrahigh-molecular weight polyethylene doped with vitamin E. J Arthroplasty. 2006 Jun;21(4):580–91.
11. Ong CS, Saffari N. Ultrasonic evaluation of ultra-high molecular weight polyethylene used in medical prostheses. Proc Inst Mech Eng H. 1998;212(1):65–9.
12. Teeter MG, Naudie DDR, Charron KD, Holdsworth DW. Three-dimensional surface deviation maps for analysis of retrieved polyethylene acetabular liners using micro-computed tomography. J Arthroplasty. 2010;25(2):330–2.
13. Teeter MG, Naudie DDR, Milner JS, Holdsworth DW. Determination of reference geometry for polyethylene tibial insert wear analysis. J Arthroplasty. 2010. In press.
14. Vicars R, Fisher J, Hall RM. The accuracy and precision of a micro computer tomography volumetric measurement technique for the analysis of in-vitro tested total disc replacements. Proc Inst Mech Eng H. 2009 Apr;223(3):383–8.
15. Bowden AE, Kurtz SM, Edidin AA. Validation of a micro-CT technique for measuring volumetric wear in retrieved acetabular liners. J Biomed Mater Res B. 2005 Oct;75(1):205–9.
16. Teeter MG, Naudie DD, McErlain DD, Brandt JM, Yuan X, MacDonald SJ, Holdsworth DW. In vitro quantification of wear in tibial inserts using microcomputed tomography. Clin Orthop Rel Res. 2011 Jan;469(1):107–12.
17. Badea CT, Drangova M, Holdsworth DW, Johnson GA. In vivo small-animal imaging using micro-CT and digital subtraction angiography. Phys Med Biol. 2008;53(19):R319–50.
18. Blunt L, Bills P, Jiang X, Chakrabarty G. Improvement in the assessment of wear of total knee replacements using coordinate-measuring machine techniques. Proc Inst Mech Eng H. 2008 Apr 7;222(3):309–18.
19. Muratoglu OK, Perinchief RS, Bragdon CR, O'Connor DO, Konrad R, Harris WH. Metrology to quantify wear and creep of polyethylene tibial knee inserts. Clin Orthop Relat Res. 2003 May'(410):155–64.
20. Kohm A, Gaumer J, Ravula V, Urban R, Gilbertson L, Bos G, Nelson L, Dyce J, Lannutti J., Three-dimensional laser micrometry characterization of surface wear in total hip arthroplasty. J Biomed Mater Res B. 2007 Aug;82(2):428–39.
21. Azzam MG, Roy ME, Whiteside LA. Second-generation locking mechanisms and ethylene oxide sterilization reduce tibial insert backside damage in total knee arthroplasty. J Arthroplasty. In press.

Journal of Long-Term Effects of Medical Implants, 20(1): 35–42 (2010)

Effects of Hydroxyapatite on Titanium Foam as a Bone Ingrowth Surface in Acetabular Shells: A Canine Study

William M. Mihalko,[1,] Craig Howard,[2] Fred Dimaano,[3] Nena Dimaano,[3] & Monica Hawkins[3]*

[1]University of Tennessee, Campbell Clinic Orthopaedics, InMotion Orthopaedic Research Center, Memphis, TN;
[2]State University of New York at Buffalo, Orthopaedic Research Laboratory, Buffalo, NY;
[3]Stryker Orthopaedics, Inc., Mahwah, NJ

*Address all correspondence to William M. Mihalko, MD PhD, Associate Professor, University of Tennessee, Campbell Clinic Orthopaedics, 1458 West Poplar Avenue, Suite 100, Memphis, TN 38017; wmihalko@campbellclinic.com.

ABSTRACT: This study investigated a highly porous titanium foam with and without a PeriApetite coating as an alternative surface for implant fixation. Twelve mongrel canines received staged total hip replacements under International Animal Care and Use Committee (IACUC) approval from our institution. Animals were randomly placed in three- or six-month groups for sacrifice. Seventeen total hips were available for evaluation. The area and depth of ingrowth was measured by SEM. At three months, PeriApetite Ti foam had 30% more depth and almost 10% more bone ingrowth. Both groups were found not to be different at the six-month mark with over 36% of ingrowth calculated on SEM. The results prove not only that titanium foam is a viable ingrowth surface but also that PA coating can enhance the time to bony incorporation.

KEY WORDS: acetabular shell, titanium foam, hydroxyapetite, bone ingrowth

I. INTRODUCTION

The ingrowth of bone as an interface for acetabular component fixation has been utilized for over a decade. The ingrowth or ongrowth surface addition to the acetabular component was devised as a solution to aseptic loosening rates with cemented all-polyethylene acetabular implants. Many different surfaces have been investigated and reported on including titanium fiber mesh and sintered cobalt chrome and titanium beads, as well as higher-porosity tantalum metal.[1–5] Many different implants have shown 5- to 10-year documented good results and survivorship of >95%.[5–11]

New ingrowth surfaces that are closer to the porosity of the surrounding cancellous bone have been investigated in the past and are now being utilized. Tantulum high-porosity metal has been reported to have good bone depth and reliable area of fixation.[2,4,5] The advent of higher-porosity metals that closely match that of cancellous bone may give multiple advantages over the previous beaded or fiber mesh surfaces. These include a higher density of bone ingrowth per unit volume due to the higher porosity and therefore possibly a higher mechanical interlock strength of the interface.[4]

Titanium has been shown to have a high affinity for bony ingrowth and has been utilized for orthopaedic and dental reconstructive implants due to this attribute for bone ingrowth.[12–14] There have been reports of a high-porosity titanium surface for ingrowth in an unloaded canine model, but no reports of its use or success with a functional implant have been reported to date.[15]

The use of titanium for a high-porosity ingrowth surface on an acetabular shell was attempted in a canine model in this study. A Titanium 3D ingrowth surface [Tritanium (Ti)] was investigated to determine the potential for ingrowth with and without a PeriApetite (PA) hydroxyapatite coating (Stryker, Mahwah, New Jersey). As with any press-fit implant, initial stability and time to bony ingrowth is essential to the success of a cementless implant. It was hypothesized that the PA coating would significantly increase the bony ingrowth and decrease the time necessary for ingrowth into the surface. Finally, comparison of previously reported canine acetabular implants will be utilized for comparison of the results.

II. METHODS

Twelve mongrel canines underwent bilateral total hip arthroplasty with a macrotextured femoral component (Stryker Orthopaedics, Inc, Mahwah, New Jersey) and a titanium foam porous surface 30 mm acetabular shell (Tritanium, Stryker Orthopaedics, Inc, Mahwah, New Jersey.). The acetabular shells consisted of a 1.5 mm thick highly porous titanium foam coating with porosity of 75–80%. The porous Ti foam coating was attached to a titanium alloy shell during the manufacturing process. The acetabular shells were randomized to uncoated foam (Ti) or with a hydroxyapatite coating (Ti-PA) applied to the Ti foam surface in a 3D manner with a 20 μm thick coating applied via a solution deposit technique. The study was approved by our institution's animal review board prior to the start of the study. The direct lateral cranial caudal approach was utilized for each operation. The acetabulum was incrementally reamed at 1 mm intervals to 29 mm. If inadequate press was felt to exist, then two or three short stainless steel acetabular screws were inserted. If it was felt there was adequate press fit, fewer screws were utilized at the discretion of the surgeon. Each hip was trialed and tested for stability prior to closure. If significant overreaming of the acetabulum and loss of the posterior and or anterior wall resulted to get to the proper reamed sized for each implant (28–29 mm), then this was documented and the positioning of the implant optimized for the best coverage. Repair of the capsule was not undertaken due to increased offset afforded by the press-fit femoral component, but repair of the musculature from the greater trochanter was undertaken. Surgical staples were utilized for all skin closures. Each canine was treated with the same postoperative protocol with a pain management regimen, intravenous antibiotic prophylaxis, and weight bearing as tolerated. The animals were taken out of their cages each day for exercise by the vivarium staff for 1 h.

Canines were sacrificed at three and six months. The surrounding bone was harvested to include the entire acetabulum, which was removed of all tissue in a subperiosteal fashion (Fig. 1) and placed in a 10% formalin neutral solution. Exclusion criteria for the postoperative canines were set as dislocation and overreaming of the acetabulum with loss of wall support. Evidence of infection was also set as an exclusion criterion as well.

II.A. Imaging

Radiographs were taken preoperatively, postoperatively, and at siv-week intervals for assessment (Fig. 2). Any noted radiolucencies were then recorded for each canine.

Anterior-posterior and lateral radiographs were also taken of specimens after harvesting to properly orient them anatomically for sectioning. Microradiography of each slide confirmed that the histological section was in the coronal plane, including the ileum part of the acetalulum, which is the weight-bearing region of the canine acetabulum (Fig. 3). The contact radiographs were used to pinpoint the region for scanning electron micrography of the ileum region of the acetabulum.

II.B. Tissue/Slide Preparation

After each canine was sacrificed, the acetabular cup and surrounding bone was retrieved and fixed in 10% neutral formalin. Radiographs were used for the orientation of trimming and sectioning.

Soft tissue was stripped and excessive bone was trimmed off. All the specimens were processed for undecalcified thin-section histology. In brief, the specimens were dehydrated in a graded series of alcohol, cleared in xylene, and embedded in methyl methacrylate. The acetabular components were sectioned in the coronal plane near the middle of the ileum regardless of the location of the implant using the Exakt diamond saw. The sections were ground to 250–350 μm and polished. Contact radiographs and backscattered scanning electron microradiographs (SEMs) were taken for each slide.

Seven images of SEM were taken sequentially to cover the whole coating of the implant across the entire area of the ileum. The area of interest was identified using the stage track mode of the SEM. Each image was taken at 20× using backscatter detector, an acceleration of 10 kV, and a spot size of 5.

Quantitative analysis was conducted on the images of SEM with the Image Pro Plus program. The histomorphometric evaluation of bone growth within the implant was done on the ileum part for each section of the acetabular components. Seven images of SEM along the circumference of the cup covered the whole coating of the implant across the entire area of the ileum. The whole area of the foam coating, the area of metal, and the area of the bone were measured. The extent of bone ingrowth was calculated by dividing the bone area by the whole area minus the metal. The depth of bone ingrowth was determined as the percentage of the length of a line from the top of the coating to the deepest point of bone toward the substrate of the shell.

II.C. Percentage of Bone Ingrowth

The distance between the substrate to the highest peak of the coating was measured and the irregular area of interest (AOI) was defined. The AOI Al, consisting of bone, metal, and pores, is the area bounded by the coating substrate interface and the highest peak of coating in that section. Areas consisting of metal coating (A2) and bone (A3) were also quantified. The percentage of bone ingrowth was then calculated using the following formula: Percent Bone Ingrowth = A3 I (A1 – A2) × 100.

II.D. Depth of Bone Ingrowth

The deepest point of bone ingrowth in each image was identified as shown in Figure 4 and measured. The depth of bone ingrowth was calculated using the following formula: Percent Bone Depth = (Bone depth/Coating thickness at the highest point in the image) × 100.

Two-factor two-way analyses of variance were performed on the depth of bone ingrowth and percent bone ingrowth with time (three and six months) and surface (with or without PA coating) as variables. When statistical differences were identified, Tukey post hoc multiple pairwise comparisons were performed. Statistical significance was assumed at $p < 0.05$.

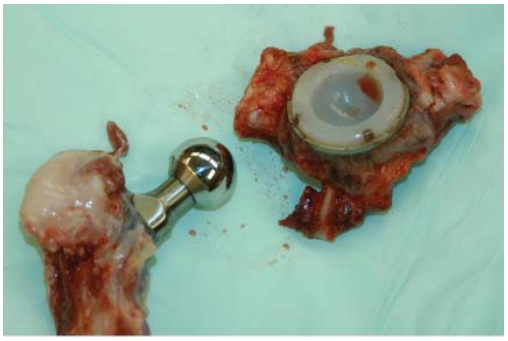

FIGURE 1. Gross anatomical resection of the acetabulum before preparation for SEM analysis.

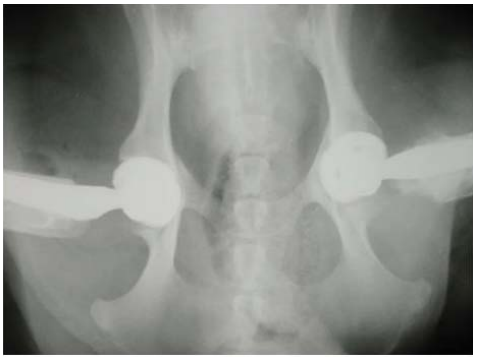

FIGURE 2. Radiograph of a canine at 4.5 months after right THR and six weeks after Left THR.

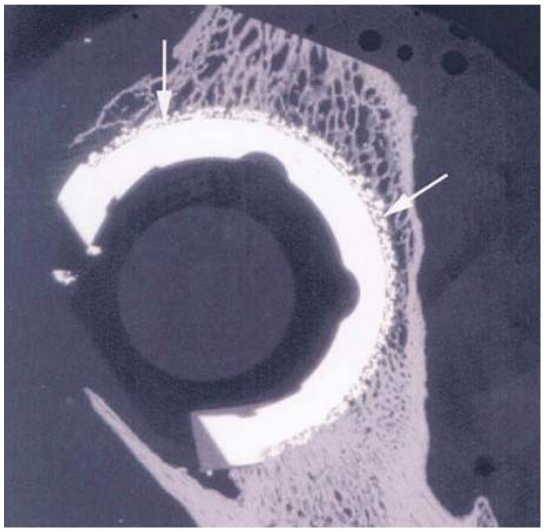

FIGURE 3. Microradiograph of acetabular section with arrows showing area along ileum analyzed for depth and percent ingrowth.

III. RESULTS

Seventeen total hips from 10 mongrel canines were included in this study after exclusion of four animals for chronic dislocation, due to implant and anatomy mismatch, and one for an infection. The size mismatch was a problem due to availability of only one size of acetabular shell (30 mm), and if significant overreaming was necessary with loss of either wall of the acetabulum, the animal was excluded from the study. Two chronic dislocations were found at six weeks due to the animals bearing weight with minimal limp. Two other dislocations occurred within the first two weeks and reduction or reoperation failed.

III.A. Radiographic Analysis

The postoperative radiographs at six weeks and three or six months for the 17 hips included in the study showed no obviouos radiolucencies. The canines that were excluded from the study showed small radiolucencies at the weight-bearing aspect and complete areas of radiolucencies for the one presumed infected case.

III.B. Histomorphometric Analysis

The depth of the bone ingrowth varied among specimens for the obtained images. At three months, bone depth was calculated with Ti-PA having 94%

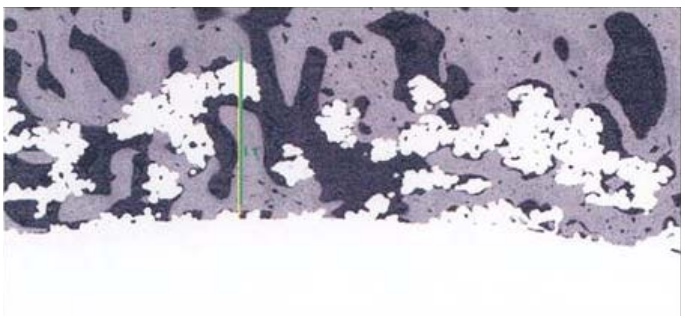

FIGURE 4. SEM showing a bone depth of 100%.

± 10.36% bone depth compared to 63.12% ± 25.6% for Ti alone. This was not statistically significant however (p = 0.081). At three months, three out of six Ti-PA specimens had 100% bone depth compared to three out of four at six months for the native Ti foam surface. At six months, the two native Ti foam specimens were nearly identical for bone depth compared to the Ti -PA group (96.42% compared to 97.31%) (Table 1).

The percentage of bony ingrowth measured at three months for the Ti foam group was calculated at 17.95% ± 9.54%. The Ti-PA group was calculated at 26.54% ± 8.06% at three months, which was not statistically significant (p = 0.28). At six months, the Ti foam percent ingrowth was calculated at 36.14% ± 8.96%. Compared to the Ti-PA group, no difference was calculated with the percentage at 38.51% ± 10.59%. The only statistical measure found to be significant was the variable of time. When bone ingrowth was compared collectively between three and six months, the results were significant with a p value of 0.048.

No surface damage in any of the microradiographs was noted to the Ti foam surface. There was no evidence that the Ti foam coating/substrate interface was damaged from the force of impaction at time of insertion during the operative procedure.

It was evident that the overreamed specimens had a gap between the Ti foam surface and the cancellous bone of the ileum (Fig. 5). The fact that little contact was visualized in these cases maintains the necessity of their exclusion for extreme size mismatch of the acetabular shell and the anatomical limitations of the bony acetabulum for each canine.

IV. DISCUSSION

The titanium foam surface proved to allow ingrowth of trabecular bone, which was continuous with the surrounding acetabular bone. The depth of bone growth proved to be complete throughout the titanium foam to the solid portion of the acetabular shell. Ti foam as an ingrowth surface performed well in this study with a significant increase in percentage of bone ingrowth between three and six months. Ingrowth depth also proved to be complete in most specimens with improvements with time as well. The depth of ingrowth as well as percentage of ingrowth for the PA-coated Ti foam appeared to have an advantage compared to the uncoated at three months, and the native Ti foam surface seemed to catch up at the six-month interval. The study results show that the high-porosity Tritanium surface with a PA coating creates a surface that appears to have a faster rate of ingrowth. At three months, there is greater ingrowth into the PA-coated Ti foam; but by six months, the two groups are equivalent. It should also be noted that with higher-porosity Tritanium surfaces, there is quantitatively more bone to interlock the shell than with beaded surfaces. This is a design advantage of the high-porosity surface whether titanium or tantalum. With 60–70% of the surface containing empty space, it allows for a greater amount of bone to be interlocked with the interface compared to ingrowth surfaces of 30 or 40% porosity.

The canine total hip model has been utilized for investigative purposes in orthopaedic surgery for decades.[13–20] These studies have been paramount in the past to gain insight into the science of biologic fixation. Some of these have comparative significance to this study.

The percentage of ingrowth area compares favorably to other reported canine studies for other types of ingrowth acetabular surfaces. These studies for cobalt chrome beads and titanium fiber mesh have been reported by Jasty et al.[3] In their canine studies, the reported ingrowth was 21.5% ± 4.4% in titanium fiber mesh and 13.4% ± 9.9% for cobalt chrome beads. For comparison, at six months, in our study,, we had favorable results with 38% for Ti + PA, and 36.1% for Ti foam alone.

Bobyn et al.[2] reported the success of highly porous tantalum acetabular cups in 22 canine hips for a total of six months. They reported a 16.8% bony ingrowth for all sections that were analyzed and a 25.1% bony ingrowth in the peripheral sections of the acetabular shell where bony contact was most consistent They concluded that the porous tantalum provided a suitable alternative to

TABLE 1. Percent Bone Ingrowth and Percent Depth of Bone Penetration into the Porous Coating for Each of the Specimens Analyzed

Animal Number	Time In Vivo	Percent Bone Depth (%)	Percent Bone Ingrowth (%)
Three Months			
Ti Foam			
4 L	3 months, 22 days	24.94	4.01
6 L	3 months, 13 days	80.70	25.98
8 L	3 months, 12 days	84.92	23.40
3 L	3 months, 7 days	48.74	12.04
1 R	4 months	76.29	24.30
MEAN		63.12	17.95
STD		25.60	9.54
Ti Foam/PA			
5 L	3 months, 21 days	94.67	25.25
9 L	3 months, 7 days	100.00	40.13
11 L	3 months, 12 days	95.85	20.20
14 R	4 months, 11 days	73.39	19.09
7 L	months	100.00	31.85
13 L	3 months, 4 days	100.00	22.72
MEAN		93.99	26.54
STD		10.36	8.06
Six Months			
Ti Foam			
9 R	7 months, 11 days	100.00	42.47
11 R	7 months, 16 days	92.83	29.80
MEAN		96.42	36.14
STD		5.07	8.96
Ti Foam/PA			
4 R	6 months, 21 days	100.00	49.29
6 R	7 months, 4 days	100.00	45.88
8 R	6 months, 26 days	100.00	30.13
10 R	7 months, 11 days	89.24	28.74
MEAN		97.31	38.51
STD		5.38	10.59

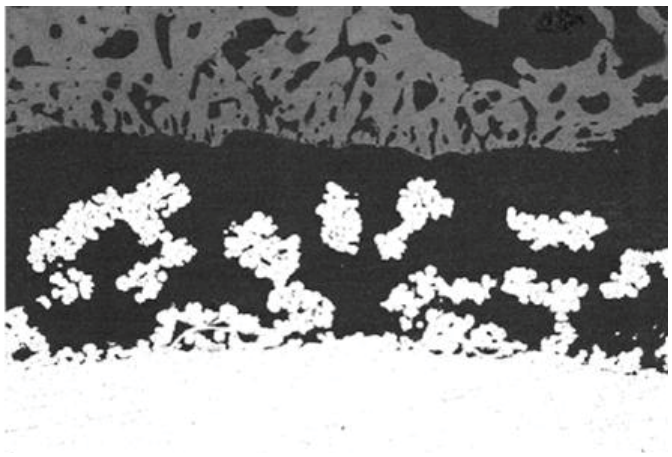

FIGURE 5. SEM of one of the overreamed specimens showing no contact of bone with the Ti foam coating.

other porous surfaces utilized for acetabular components. The acetabular ingrowth for our study compares favorably to these results, with 23% at three months and 38% at six months with Ti and PA coating. In our Ti foam group at six months, the average was 36.1%, which again compares favorably to the tantalum at six months as well (25.1% in the periphery).

Downfalls of our reported study include exclusion of chronic and failed dislocations, exclusion of overreamed acetabuli, and exclusion of one presumed infected hip at six weeks. These exclusions also limited the number of hips in the uncoated Ti foam group. With inclusion of the overreamed specimens, the percent bony ingrowth at six months from our study would still compare favorably with previously reported studies.

The conclusions of this canine study on the simplest levels tells us that trabecular bone was present inside the pores of the Ti foam both with and without PA coating, and was continuous with the surrounding acetabular bone. The study also proved that bone readily grew into the pores and throughout the depth of the Ti foam coating. The addition of the PA coating on the Ti foam resulted in faster bone ingrowth into the full depth of the porous surface. This was evident with an average percent bone ingrowth into the pores increasing significantly from 23% at three months to 38% at six months. The average depth of bone ingrowth into the porous coating was much greater for PA-coated Ti foam than for Ti foam alone. These differences were attributed entirely to the greater depth of ingrowth for PA-coated than uncoated at three months, and the increase between three and six months for the uncoated Ti foam. The new highly porous 1.5 mm Ti foam coating both with and without PA coating proved to create a viable biologic interface that has promise for an improved fixation method in total hip arthroplasty.

AKNOWLEDGMENTS

All funding for this project was provided by a research grant from Stryker Orthopaedics, Inc. William M. Mihalko, MD PhD was a consultant for Stryker Orthopaedics, Inc. and now for Aesculap, Inc.

REFERENCES

1. Bobyn JD, Pilliar RM, Cameron HU, Weatherly GC. The optimum pore size for the fixation of porous surfaced metal implants by the ingrowth of bone. Clin Orthop. 1980;150: 263-70.
2. Bobyn JD, Toh K, Hacking A, Tanzer M, Krygier JJ. Tissue response to porous tantalum acetabular cups, J Arthoplasty. 1999;14:3:347-354.

3. Jasty M, Bragdon CR, Haire T, Mulroy RD Jr, Harris WH. Comparison of bone ingrowth into cobalt chrome and titanium fibre mesh porous coated cementless canine acetabular components, J Biomed Mater Res, 1993;27:639-.
4. Komarasamy B, Vadivelu R, Bruce A, Kershaw C, Davison J. Clinical and radiological outcome following total hip arthroplasty with an uncemented trabecular metal monoblock acetabular cup. Acta Orthop Belg. 2006 Jun;72(3):320-5.
5. Macheras GA, Papagelopoulos PJ, Kateros K, Kostakos AT, Baltas D, Karachalios TS. Radiological evaluation of the metal-bone interface of a porous tantalum monoblock acetabular component. J Bone Joint Surg Br. 2006 Mar;88(3):304-9.
6. Engh CA, Hooten JP Jr, Zettl-Schaffer KF, Ghaffarpour M, McGovern TF, Macalino GE, Zicat BA. Porous coated total hip replacement. Clin Orthop , 1994, 298:89-96.
7. Sumner DR, Jasty M, Jacobs JJ, Urban RM, Bragdon CR, Harris WH, Galante JO: Histology of porous-coated acetabular components. 25 cementless cups retrieved after arthroplasty. Acta Orthop Scand. 1993 Dec:64(6):619-26.
8. Goldberg VM, Ninomiya J, Kelly G, Kraay M. Hybrid total hip arthroplasty: a 7- to 11-year followup. Clin Orthop. 1996, 333:147-54.
9. Schmalzried TP, Harris WH. Hybrid total hip replacement: a 6.5 year follow-up study. J Bone Joint Surg Br. 1993, 75:608-15.
10. Cook SD, Barrack RL, Thomas KA, Haddad RJ. Quantitative analysis of tissue growth into human porous total hip components. J Arthroplas. 1988;3:249-62.
11. Engh CA, Zettl-Schaffer KF, Kukita YSweet D, Jasty M, Bragdon C. Histological and radiographic assessment of well functioning porous-coated acetabular components: a human postmortem retrieval study. J Bone Joint Surg Am. 1993, 75:814-24.
12. Bragdon CR, Jasty M, Greene M, Rubash HE, Harris WH. Biologic fixation of total hip implants. insights gained from a series of canine studies. J Bone Joint Surg Am. 2004;86-A Suppl (2):105-17.
13. Munting E. Ingrowth and formation of bone in defects in an uncemented fiber-metal total hip-replacement model in dogs. J Bone Joint Surg Am. 1991 Dec;73(10):1576-7.
14. Kang JD, McKernan DJ, Kruger M, Mutschler T, Thompson WH, Rubash HE. Ingrowth and formation of bone in defects in an uncemented fiber-metal total hip-replacement model in dogs. J Bone Joint Surg Am. 1991 Jan;73(1): 93-105.
15. Frenkel SR, Jaffe WL, Dimaano F, Iesaka K, Hua T. Bone response to a novel highly porous surface in a canine implantable chamber. J Biomed Mater Res B. 2004 Nov 15;71(2): 387-91.
16. Al Hertani W, Waddell JP, Anderson GI. The effect of partial vs. full hydroxyapatite coating on periprosthetic bone quality around the canine madreporic femoral stem. J Biomed Mater Res. 2000 Sep;53(5):518-24.
17. Christie MJ. Clinical applications of trabecular metal. Am J Orthop. 2002 Apr;31(4):219-20. Review.
18. Ido K, Matsuda Y, Yamamuro T, Okumura H, Oka M, Takagi H. Cementless total hip replacement: bio-active glass ceramic coating studied in dogs. Acta Orthop Scand. 1993 Dec;64(6):607-12.
19. Munting E. Ingrowth and formation of bone in defects in an uncemented fiber-metal total hip-replacement model in dogs. J Bone Joint Surg Am. 1991 Dec;73(10):1576-7.
20. Kang JD, McKernan DJ, Kruger M, Mutschler T, Thompson WH, Rubash HE. Ingrowth and formation of bone in defects in an uncemented fiber-metal total hip-replacement model in dogs. J Bone Joint Surg Am. 1991 Jan;73(1): 93–105.

Journal of Long-Term Effects of Medical Implants, 20(1): 43–48 (2010)

Evidence That In Vivo Wear Damage Alters Kinematics and Contact Stresses in a Total Knee Replacement

John L. Williams,[1,2] David A. Knox,[2] Matthew G. Teeter,[3] David W. Holdsworth,[3] & William M. Mihalko[1,2,]*

[1]University of Tennessee, Memphis, TN; [2]University of Memphis, Memphis, TN; [3]University of Western Ontario, London, ON, Canada

*Address all correspondence to William M. Mihalko, MD PhD, 1458 W. Poplar Avenue, Suite 100, Memphis, TN 38017; Tel.: 901-759-5512; Fax: 901-759-5571; wmihalko@campbellclinic.com.

ABSTRACT: Polyethylene wear after a total knee arthroplasty is inevitable. The effects of the wear particles on the surrounding soft tissue causing inflammatory responses and eventual aseptic loosening are well documented, but the biomechanical changes from polyethylene wear have been less understood. This study investigated how wear from a retrieved polyethylene insert from a total knee arthroplasty changed the kinematics and contact stresses. A cruciate-retaining total knee implant (Natural-Knee, Intermedics Orthopedics, Inc., Austin, Texas) was retrieved from a donor program. The polyethylene insert was then scanned and modeled. KneeSIM (LifeMOD/KneeSIM, San Clemente, California) was used to simulate one cycle of gait of three second duration (100% of cycle). A threefold increase in contact stress as well as resulting kinematic changes were seen when the model was used to compare the retrieved versus a modeled off-the-shelf new polyethylene insert. Total knee designs should take into account the wear patterns that result from years of use and how they may affect the biomechanics of the knee long term.

KEY WORDS: knee, arthroplasty, wear, retrieval, biomechanics

I. INTRODUCTION

Retrieval analysis studies in orthopaedic surgery have mostly focused on tribology and mechanical fixation.[1–3] Little has been done to analyze how the effect of wear in a total knee replacement impacts the functional aspects of the joint. Today, with health care dollars being highly scrutinized, the more knowledge we have pertaining to functional outcome basis and effects of wear on those functional parameters, the more we will be able to address long-term concerns on a material and design basis.

Flouroscopic kinematic analysis studies have now been utilized to predict how a total knee replacement is functioning in situ. These studies, however, are often variable within the same design of an implant,[4–7] which makes it difficult in current analyses to determine the effects of wear on a certain design of an implant. If certain designs of current total knee arthroplasties (TKAs) exist that are more susceptible to wear once the process occurs, then knowing the parameters that can be avoided at the design phase would be an extremely beneficial tool.

Wear simulators often do not correlate to true in vivo conditions,[8–10] nor do they account for clinical and surgical variations that can have a significant effect on the resulting kinematics and function of the joint. Although ISO and ASTM standards exist for wear analysis studies of medical devices, the effects on the mechanics and biomechanics of the joint are not the aim of these standards.

1050-6934/10 $35.00

The polyethylene bearing on the tibial side of a total knee replacement (TKR) is subjected to large forces from the metal femoral component while allowing the required motions of rolling, gliding, and rotation. Over time, the polyethylene bearing surface topography is expected to undergo change due to creep and wear. These effects are often not accounted for during the design, development, or testing phases of an implant. If the change in kinematics and contact stresses once a TKA started a certain in vivo wear pattern allowed for a detrimental cycle to start, then knowing this ahead of time could allow engineers to avoid a potentially catastrophic situation for both the patient and the design of the implant.

We hypothesized that changes in surface topography would alter joint kinematics and contact stresses. This study sought to investigate tibiofemoral kinematics and patterns of motion of contact stresses at the tibiofemoral bearing using a virtual simulation of gait of a retrieved TKR for comparison to the same parameters for simulations of an unworn TKR.

II. METHODS

A cruciate-retaining total knee implant (Natural-Knee, Intermedics Orthopedics, Inc., Austin, Texas) was retrieved from the right knee of a deceased 86-year-old, 91 kg, male subject with institutional review board approval. The retrieval was part of a program established at the Medical Education and Research Institute (MERI) in Memphis, Tennessee. All retrieval protocols were performed under current ASTM standards. For this report, a polyethylene highly congruent tibial insert was retrieved along with a Ti base plate, a CoCr femoral component, and an all-polyethylene (three-peg design) patellar component through a midline incision. The posterior cruciate ligament (PCL) was intact and appeared to be functioning since it resisted a posterior drawer. All components were cemented and well fixed. The knee was in a tibiofemoral angle of 7 deg of varus. Utilizing fluoroscopic imaging, the Q-angle was determined to be 13 deg as measured by a radiopaque goniometer. The range of motion was measured and was below average at 5–78 deg of flexion. A new tibial insert (Zimmer Natural-Knee System Congruent Tibial Insert, Zimmer, Inc., Warsaw, Indiana) of the same size and type was also obtained. All components were scanned by white light and reverse engineered to generate parasolid models. Both tibial inserts were also scanned by micro-CT with 50 μm resolution, at an X-ray tube voltage of 90 kV and current of 40 mA. Twelve hundred views were taken, with 10 frames averaged per view, each using an exposure of 16 ms. Isosurface rendering of the resulting micro-CT images was performed to generate STL files. The worn and new tibial insert geometries were coregistered and the deviations between the two were measured in a previously described fashion.[11]

KneeSIM (LifeMOD/KneeSIM, San Clemente, California) was used to simulate one cycle of gait of 3 s duration (100% of cycle) including 0.3 s of equilibrium (10% of cycle) for the new and worn tibial insert components. The components were positioned in the model of the knee in the orientation determined from whole leg CT scans and fluoroscopy images. The KneeSIM simulations included the patellofemoral and tibiofemoral joints, the quadriceps extensor mechanism and hamstrings muscle, PCL, MCL, LCL, and joint capsule. Kinematics of the knee was analyzed using similar measures employed in fluoroscopy studies, i.e., by tracking the antero-posterior motion of the computed lowest condylar positions, closest to the tibial base plate.

III. RESULTS

The retrieved tibial insert had significant delamination in the medial compartment and pitting in the postero-lateral margin. The surrounding areas had notable thinning as seen from micro-CT analysis (Fig. 1).

Differences were noted in the predicted fluoro-style kinematics (Fig. 2) of the TKRs with worn versus new tibial insert geometries and in the internal-external rotations (Fig. 3). Peak contact stresses in the medial and lateral plateaus increased

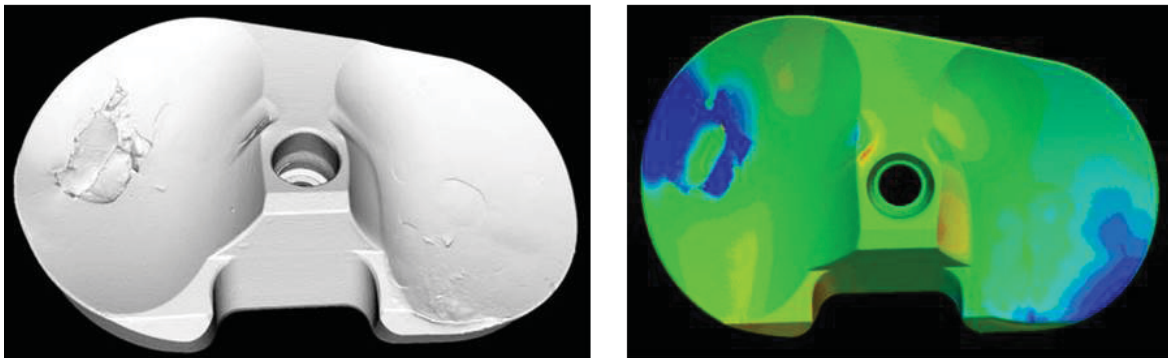

FIGURE 1. Surface damage (left) of retrieved tibial insert and contour plot (right) showing elevation deviations between the worn and new inserts with cool colors indicating lower and warm colors higher elevation than the new insert (blue = −0.75 mm, red = +0.75mm).

threefold after wear (Fig. 4), while the intercondylar eminence stress decreased. Most of the severe pitting and delamination damage occurred in a region where the model predicted peak contact stress and cross-shear motion (Fig. 5). Peak stresses occurred mostly during heel strike and the stance phase on the medial plateau, while the lateral side experienced peak stresses during the latter part of the swing phase. The greatest excursion of the center of pressure points occurred at the end of the swing phase (80–100% of the total cycle).

IV. DISCUSSION

Many orthopaedic implants have shown demise earlier than expected.[12–15] Although many of these performed well in the laboratory, they proved to be bad solutions in vivo. This study has shown another consequence of wear in a total knee replacement implant that has not been previously described. The modeling analysis has shown that as wear increases in the polyethylene insert, there are large increases in the contact stress and measureable changes in the

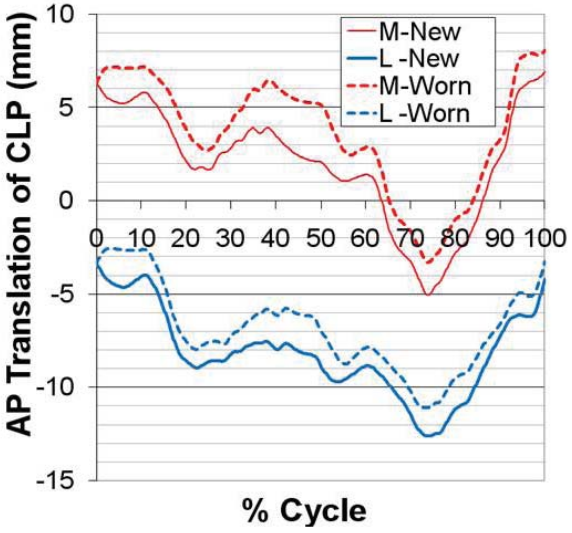

FIGURE 2. Antero-posterior (+ANT) motion of the condylar low points (CLPs) relative to dwell positions.

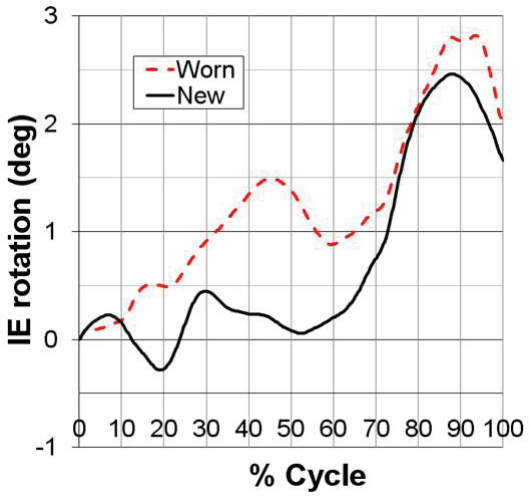

FIGURE 3. Internal-external (+INT) rotation of the tibia relative to the femur.

kinematics of the joint. These issues should be taken into consideration when designing total knee implants in order to minimize these long-term effects.

Tractive forces during rolling occur during the stance phase of gait and may be associated with the phenomenon of cross-shear wear, which appears to occur around midstance (Fig. 5). In this study, observed damage to the intercondylar eminence was predicted by simulation to occur between 30 and 50 % of the gait cycle, and appeared to limit internal rotation of the tibia and force it into external rotation. IE rotational differences before and after wear were most notable between heel strike and swing phase with a reversal of direction following heel

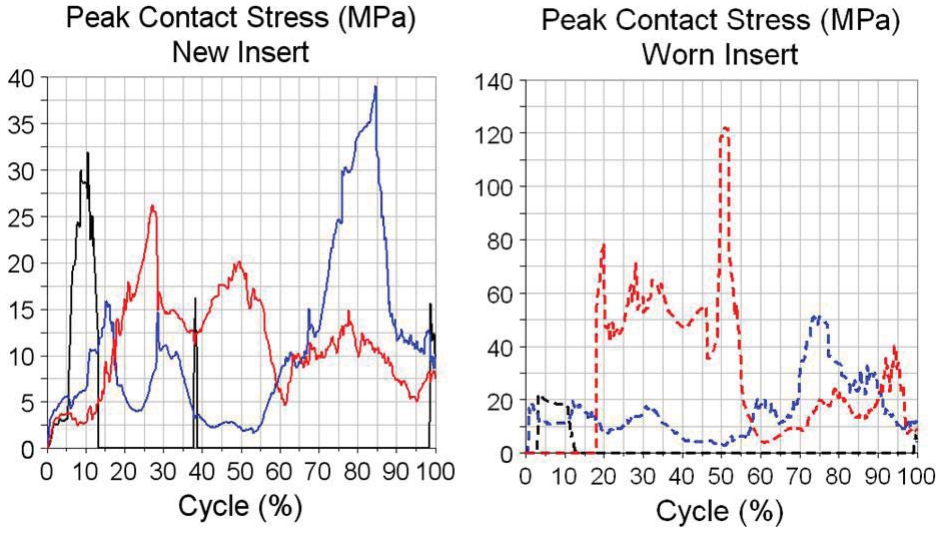

FIGURE 4. Peak medial (red) and lateral (blue) contact stresses after wear (right) were three times larger than for a new insert (left), but lower on the intercondylar eminence (black) after notching of the eminence.

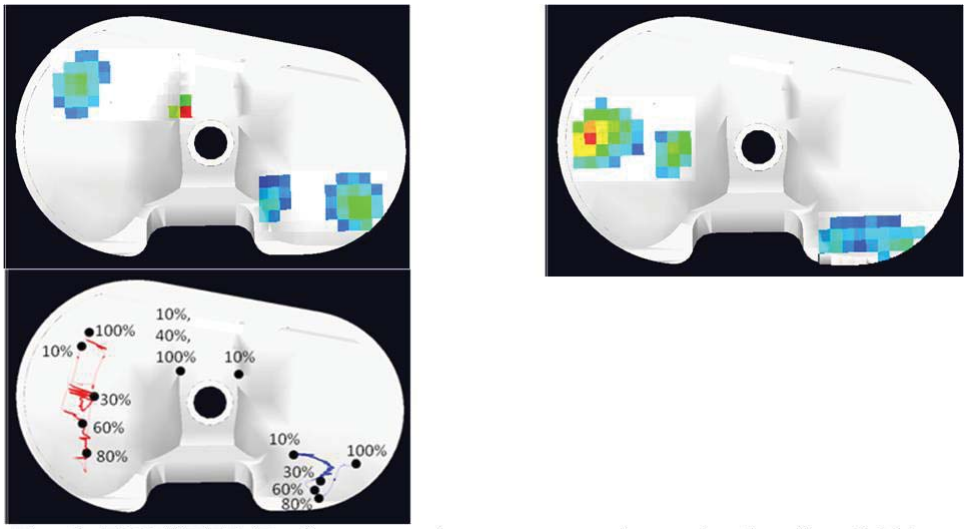

FIGURE 5. Top left: Peak stresses in contact patches at heel strike (10% total cycle) and at midstance (30% total cycle, top right). Red: high stress; blue: low stress. Left: Centers of contact pressure traced on the medial (red) and lateral (blue) plateaus for a new tibial insert. Black dots indicate centers of pressure as percent of gait cycle.

strike into early stance.[16] Anterior fluoro-style relative motion of the femur on the tibia was predicted to increase by as much as 2.5 mm after wear.

Retrieval analysis of a functioning TKR can offer significant insight into current implant designs, even when these designs have not yet seen overt clinical failures that result in revision surgery. As much as the argument is made for the need in the United States for a hip and knee registry to follow the survivorship of all implant designs, the need for retrieval analysis of both failed and well-functioning implants is a necessity that can allow progression of better designs that have longer survivorship and save the health care system billions of dollars in the future. This study suggests that further retrieval analyses of well-functioning TKRs are warranted to determine the defining design characteristics that minimize wear and mechanical effects and optimize functional outcome and survivorship.

ACKNOWLEDGMENT

This study was funded by a grant from the Arthritis Foundation and an in-kind donation of software from LifeModeler, Inc.

REFERENCES

1. Grupp TM, Weik T, Bloemer W, Knaebel HP. Modular titanium alloy neck adapter failures in hip replacement--failure mode analysis and influence of implant material. BMC Musculoskelet Disord. 11:3doi:10.1186/1471-2474-11-3. Open Access article (12 pages), published 4 Jan 2010: http://www.biomedcentral.com/1471-2474/11/3.
2. Milosev I, Trebse R, Kovac S, Cör A, Pisot V. Survivorship and retrieval analysis of Sikomet metal-on-metal total hip replacements at a mean of seven years. J Bone Joint Surg Am. 2006 Jun;88(6):1173–82.
3. Cuckler JM, Lemons J, Tamarapalli JR, Beck P. Polyethylene damage on the nonarticular surface of modular total knee prostheses. Clin Orthop Relat Res. 2003 May;(410):248–53.
4. Li G, Suggs J, Hanson G, Durbhakula S, Johnson T, Freiberg A. Three-dimensional tibiofemoral articular contact kinematics of a cruciate-retaining total knee arthroplasty. J Bone Joint Surg Am. 2006 Feb;88(2):395–402.
5. Mikashima Y, Tomatsu T, Horikoshi M, Nakatani T, Saito S, Momohara S, Banks SA. In

vivo deep-flexion kinematics in patients with posterior-cruciate retaining and anterior-cruciate substituting total knee arthroplasty. Clin Biomech (Bristol, Avon). 2010 Jan;25(1): 83–7.
6. Kitagawa A, Tsumura N, Chin T, Gamada K, Banks SA, Kurosaka M. In vivo comparison of knee kinematics before and after high-flexion posterior cruciate-retaining total knee arthroplasty. J Arthroplasty. 2009;25(6):964–97.
Sharma A, Komistek RD, Scuderi GR, Cates HE Jr. High-flexion TKA designs: what are their in vivo contact mechanics? Clin Orthop Relat Res. 2007 Nov;464:117–26.
8. Scholes SC, Unsworth A. Wear studies on the likely performance of CFR-PEEK/CoCrMo for use as artificial joint bearing materials. J Mater Sci Mater Med. 2009 Jan;20(1):163–70. Epub 2008 Aug 14.
9. Scholes SC, Inman IA, Unsworth A, Jones E. Tribological assessment of a flexible carbon-fibre-reinforced poly(ether-ether-ketone) acetabular cup articulating against an alumina femoral head. Proc Inst Mech Eng H. 2008 Apr;222(3):273–83.
10. Pace N, Marinelli M, Spurio S. Technical and histologic analysis of a retrieved carbon fiber-reinforced poly-ether-ether-ketone composite alumina-bearing liner 28 months after implantation. J Arthroplasty. 2008 Jan;23(1):151–5.
11. Teeter MG, Naudie DD, Milner JS, Holdsworth DW. Determination of reference geometry for polyethylene tibial insert wear analysis. J Arthroplasty. 2010 In press.
12. Langton DJ, Jameson SS, Joyce TJ, Hallab NJ, Natu S, Nargol AV. Early failure of metal-on-metal bearings in hip resurfacing and large-diameter total hip replacement: a consequence of excess wear. J Bone Joint Surg Br. 2010 Jan;92(1):38–46.
13. Campbell P, Takamura K, Lundergan W, Esposito C, Amstutz HC. Cement technique changes improved hip resurfacing longevity—implant retrieval findings. Bull NYU Hosp Jt Dis. 2009;67(2):146–53.
14. Blumenfeld TJ, Bargar WL. Early aseptic loosening of a modern acetabular component secondary to a change in manufacturing. J Arthroplasty. 2006 Aug;21(5):689–95.
15. Sylvain GM, Kassab S, Coutts R, Santore R. Early failure of a roughened surface, precoated femoral component in total hip arthroplasty. J Arthroplasty. 2001 Feb;16(2):141–8
16. Johnson C, Hull ML. Parameter identification of the human lower limb under dynamic, transient torsional loading. J Biomech. 1988;21(5):401–15.

Journal of Long-Term Effects of Medical Implants, 20(1): 49–56 (2010)

Regional Measurements of Surface Deviation Volume in Worn Polyethylene Joint Replacement Components

Matthew G. Teeter,[1,2,] Jaques S. Milner,[1] Jennifer L. Au,[1] Daniel Lorusso,[1] Douglas D.R. Naudie,[3] & David W. Holdsworth[1,2,3]*

[1]Imaging Research Laboratories, Robarts Research Institute, London, Ontario, Canada; [2]Department of Medical Biophysics, The University of Western Ontario, London, Ontario, Canada; [3]Department of Surgery, The University of Western Ontario, London, Ontario, Canada

*Address all correspondence to Matthew G. Teeter, BSc, Robarts Research Instite, The University of Western Ontario, P.O. Box 5015,100 Perth Drive, London, Ontario, N6A 5K8, Canada; mteeter@imaging.robarts.ca.

ABSTRACT: Total joint replacements can be subject to the loss of polyethylene material due to wear, leading to osteolysis and decreased implant longevity. Micro–computed tomography (micro-CT) techniques have recently been developed to calculate 3D surface deviations in worn implant components. We describe a micro-CT technique to measure the volume of the surface deviations (volume of wear plus creep) within a specific region or compartment, and report its repeatability and reproducibility. Six worn polyethylene tibial inserts were scanned using a laboratory micro-CT scanner and subsequently reconstructed at 50 μm voxel spacing. A previously developed custom software application was used to quantify the 3D surface deviations between the worn tibial inserts and an unworn reference geometry. Three observers (two trained and one expert) used new custom software to manually outline the localized regions of surface deviation (three times for each of the worn inserts) and calculate the volume of the deviations. The overall intraobserver variability in the surface deviation volumes was 3.6% medially and 1.1% laterally. The overall interobserver variability was 4.8% medially and 1.7% laterally. Placement of points in outlining the region of deviation contributed the greatest variability to the measurements. Repeatability and reproducibility of the volume measurements are similar to measurements of total (nonregional) wear volume including a previous micro-CT technique (10%), fluid displacement (4.8%), and radiographic measurements (15.7%). The principles of this technique can likely be used to measure regional wear and creep volume in knee and hip joint replacement components from wear simulator, pin-on-disk, and retrieval studies.

KEY WORDS: total joint replacement, polyethylene wear, micro–computed tomography

I. INTRODUCTION

The loss of polyethylene material due to wear in joint replacement components continues to be of interest to the orthopaedics community. Polyethylene wear may lead to aseptic loosening and osteolysis, decreasing the longevity of the implant.[1] A number of in vitro laboratory methods have been developed to quantify the gravimetric or volumetric changes (due to wear and creep) in polyethylene components that have been retrieved from patients or undergone wear simulator testing. These methods include micro–computed tomography (micro-CT), gravimetric analysis, fluid displacement, and coordinate measuring machines.[2–4]

Micro-CT has been used to measure the overall volume of polyethylene tibial inserts and spinal discs,[5,6] and to measure the volume loss due to wear in retrieved polyethylene acetabular liners.[7] Techniques have

also been developed to measure and map the 3D surface deviations due to wear and creep in tibial inserts and acetabular liners.[4,5] A similar technique to measure the localized volume change within specific operator-selected regions of interest would be useful for comparing the location (e.g., medial versus lateral side of a tibial insert) and type of deviation (e.g., burnishing versus pits). Operator input is required to ensure that only "true" wear damage is quantified, ignoring erroneous surface deviations such as damage from the retrieval process, residual errors in component geometry coregistration, and residual differences (from manufacturing tolerances) between a retrieved component and a never-implanted reference geometry.[8]

The objectives of the present study were to describe the development of a technique to measure the regional volumes of surface deviations due to wear in polyethylene tibial inserts, and to measure the intraobserver repeatability and interobserver reproducibility of the technique. The technique was first established using a group of tibial inserts from a wear simulator study, then demonstrated using a tibial insert retrieved from a patient.

II. METHODS

II.A. Micro-CT Scanning of the Tibial Inserts

A group of 12 polyethylene tibial inserts (AMK, DePuy Inc., Warsaw, Indiana) of the same design and size were included in this study for establishing the technique. Six of the inserts had undergone wear testing to 5.5 million cycles in a prior wear simulator trial.[9] Patches of damage from the wear testing were observed macroscopically on both the medial and lateral sides of the articular surface for each of the six worn inserts. The remaining six inserts had experienced no wear and were used to construct an unworn reference geometry. This reference geometry was necessary to enable quantification of the worn surface deviations, since the worn inserts were not scanned before the wear trial (and thus the pre-wear geometry of the inserts was unknown).

Each insert was scanned with a laboratory micro-CT scanner (eXplore Vision 120, GE Healthcare, London, Otario) as part of a previous study.[5] Inserts were scanned at 50 μm isotropic voxel spacing, with an X-ray tube voltage of 90 kVp and current of 40 mA. In each scan, 1200 views were obtained in 0.3° deg increments with 10 frames averaged per view at an exposure of 16 ms per frame. The scans were reconstructed at the full 50 μm isotropic voxel spacing and analyzed with micro-CT analysis software (MicroView, GE Healthcare, London, Ontario). Isosurface rendering of the insert geometry was performed at the highest possible quality, using a threshold automatically determined by the software. The resulting geometry was saved in stereolithography file format.

II.B. Measurement of 3D Surface Deviations

A custom software application, developed for a previous study, was used for the construction of the unworn reference geometry and the quantification of the worn insert 3D surface deviations.[8] The application coaligns a source insert surface to a target surface using an iterative closest-points algorithm, with convergence set for when the rms average distance dropped below 0.1 μm for the 1000 sample points. To construct the unworn reference geometry, each of the six unworn inserts were imported into the application and the geometries were averaged to minimize any between-insert deviations due to the manufacturing process.

Each of the six worn inserts were then imported into the application and coaligned to the unworn reference geometry. The 3D deviations between the worn insert and the unworn reference geometry (in millimeters) were then calculated continuously across the entire surfaces of the inserts. The calculated 3D surface deviations were then mapped across the insert surface (Fig. 1) and visualized in ParaView (Kitware Inc., Clifton Park, New York).

II.C. Measurement of Regional Wear Volume

Custom software was developed using The Visualization Toolkit (Kitware Inc., Clifton Park, New

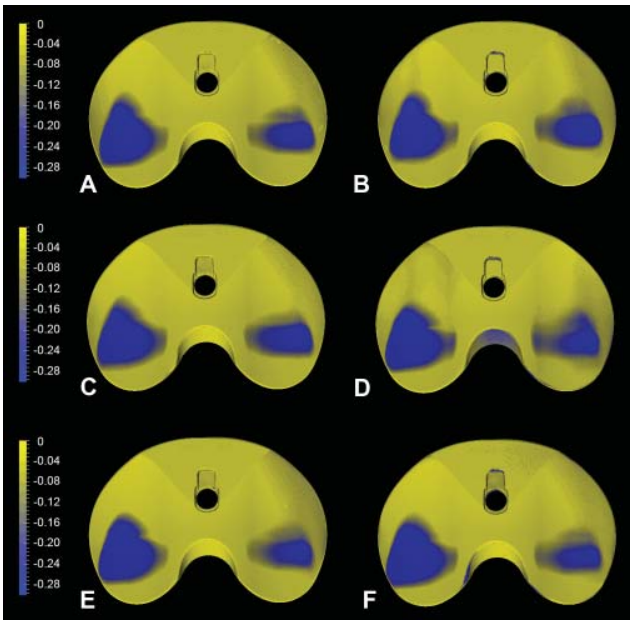

FIGURE 1. Maps of articular surface deviation (in millimeters) for the six worn inserts. Inserts are oriented so that the medial side is on the right of the figure.

York) to compute the volume deviation of the worn implant from the unworn reference geometry for operator-defined regions of interest. Input to the software was the unworn reference geometry, with mapped surface deviations computed from the worn implant as described in Section B above. The geometric model consisted of over 8.8 million points and 4.4 million triangles with a mean and median point spacing of 0.0501 and 0.0508 mm, respectively.

In order to define the worn region of interest, operators were required to (i) identify the worn area and (ii) outline the region boundary. Identification was carried out using interactive features built into the software, which allowed operators to arbitrarily reorient the surface geometry in 3D space and to modify the color lookup table range used to map the surface deviation values onto the visual model. Once the region of interest had been identified, nonessential surface geometry was cropped away in order to accelerate later computation. To outline the region of interest, points were manually placed on the surface around the extent of the worn region as determined by the operator. The points were then used to define a closed selection loop residing on the surface geometry (Fig. 2). Having outlined the worn region, three analysis quantities were computed and reported on for this study, namely, the deviation volume, the number of points used to outline the surface deviation, and the PSI.

The deviation volume of the discrete triangulated surface patch enclosed by the selection loop was computed as

$$V = \sum_{i=1}^{n} A_i \left(\frac{1}{3} \sum_{j=1}^{3} d_{i,j} \right) \tag{1}$$

where V is the total deviation volume of the surface patch, n is the total number of surface facets, A_i is the area of the ith triangular surface facet, and $d_{i,j}$ is the surface deviation at the jth vertex of the ith surface facet.

We define point spacing index (PSI) as a normalized measure of the uniformity in the spacing between adjacent points placed by the operator in outlining the surface deviation. Possible values range from 0 to 1, with a value of 1 representing

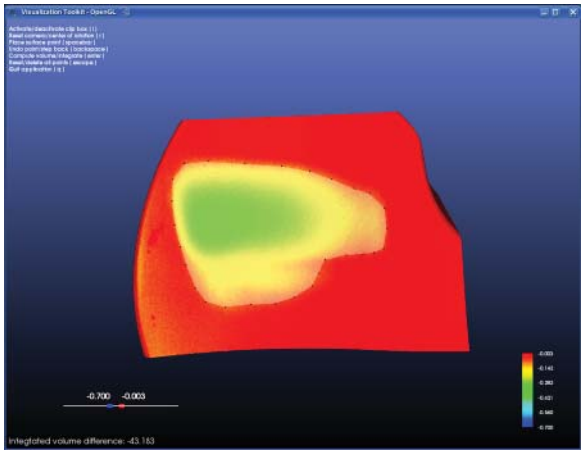

FIGURE 2. Screen shot of the volume measurement program, showing a cropped region of surface deviation outlined with points.

completely uniform point spacing with no dispersion in distance between points from the mean value. The value is computed as PSI = 1 $-C_V$ where C_V is the coefficient of variation calculated using the standard deviation of the distance between manually placed points and the mean distance between points.

II.D. Data Analysis

One expert observer (MGT) and two trained observers (JLA and DL) performed the volume-outlining task. The region of surface deviation on both the medial and lateral sides of the articular surface for each of the six worn inserts was identified visually, and manually outlined. The deviation volume, number of points used in the outlining, and PSI was recorded. The observers measured each region of surface deviation three times for all of the worn inserts. All measurements were made in one sitting. The six inserts were each measured once in consecutive order before repeating the measurements.

The mean medial and lateral deviation volume of each worn insert, as calculated by each observer and across all observers, was determined. The intraobserver variability (i.e., the coefficient of variation between repeated measurements of the same surface deviation volume by an observer) was calculated for each of the three observers. The interobserver variability (i.e., the coefficient of variation between measurements of the same surface deviation volume by the three observers) was also calculated. In addition, the mean and standard deviations of the number of points used to outline the surface deviation volume by each observer, along with the PSI, were calculated. Statistical analysis of the deviation volumes, number of points, and PSI was performed using one-way repeated measures ANOVAs with Tukey post hoc multiple comparison tests. Pearson correlations between the deviation volumes and number of points, and between the deviation volumes and PSI, were also performed. Statistical significance was set at $p < 0.05$.

II.E. Analysis of a Retrieved Insert

An additional insert that was retrieved from a patient after seven years implantation (Genesis II, Smith & Nephew, Memphis, Tennessee) was obtained. A never-implanted insert of the same model and size of the retrieved insert was also obtained for use as the unworn reference geometry. In the fashion described previously for the inserts from the wear simulator, both the retrieved and never-implanted inserts were scanned with micro-CT and their 3D geometries were generated from isosurface rendering. The retrieved and unworn geometries were coaligned, and the deviations be-

tween the two were quantified. The resulting deviation map was loaded into the volume measurement software, and the deviation volumes within specific regions of interest on the articular surface were measured.

III. RESULTS

The overall surface deviation volume across all observers was 42.3 ± 6.5 mm^3 medially and 101.7 ± 8.5 mm^3 laterally (Fig. 3). Significant differences (p < 0.05–0.001) were found between the mean volumes calculated by the three observers both medially and laterally. This interobserver variability was found to be 4.8% (2.0 mm^3) medially and 1.7% (1.8 mm^3) laterally. The overall intraobserver variability was slightly lower than the interobserver variability, at 3.6% (1.5 mm^3) medially and 1.1% (1.2 mm^3) laterally. In both cases, the observer-dependent variability was less than the standard deviation between the six insert volumes.

The number of points used by each observer to outline the surface deviation volume differed greatly between observers. Medially, the expert observer used a mean of 23.7 ± 6.8 points, significantly less (p < 0.001) than either of the two trained observers (49.1 ± 4.5 and 55.2 ± 14.2 points). Laterally, the expert observer used a mean of 24.7 ± 6.3 points, also significantly less (p < 0.001) than either of the two trained observers (54.7 ± 3.0 and 69.8 ± 6.8 points). However, no correlation was found between the surface deviation volume and number of points medially (r = 0.23, p = 0.35) or laterally (r = 0.12, p = 0.64).

Side (medial or lateral) had no effect on the mean PSI for any observer, which was identical on both sides for the expert observer (0.65) and two trained observers (0.71 and 0.64). As with the number of points, no correlation was found between the surface deviation volume and PSI medially (r = 0.10, p = 0.70) or laterally (r = –0.16, p = 0.53).

Both large (e.g., burnishing) and small (e.g., pits) deviation features were present on the retrieved insert (Fig. 4). On the medial side, the total volume of the burnished region was 107.8 mm^3. Within this region, there was a distinct area of increased depth with a volume of 45.7 mm^3. On the lateral side, the total volume of the burnished region was 115.1 mm^3. Two large pits were present on the lateral side, with volumes of 0.3 mm^3 and 0.1 mm^3. Overall, the deviations were less distinct than those in the inserts from the wear simulator trial.

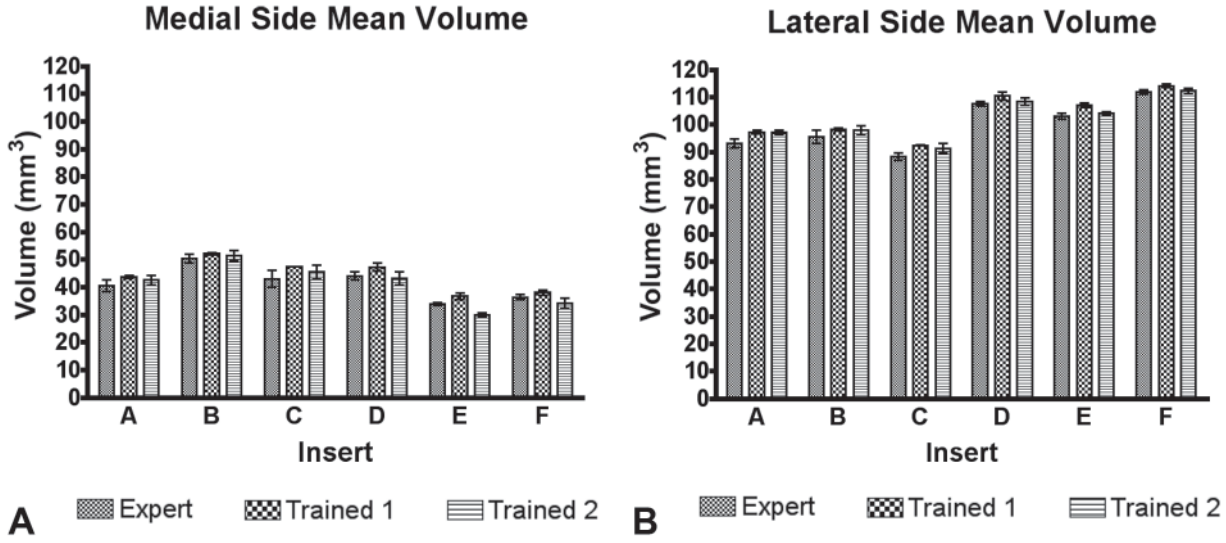

FIGURE 3. Mean surface deviation volumes (in cubic millimeters) of the **(A)** medial and **(B)** lateral sides as measured by each observer for the six worn inserts. Bars are standard deviation.

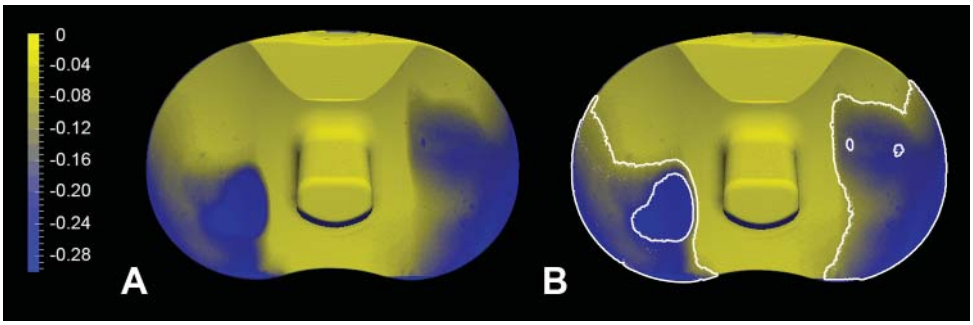

FIGURE 4. Map of the articular surface deviations (in millimeters) for the retrieved tibial insert **(A)** and overlay of regions selected for volume measurements **(B)**.

IV. DISCUSSION

The medial surface deviation volume measurement showed greater intraobserver and interobserver variability than the lateral surface deviation volume measurement (3.6% versus 1.1%, and 4.8% versus 1.7%, respectively). In examining the surface deviation maps (Fig. 1), the lateral deviations appear to be both larger and more distinct (i.e., have a stronger edge) than the medial deviations, perhaps resulting in easier point placement laterally. Although a statistically significant difference was found between the observer-reported volumes, we do not believe these differences (of ~2 mm^3) are clinically relevant. The differences between observers were three to four times less than the differences between the actual inserts. For wear simulator studies, the wear volume for wear-resistant highly cross-linked polyethylene has been reported to be 32 mm^3 over seven million cycles, with retrieved inserts demonstrating even greater wear volumes, at up to 85 mm^3 per year.[5] Therefore, even at short implant durations or low wear cycles, the relative contribution of observer error to the measurements should have minimal effect. Surface deviation volumes were measurable on the retrieved insert, including both large features such as burnishing and small features such as pits.

When using this technique, the primary variables that can contribute to differences between observers are the placement of the points, number of points used, and spacing between the points. If there is a true edge where the component surface changes from damaged (with deviations) to undamaged (no deviations), then an overestimate that places points within the undamaged region should contribute minimal error to the volume measurement, and is preferable to an underestimate of the wear volume. Observers must be mindful of point location, since it is likely the greatest source of potential error when using the application. No correlation was found between the number of points or point spacing and the resulting surface deviation volume. In comparing one of the trained observers to the expert observer, the expert observer used significantly fewer points, yet no significant difference resulted in the deviation volume. The PSI appeared to be fairly consistent among all observers (mean of 0.64–0.71), regardless of the number of points they used (mean of 23.7–69.8). We believe the location the observer places the points will contribute a larger error in the volume calculations than the number of points used or the spacing between the points.

The intraobserver and interobserver variability reported here compares well to other wear volume measurement techniques, which have been primarily applied to components from total hip replacement. Bowden et al.[7] used micro-CT to measure the wear volume in retrieved acetabular liners. They reported intraobserver and interobserver variability of approximately 10%, with the variability increasing to 50% for one liner with a low volume of wear. Chuter et al.[3] compared coordinate measuring, fluid displacement, and a radiographic technique for measuring wear in acetabular liners. Coordi-

nate measuring was found to be the most repeatable at 2.5% (range 0.25–9.8%), followed by fluid displacement at 4.8% (range 1.6–6.9%), and finally the radiographic technique at 15.7%.

The primary limitation of this surface deviation volume measurement tool is that it relies on observers. However, observers are necessary to ensure that the deviation volumes being quantified are "true" and not from damage during the retrieval process or errors in the geometry coregistration. The inserts used in this study for determining the repeatability and reproducibility of the measurements came from a wear simulator trial, and therefore likely have a more consistent pattern of surface damage than inserts retrieved from patients during revision surgery.[10] In the current study, the deviations in the retrieved insert were less distinct than those of the inserts from the wear simulator. In addition, a high number of wear cycles (5.5 million) was performed on the inserts from the wear simulator trial, using conventional polyethylene without cross-linking. This resulted in measured wear volumes approaching 100 mm^3. Components implanted for a shorter duration or having undergone low wear cycles, as well as those components manufactured from newer highly cross-linked polyethylene, could experience lower wear volumes.[11] As previously discussed, the expected wear volumes would still be an order of magnitude greater than the observer error. However, examining high-volume regions of wear with a consistent pattern as in this study may have resulted in slightly more repeatable and reproducible measurements than low-volume, inconsistent regions of wear.

In summary, we have developed a technique to measure the regional volume of surface deviations due to wear and creep in polyethylene tibial inserts. This technique enhances the utility of micro-CT for wear measurement, adding to existing capabilities of surface deviation mapping and measurements of whole-component volume.[4,5] This method ensures that only "true" wear damage is quantified, ignoring erroneous deviations such as damage from the retrieval process. The intraobserver repeatability and interobserver reproducibility of the method was found to be similar to other wear volume measurement techniques such as fluid displacement and radiographic methods. The technique described in this study can likely be used in wear simulator, pin-on-disk, and retrieval studies of polyethylene components used in joint replacement, including total knee and total hip replacement.

ACKNOWLEDGMENTS

This study was funded by a grant from the Canadian Institutes of Health Research (No. MOP-89852). MGT received support from an Ontario Graduate Scholarship and is supported in part by the Joint Motion Program—A CIHR Training Program in Musculoskeletal Health Research and Leadership. DWH holds the Dr. Sandy Kirkley Chair for Musculoskeletal Research at the Schulich School of Medicine & Dentistry.

REFERENCES

1. Naudie DD, Ammeen DJ, Engh GA, Rorabeck CH. Wear and osteolysis around total knee arthroplasty. J Am Acad Orthop Surg. 2007 Jan;15(1):53–64.
2. Blunt L, Bills P, Jiang X, Chakrabarty G. Improvement in the assessment of wear of total knee replacements using coordinate-measuring machine techniques. Proc Inst Mech Eng H. 2008 Apr 7;222(3):309–18.
3. Chuter GS, Cloke DJ, Mahomed A, Partington PF, Green SM. Wear analysis of failed acetabular polyethylene: a comparison of analytical methods. J Bone Joint Surg Br. 2007 Feb;89(2):273–9.
4. Teeter MG, Naudie DDR, Charron KD, Holdsworth DW. Three-dimensional surface deviation maps for analysis of retrieved polyethylene acetabular liners using micro-computed tomography. J Arthroplasty. 2010;25(2):330–2.
5. Teeter MG, Naudie DD, McErlain DD, Brandt JM, Yuan X, MacDonald SJ, Holdsworth DW. In vitro quantification of wear in tibial inserts using microcomputed tomography. Clin Orthop Rel Res. 2011 Jan;469(1):107–12.
6. Vicars R, Fisher J, Hall RM. The accuracy and precision of a micro computer tomography vol-

umetric measurement technique for the analysis of in-vitro tested total disc replacements. Proc Inst Mech Eng H. 2009 Apr;223(3): 383–8.
7. Bowden AE, Kurtz SM, Edidin AA. Validation of a micro-CT technique for measuring volumetric wear in retrieved acetabular liners. J Biomed Mater Res B. 2005 Oct;75(1):205–9.
8. Teeter MG, Naudie DDR, Milner JS, Holdsworth DW. Determination of reference geometry for polyethylene tibial insert wear analysis. J Arthroplasty. 2010;In press.
9. Brandt J-M, Charron KD, Zhao L, MacDonald SJ, Medley JB, editors. Serum composition affects the fluid uptake and wear of polyethylene in total knee simulator testing. Society for Biomaterials Annual Meeting, Chicago; 2007.
10. Harman MK, DesJardins J, Benson L, Banks SA, LaBerge M, Hodge WA. Comparison of polyethylene tibial insert damage from in vivo function and in vitro wear simulation. J Orthop Res. 2009 Apr;27(4):540–8.
11. Jacobs CA, Christensen CP, Greenwald AS, McKellop H. Clinical performance of highly cross-linked polyethylenes in total hip arthroplasty. J Bone Joint Surg Am. 2007 Dec;89(12):2779–86.

Journal of Long-Term Effects of Medical Implants, 20(1): 57–72 (2010)

Assessment of the Damage in Retrieved Patellar Components

Peter Ellison[1,] & John Fisher[2]*

Department of Surgical Sciences, University of Bergen, Bergen, Norway[1]; Institute of Medical and Biological Engineering, University of Leeds, Leeds, United Kingdom[2]

*Address all correspondence to Dr. Peter Ellison; 'Universitetet i Bergen, Institutt for Kirurgiske Fag, Biomateriallaboratoriet, Laboratoriebygget, Haukeland Universitetssjukehus, 5021 Bergen, Norway; Peter.Ellison@kir.uib.no.

ABSTRACT: Patellofemoral complications are cited as a leading cause for revision surgery following total knee arthroplasty. Despite widespread clinical use, the decision to resurface the patella, or not, is controversial and remains surgeon dependent. Damage to the patellar component can lead to revision surgery; however, little work exists investigating the damage they sustain in vivo. Twenty-four retrieved patellar components were assessed for damage. There was a wide variation in wear scar morphology, although the mean wear scar area spanned mediolaterally in a band across the articular surface and was 364.32 ± 64.7 mm^2 in area. Maximum linear penetration was located in the lateral region of the articular surface. Assessment of damage mode grading indicated that it was more severe in the lateral quadrant, although the method's lack of consideration of the chronological progression of wear creates uncertainty over this finding. Volume change ranged from –1.3 to –45.16 mm^3/year, and maximum penetration was in the lateral region. Damage to the patellar component of knee replacement has been shown to be significant. The number of components in the study was too small to determine a difference in damage in all-polyethylene and metal-backed designs; however, the volume loss of all-polyethylene patellae was found to be significant.

KEY WORDS: patella retrieval total knee replacement arthroplasty

I. INTRODUCTION

The use of total knee arthroplasty (TKA) in the treatment of arthritis carries a high rate of success providing improvement in function and relief of pain for the patient. Patellofemoral complications remain one of the most prevalent causes of revision surgery in TKA,[1–15] and despite widespread clinical use the debate on whether the patella should be resurfaced, or not, remains open.[7,16] Use of a patellar button for TKA varies considerably between countries. It is popular in Denmark (76%) and Australia (43%), but not in England and Wales (33%), Norway (11%), or Sweden (14%).[17–19] The potential complications related to patellar resurfacing include loosening, infection, pain, instability, fracture, and tear of the extensor mechanism.[18,20] Damage to the patellar component is also a cause of revision surgery. Following the introduction of metal-backed designs, many studies documented the failure of such devices.[21–32] A high incidence of significant wear has also been documented for all-polyethylene patellar components,[27,33] as well as creep deformation with a potential for cracking at the periphery of the articular surface.[27] Excessive loosening in all-polyethylene,dome-type patellar components has been reported.[34] Experimental contact stress analysis has shown that this may be caused by deformation of the polymer leading to failure of the underlying bone.[35] Wear simulator studies have predicted that the absolute

volume of wear generated is low;[36–39] however, the debris is of the same functional biological activity as debris from the tibiofemoral compartment[40] and therefore must be considered.

The analysis of in vivo damage mechanisms is a vital part of evaluating the performance of orthopaedic joint replacements. Considerable effort has been focused on assessing in vivo wear mechanisms within acetabulatar and tibial components manufactured from UHMWPE.[34,41–53] In contrast, few studies have investigated the in vivo damage mechanisms of UHMWPE patellar components[33,47,54] and as a result comparatively little is know about the mechanisms of damage. This study investigates the damage sustained in vivo in a series of 24 retrieved patellar components by quantifying volume change, wear scar area, and damage grading of the articular surface.

II. METHOD

In total, 24 knee prostheses were retrieved during revision surgery or at postmortem. Immediately following retrieval, components were sterilized and cleaned with a mild detergent solution, and all extraneous tissue was removed. On arrival at the university, the sterilization and cleaning procedure was repeated. Finally, components were cleaned with isopropanol in an ultrasonic bath prior to analysis. Care was taken in handling the components throughout the cleaning and analysis process so as not to create artificial damage.

II.A. Femoral Components

The femoral components were examined for evidence of scratches, corrosion, and fracture with the naked eye and light stereo microscopy. Average surface roughness, R_a, measurements were taken using a Form Talysurf stylus profilometer 120L (Rank-Taylor Hobson, Leicester, UK) with a conical diamond stylus of 2.5 μm radius.

II.B. Patellar Components

As with the femoral components, a Form Talysurf stylus profilometer was used to measure the R_a of the articular surface of the patellar components. The condition of the articular surfaces was inspected and evaluated. Damage modes were quantified through visual inspection, stereo microscopy, and scanning electron microscopy (SEM). Observations of the UHMWPE surface morphology were matched to findings of previous investigations.[34,41–47,51–56] The level of damage was assessed using the semi-quantitative damage grading method outlined by Hood et al.[47] The basis of this method was to record the variation of seven predefined damage modes across the articular surface. The seven damage modes were defined as surface deformation, pitting, embedded PMMA debris, scratching, burnishing, abrasion, and delamination.[47]

The articular surface of the patella was divided into quadrants (Fig. 1). The level of each damage mode within the quadrant was quantified on a scale

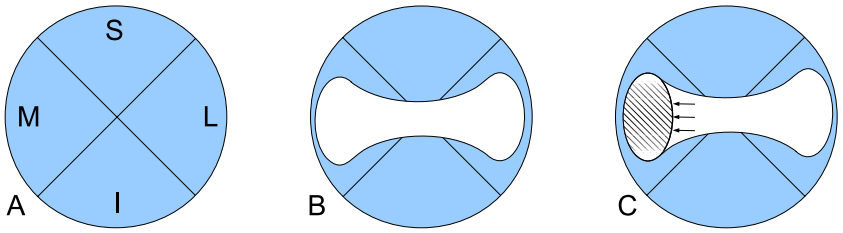

FIGURE 1. Quadrants used to categorise patellar wear: **(A)** Medial (M), lateral (L), superior (S), and inferior (I); **(B)** Illustration of a "bow tie" shaped total wear scar area; **(C)** Example of how the perimeter of the wear scar increases if a damage mode is outlined within the total wear scar area. The additional perimeter is indicated by three arrows.

of zero to three, defined as zero (none), one (light), two (moderate), and three (severe). Definition of these grading bands was assessed by the means of extent and severity. Extent was measured by the percentage area of the quadrant covered by the mode. Zero to three damage grades related to 0, <10, 10–50, and >50% areas, respectively. Severity was assessed via a more subjective method considering the severity of individual artifacts. For example, an abnormally severe level of damage mode covering a smaller area would be graded higher than the area alone would indicate. The total damage score for each quadrant was then calculated by summing the scores due to each damage mode, which were in turn summed to give a total damage score for the component. This gave a total maximum score of 84 for each patella.

To assess the repeatability of the grading scheme, 10 patellar buttons were selected at random from the sample group and scored by the primary author and an experienced researcher independent from the investigation. The statistical significance between the observations was compared using the Wilcoxon signed-rank test.[57] No statistical difference could be found between the two groups for the total damage score at the 5% level. In order to assess the intraobserver repeatability the same 10 patellae were scored by the author a second time and the observations compared using the Wilcoxon signed-rank test.[57] No statistical difference could be found between the two group's total scores at the 5% level. Therefore, the damage grading method was shown to be repeatable on the level of inter- and intraobservations.

The area of the total wear scar and the associated damage modes on the patellar button's articular surface were quantified for each component, the latter forming the basis of the Hood et al.[47] grading method. The wear scar and contained damage mode regions were manually outlined using removable ink. A calibrated 2D image of the wear scar was then captured using an Epson Perfection 2480 Digital Scanner (Seiko Epson, Japan). Regions were measured using image analysis software functions within Image Pro Plus 3.0 (Media Cybernetics, Bethesda, Maryland). Evaluation of this technique showed that areas in the range of 25–1000 mm^2 could be measured with a standard deviation of 1–9 mm^2. Further tests showed that increasing the length of the scar's perimeter significantly reduced the absolute value of area measured (Fig. 1). The error introduced was minimized by ensuring the perimeters were marked as thinly as possible. Nevertheless, a maximum variation of 71 mm^2 was found when comparing measurements from a specimen where only the total wear scar was marked (Fig. 1B) to that where the total scar and contained regions were outlined (Fig. 1C). As a consequence, total wear scar measurements were collected initially by outlining the total wear scar. A second measurement was then taken in which the enclosed regions were highlighted. Since the grading of wear regions was based on percentage area quantification of regions, this technique was deemed acceptable. Repeatability tests of the total wear scar measurement reported values in the range of 380 ± 1.8 mm^2 (SE). The length of perimeter was not found to affect the repeatability of the total wear scar measurement.

Volume loss from the articulating surface of the patellar button was calculated by measurement of the existing articular surface form and comparison to an assumed virgin geometry reconstructed from unworn portions of the component. The articular surface geometry was digitized using a coordinate measuring (CM) machine, Kemco 400 (Keeley Measurement Company, UK) equipped with a Renishaw PH10T probe head, TP20 touch probe, and PS2R 2 mm ruby ball stylus (Renishaw, UK). The CM machine took a sequence of point measurements in order to digitize the articular surface (Fig. 2A). The data point cloud was collected through QCT-2000 Inspect2CAD software (QCT Ltd, UK) from which the surface was reconstructed using TriboSol SR3D v4.1.1 (Tribology Solutions Ltd, UK) software. In order to estimate the volume loss from the articular surface, a nominal sphere assumed to represent the unworn geometry was created by applying least-squares minimization to unworn sections identified from the physical component (Fig. 2B). Prior to all measurements, specimens were subject to a 48 h temperature stabilization period to remove the variability of

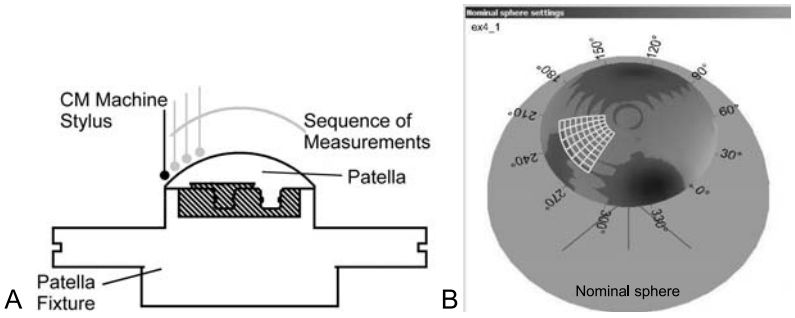

FIGURE 2. Details of the methodology used to measure the volume change of the patella: **(A)** CM machine took a sequence of point measurements in order to digitize the articular surface; **(B)** A nominal sphere was fitted to the unworn region of the patella (shown a white hatching between 240 and 270 deg).

UHMWPE geometry due to temperature. The accuracy of the Kemco 400 working with QCT-2000 Inspect2CAD software was calibrated to the range of 1–3 μm for linear, length, and squareness measurements. This was less than the maximum axial position error (*D*) outlined in current international standard for dimensional measurement of wear in hip prostheses.[58]

III. MATERIALS

A total of 24 knee prostheses were retrieved during revision surgery or at postmortem from Nottingham City Hospital, Glenfield Hospital Leicester, Bradford Royal Infirmary, and Leeds General Infirmary (Table 1). Unfortunately, full patient histories and femoral components were not available in all cases. Therefore, analyses were based on subsets of the total data set depending on the availability of the variable of interest.

The mean age of the patient sample at retrieval was 70.6 years (58.7–85 years). Male to female split was 50% to 50%. Seventy one percent of retrievals were taken from the right limb and 29% from the left. Mean weight and height was 80 kg (56–106 kg) and 161 cm (110–186 cm), respectively. The data set was made up from the following designs of replacement: PFC, Johnson and Johnson Orthopaedics, USA (6); Tricon, Smith and Nephew, Memphis, TN, USA (4); PFC Σ, DePuy International, UK (3); Leicester Patella Femoral Knee (PFK), Corin Medical Ltd, UK. (3); Insall-Burstein II, Zimmer Inc, USA (2); Kinemax, Stryker Orthopaedics, USA (2); Johnson-Elloy (Accord) Knee, Thackeray, UK (1); Interax, Stryker Orthopaedics, Mahwah, NJ, USA (1); and LCS MB DePuy International, UK (1). The Tricon, LCS MB design and one unidentified patellar component were metal backed; all remaining components were all-polyethylene. It should be noted that the Leicester PFK prostheses was a unicompartmental PFJ replacement; the remainder were total knee systems. Mean time in situ was 8.2 years (2.1–19.1 years). The average activity level was judged to be low, with only two patients walking without support. One patient had suffered from rheumatoid arthritis (sample B), with all others suffering OA.

IV. RESULTS

IV.A. Femoral Components

Twelve of the samples were retrieved with femoral components. Scratching of the trochlear groove could be seen with the naked eye in all samples. No consistent trend was found with observations ranging from densely populated areas of fine scratches ($R_a \approx 0.03$ μm) aligned to the primary direction of sliding (S-I), to an array of deeper, randomly orientated scratches ($R_a \approx 0.06$ μm). No correlation between R_a and time in situ was found, ($r^2 = 0.07$), or patellar total damage score with mean R_a ($r^2 = 0.0135$). Two

TABLE 1. Clinical Data for Revised Prostheses and Patients

No.	TKR System	Implant Date	Time In Situ (years)	Activity Level	Cemented	Metal Backed	Patella Design	Joint Side	Gender	Age (years)	Weight (kg)	Height (cm)	Reason for Revision
A	PFC	1994	-	Stick	☑	☒	Oval sombrero	R	F	-	58	-	Functioning normally, retrieved at postmortem
B	PFC	1995	10	-	☑	☒	Oval sombrero	L	F	-	58	110	Functioning normally, retrieved at postmortem
C	PFC	1998	2.1	No support	☑	☒	Oval sombrero	R	F	77	63	160	PFJ Pain
D	PFC	1999	4.9	Sedentary	☑	☒	Oval sombrero	R	F	68	56	-	Loose components
E	PFC	1999	7.2	Stick	☑	☒	Oval sombrero	R	M	76	87	177	Joint pain, osteolysis of the lateral femoral condyle
F	PFC	2001	5.5	Sedentary	☑	☒	Oval sombrero	L	F	63	77	152	Joint pain, patellar clunk and loosening of femoral component
G	Tricon	1987	19.1	Stick	☒	☑	Round dome	R	F	64	100	160	Loose femoral and tibial components
H	Tricon	1988	14.2	Sedentary	☒	☑	Round dome	L	F	72	100	-	Joint pain
I	Tricon	1992	14.1	Stick	☒	☑	Round dome	R	M	71	90	-	Pain and instability
J	Tricon	1995	10.8	immobile	☒	☑	Round dome	R	M	70	80	-	Loose femoral and tibial components
K	PFC ∑	2002	3.4	Sedentary	☑	☒	Oval dome	R	F	64	76	157	Aseptic loosening of tibial and patellar components.
L	PFC ∑	2002	3.9	-	☑	☒	Oval dome	R	M	85	105	186	Dislocation of patella
M	PFC ∑	-	-	Stick	☑	☒	Oval dome	L	M	-	-	-	Sepsis

TABLE 1. (continued)

No.	TKR System	Implant Date	Time In Situ (years)	Activity Level	Cemented	Metal Backed	Patella Design	Joint Side	Gender	Age (years)	Weight (kg)	Height (cm)	Reason for Revision
N	Leicester PFK	1996	9	Seden-tary	☑	☒	Round sombrero	L	M	64	84	177	Progression of OA to medial compart-ment
O	Leicester PFK	1997	9.2	Two sticks	☑	☒	Round sombrero	L	F	72	69	155	Progression of OA to medial and lat-eral compartments
P	Leicester PFK	1999	6	Seden-tary	☒	☒	Round sombrero	R	M	69	86	166	Progression of OA to medial compart-ment
Q	Insall-Burstein II	1998	7.5	Stick	☑	☒	Round dome	R	M	71	85	173	Joint pain, PFJ stuffed despite resurfacing ma-laligned tibial com-ponent
R	Insall-Burstein II	-	10	No sup-port	☑	☒	Round dome	R	-	-	-	-	Failure of tibial spine
S	Kinemax	2003	2.9	Manual	☑	☒	Sombrero (offset)	R	F	59	106	155	Osteolysis leading to collapse of me-dial tibial plateau
T	Kinemax	-	-	-	☑	☒	Pyramid (offset)	R	F	-	-	-	-
U	Accord Knee	1993	13.1	Stick	☑	☒	Round flat	R	F	77	65	170	Instability leading to dislocated bear-ing
V	Interax	2001	2.5	Stick	☑	☒	Pyramid (offset)	L	M	78	-	-	Inflammation
W	LCS MB	1994	-	-	☒	☑	Conform-ing	R	-	-	-	-	-
X	-	-	-	-	☑	☑	Round sombrero	R	M	-	-	-	-

of the samples, G and H, showed areas of severe wear (Fig. 3).

1. Patellar Component—Surface Roughness

The mean R_a was calculated from the series of roughness measurements taken at discrete locations on the articular surface. Four roughness measurements were from each patella. Figure 4 shows the variation of mean R_a with respect to time in situ for the patellar components. No correlation between mean R_a and time in situ was found ($r^2 = 0.04$).

2. Patellar Components—Damage Grading

In general, wear scars on the patellar components spanned from medial to lateral with a slight bias toward the superior. Mean scar areas of 78.4 ± 27.3 mm^2 [mean (n = 24) ± 95% CI], 92.4 ± 24.9 mm^2, 51.7 ± 20.3mm^2, and 129.6 ± 32.4 mm^2 were recorded for the superior, medial, inferior, and lateral quadrants, respectively. The average total wear scar area was 364.3 ± 64.7 mm^2. There was no correlation between wear scar area variation and time in situ (Fig. 5, $r^2 = 0.002$).

The mean total damage grade score of the sample group was observed to be 21. The individual scores for the superior, medial, inferior, and lateral quadrants were 5, 5, 4, and 7, respectively. There was no significant correlation between the variation of total damage score and time in situ (Fig. 6, $r^2 = 0.12$), height and time in situ (Fig. 7, $r^2 = 0.0002$), or mass and time in situ (Fig. 8, $r^2 = 0.006$).

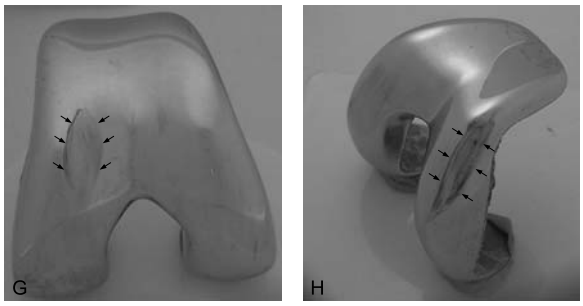

FIGURE 3. Images of explants G and H showing clear evidence of metal on metal wear between the patella femoral component and the patella's metal backing due to polymer wear through.

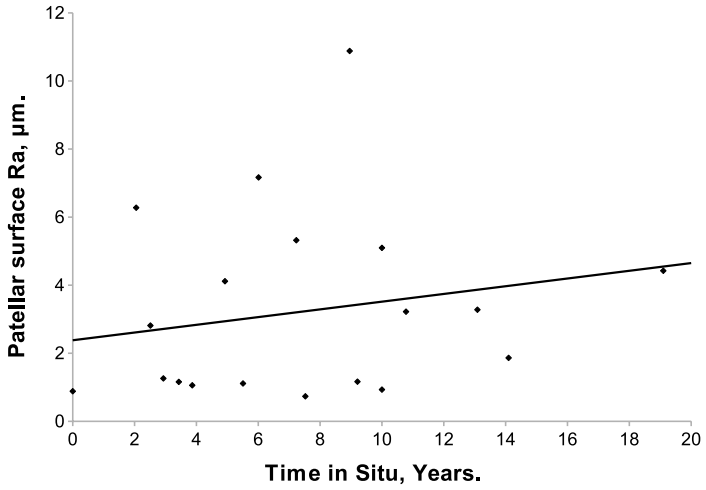

FIGURE 4. Variation of patellar counterface mean R_a with time in situ.

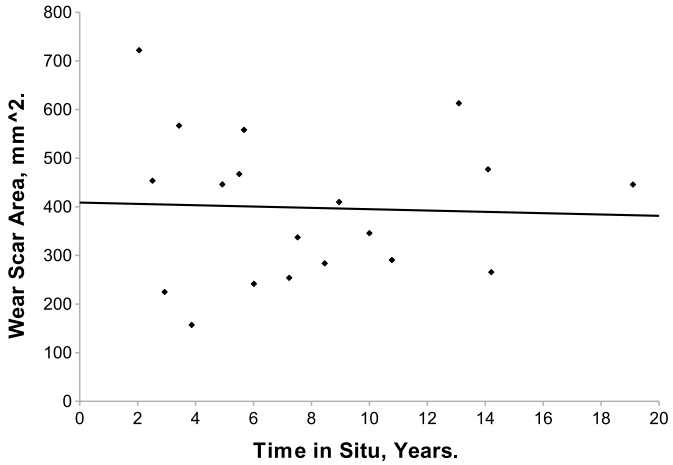

FIGURE 5. Variation of patellar wear scar area with time in situ.

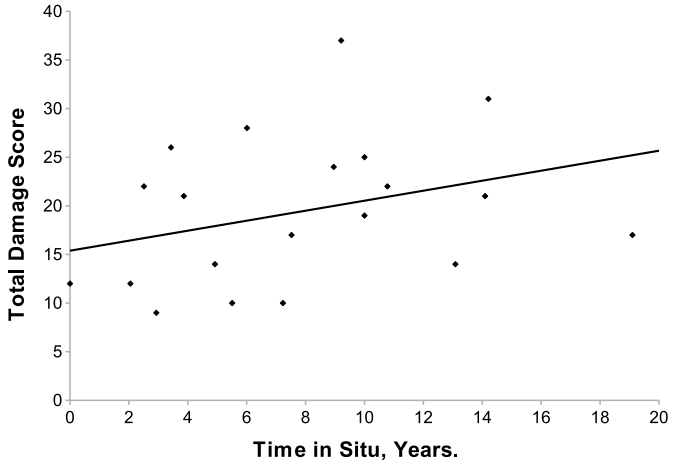

FIGURE 6. Variation of patellar total damage score area with time in situ.

3. Patellar Component—Wear Volume Loss

The technique available for the CM analysis of the patellae was only applicable to round dome components with a cross-sectional radius of single curvature. This restricted the number of samples that could be analyzed to two all-polyethylene samples, Q and R. The total change calculated was –9.77 ± 0.28 mm^3 and –486.85 ± 4.6 mm^3 [mean (n = 5) ± 95% CI], respectively, equating to –1.3 and –45.16 mm^3/year. A maximum penetration of –0.591 mm was observed for sample Q at 0 deg on the lateral region of the articular surface. The maximum penetration observed for sample R was –2.705 mm, again occurring at 0 deg on the lateral region of the articular surface (Fig. 9).

V. DISCUSSION

Analysis of the retrieval samples allowed quantification of the surface damage sustained by femoral components in vivo. Scratching was observed on the trochlear groove of all femoral components. No trend could be observed in the severity or frequency of the scratches. It was presumed that the variation was due to subtleties in the host patients.

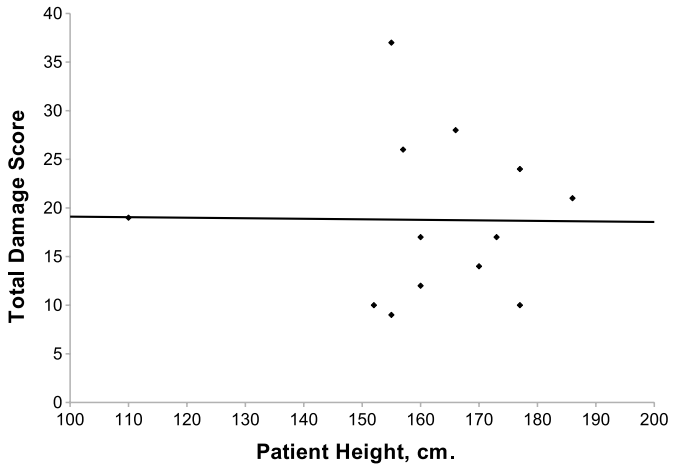

FIGURE 7. Variation of patellar total damage score area with patient height.

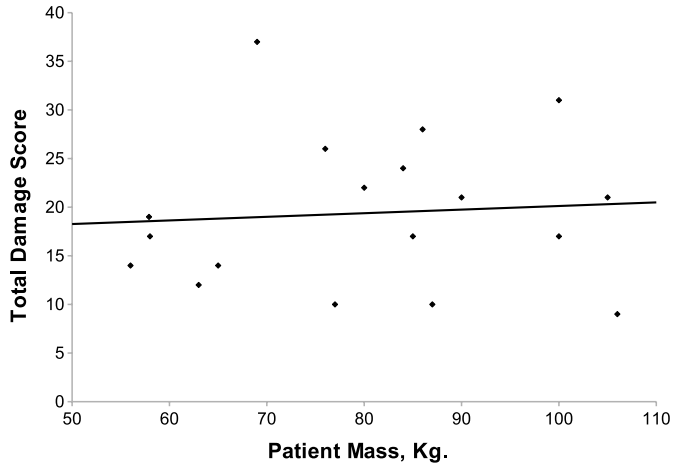

FIGURE 8. Variation of patellar total damage score area with patient mass.

The limited clinical data and small sample size did not allow investigation of these details. Femoral components from samples G and H showed areas of severe wear (Fig. 3). On inspection of the associated patellae, the UHMWPE was found to have worn through to the metal backing allowing it to come into contact with the femoral component (Fig. 11B).

The mean R_a of the femoral components' trochlear grooves varied from 0.03 μm to 0.06 μm. Articular surfaces of the femoral components are typically manufactured to an R_a of 0.02 μm; thus, the range recorded for the retrieved prostheses clearly indicated surface damage. Although no previous data was found for the roughness of the retrieved femoral components' trochlear grooves, the values observed are in a similar range to those reported for the condyles of retrieved femoral TKR components.[52] No correlation between R_a of the femoral component and time in situ was found. This was not surprising considering the small sample size and the high variability commonly found in retrieval studies. Previous research investigating the tibiofemoral articulation of CoCr femoral components[52] and titanium alloy hip components[59] found no correlation between surface roughness

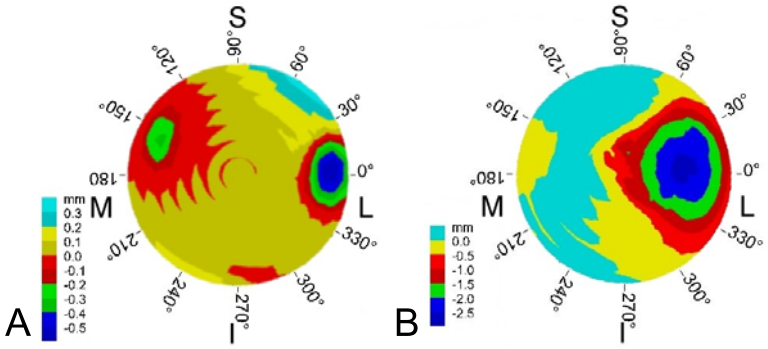

FIGURE 9. Wear penetration across the patella's articular surface of two all-polyethylene samples: (A) Sample Q; (B) Sample R.

and clinical parameters (patient age, sex, weight, or the time the implant was in situ). However, Nasser et al.[60] have suggested a relationship between the abraded surface area on titanium alloy hip components and time in situ.

Visual inspection of the patellae showed that the wear scar typically spanned from medial to lateral, with a bias to superior and lateral regions, although the difference between the superior and inferior quadrants, or the medial and lateral quadrants, was not significant at the 5% level. Previous investigators have also found a tendency for in vivo wear to be on the medial and lateral regions of patellar buttons.[33,47,54] Schwartz et al.[33] described the wear scar as "bow tie" shaped, being more extensive at the medial and lateral edges (Fig. 1B). Examples of this wear scar morphology were observed (Fig. 10A) as well as stripe-shaped scars predominantly in the S-I direction (Fig. 10B), scars made up from isolated pockets of wear (Figure 10-C) and those which engulfed the majority of the articular surface (Fig. 10D). This variation in the wear scar morphology reflects the movements at the patellofemoral joint, which have been reported to vary significantly, even for well-functioning healthy subjects.[61] The mean total wear scar area was 364.32 ± 64.7 mm^2 [mean (n = 24) ± 95% CI]. These values compared positively to previously published data.[26,38]

The mean total damage score for the patellae was found to be 21 after a mean of 8.2 years in situ.

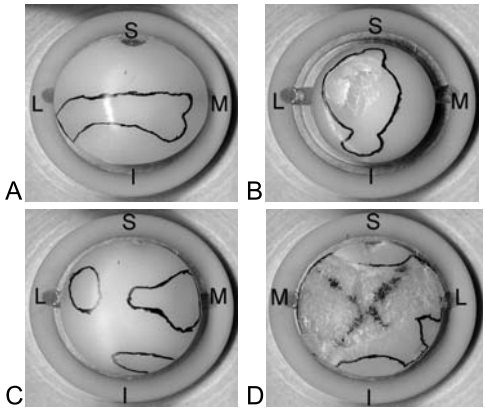

FIGURE 10. Images of the various wear scar shapes found on the retrieved patellae: **(A)** Typical M-L band wear scar, sample F; **(B)** S-I stripe wear scar, sample J; **(C)** Isolated pockets of wear, sample Q; **(D)** Extreme surface damage engulfing the majority of the articular surface, sample N.

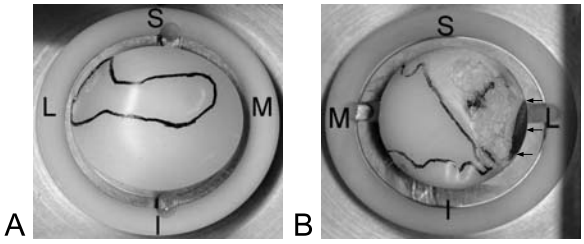

FIGURE 11. Comparison of damage sustained to samples: (A) Sample B showing only moderate wear and the initial signs of delamination; (B) Sample G showing heavy delamination and clear evidence of wear through the UHMWPE on to the metal backing (indicated by black arrows).

This was considerably higher than the previously reported mean damage score of 6 (n = 28) at a mean time in situ of 1.7 years.[47] Previous investigators have found time in situ to be positively correlated to damage of UHMWPE tibial and acetabular components[34]; however, we did not find a similar trend (Fig. 6, r^2 = 0.12). The difference is likely to be related to limitations in the damage grading system since it was not able to consider the chronological progression of wear. The limitation can be illustrated by considering samples B and G (Fig. 11). Sample B was retrieved at autopsy following 10 years in situ. Sample G was retrieved following 19 years in situ due to loose femur and tibial components. Sample G shows heavy signs of wear with extensive delamination in the lateral and inferior quadrants (Fig. 11). Wear has fully penetrated the UHMWPE surface such that the metal backing has worn against the femoral component. Sample B was seen to have low to moderate wear, showing only initial signs of delamination; however, the total damage score reported for the samples were 17 and 19, respectively. Thus, the assessment of damage based on a simple visual evaluation contradicts the score derived using the damage grading system. It is suggested that the semiquantitative grading method used in this study was unable to rank patellar UHMWPE damage in a logical manner since it does not account for the chronological progression of wear. This is based on the fact that if the extent of a later damage mode eradicated evidence of the previous modes, the prior modes will not be taken into account. This has particular relevance to delamination due to its destructive nature, but could also affect other modes. Therefore, while the semiquantitative damage grading method did offer some basic insight into the severity and location of in vivo damage modes, more detailed studies of UHMWPE wear mechanisms and surface morphology are required to allow the damage to be accurately quantified.

The mean total damage scores for the superior, medial, inferior, and lateral quadrants were 5, 5, 4, and 7, respectively. The trend supports the data presented for the wear scar area, indicating that damage tended to occur in a band spanning the mediolateral direction. The bias between the quadrants was tested for significance using the Mann-Whitney U-test.[62] Damage of the superior and inferior quadrants was not significantly different at the 5% level. However, damage of the medial and lateral quadrants was found to be significantly different at the 5% level, with a bias toward the lateral.

Linear correlation coefficients of r^2 = 0.12, 0.0002, and 0.006 indicate that there was no relationship between patellar total damage score and time in situ, patient height, and patient mass, respectively. Previous retrieval studies of tibial and acetabular components have indicated positive correlations between UHMWPE total damage score and both patients' weight and the length of time the component was implanted for.[34,47] However, Hood et al.[47] did not report any correlations for patellar components, and it is therefore assumed that none were found. No correlation was expected in the present investigation considering the evidence suggesting that the method is unable to consistently grade all instances of patellar damage.

The total damage observed was made up from burnishing, pitting, scratching, delamination, and surface deformation. There were no instances of embedded PMMA debris or abrasion damage. Frequency of each mode's occurrence was calculated as a percentage of the sample data set (Table 2). As shown, neither of the previous investigators reported evidence of abrasion. Burnishing was the most prevalent damage mode, being observed in 100% of samples. Previous investigations have also reported burnishing to be the most common damage mode. There was no apparent difference between the damage of metal-backed or all-polyethylene designs, although the number of components was too small to determine this statistically. These results highlight the wide variation in damage modes reported for patellar components.

Volume changes of –1.3 and –45.16 mm^3/year were observed for the two components analyzed. To the author's knowledge, this is the first recorded estimation of the patellar button's volume change during clinical usage. Unfortunately, the level of supporting clinical data was not sufficient to allow the reason for the variation to be identified. However, the range does highlight the variability in the volume change that can be sustained to patellae in vivo. The peak value of volume change indicates that under clinical conditions, the wear of all-polyethylene patellar buttons is sufficient to cause concern over joint laxity, due to gross shape change, and wear debris–induced osteolysis.

For samples Q and R, the maximum penetration was –0.591mm and –2.705 mm, respectively, and was located in the lateral region of the articular surface (Fig. 9). This result of high damage in the lateral region supports that from the damage grading and wear scar area measurements. This damage is presumably caused by lateral loading of the patellar, high lateral patellar tilt, or a combination of both.

It should be noted that CM analysis is susceptible to errors at low volumes. Derbyshire et al.[63] stated that data captured using a similar specification of CM machine had a repeatability error of as much as ±1.8 mm^3 when measuring a 22 mm diameter acetabular cup. Therefore, in order for results to be of high accuracy, it is suggested that the present technique can only be applied to patellae with greater than 10 mm^3 wear. Comparison of the recreated volume to the design volume could act as a method of reducing this error. No assessment of this could be made in the present study since original component dimensions for the Insall-Burstein II prosthesis was not available. Precise measurement of volume change sustained by in vivo usage remains a challenging obstacle in the assessment of orthopaedic devices. Measurement of wear volume loss through gravimetric techniques has been used

Table 2. Frequency of Patellar Damage Modes Recorded for Samples in the Present Retrieval Study Compared to Those Reported in the Literature

	Present Study (*n* = 24)	Hood et al. [47] (*n* = 28)	Schwartz et al.[33] (*n* = 17)
Burnishing	100%	71%	76.5%
Pitting	88%	18%	0%
Scratching	75%	25%	17.6%
Delamination	67%	11%	70.6%
Surface deformation	50%	46%	35.3%
Embedded PMMA debris	0%	14%	[1]
Abrasion	0%	0%	0%

[1]Schwartz et al.[33] did not comment on the presence of embedded PMMA debris

extensively for in vitro simulator testing of orthopaedic joints[64–67] and remains the gold standard. Such methods are not suitable for measurement of UHMWPE components retrieved from patients.[68] The lack of soak control specimens, cement ingression, manufacturing tolerances, deviation from target dimensions, and the fact that material can be lost during retrieval are all reasons why this technique is not applicable. CM techniques have been used to successfully quantify the volume change in acetabular cups both in vitro and in vivo.[63,68,69] The application of micro-CT has been used to measure volume change in other polyethylene replacement joints and may prove to viable solution.[70,71]

The purpose of this study was to investigate the damage to patellar components in vivo. A series of 24 retrieved TKR prostheses consisting of nine designs of patellar button was analyzed. This study provides a preliminary assessment of the damage sustained to patellae in vivo. While the majority of samples were retrieved at revision, and therefore the reported damage may be closely related to the reason for revision, it is more likely that the general condition reflects that of components that are functioning well clinically. Damage to the patellar component of knee replacement has been shown to be significant in clinically well-functioning and dysfunctional knees irrespective of design. On average, the wear scar formed a band spanning in the mediolateral direction. Maximum linear penetration was located in the lateral region of the articular surface. In addition, grading of the damage indicated that it was more extreme in the lateral quadrant, although the method's lack of consideration of the chronological progression of wear reduces the confidence in this finding. The number of components in the study was too small to determine a difference in damage in all-polyethylene and metal-backed designs; however, the volume loss of all-polyethylene patellae has been shown to be significant.

ACKNOWLEDGMENTS

This study was funded by the EPSRC, DePuy International, Leeds, UK, and the Health Technologies Knowledge Transfer Network. The authors thank C. Esler, D. L. Shaw, and M. H. Stone for retrieval of the prostheses, and A. M. Eagles for technical support regarding metrological analysis.

REFERENCES

1. Clayton ML, Thirupathi R. Patellar complications after total condylar arthroplasty. Clin Orthop Relat Res. 1982;170:152–5.
2. Lewallen DG, Rand JA. Failure of metal-backed patellar components after total knee athroplasty. The Knee. 1995;2(1):37–41.
3. Francke EI, Lachiewicz PF. Failure of a cemented all-polyethylene patellar component of a press-fit condylar total knee arthroplasty. J Arthroplasty. 2000;15(2):234–7.
4. Thadani PJ, Vince KG, Ortaaslan SG, Blackburn DC, Cudiamat CV. Ten- to 12- year follow-up of the Insall-Burstein I total knee prosthesis - the Insall award. Clin Orthop Relat Res. 2000;380:17–29.
5. Hooper GJ. Patella complications. In: Hamelynck Kj SJB, editor. LCS mobile bearing arthroplasty: 25 years worldwide experience. New York: Springer; 2002. p. 260–3.
6. Jordan LR, Sorrells RB, Jordon LC, Olivo JL. The long-term results of a metal-backed mobile bearing patella. Clin Orthop Relat Res. 2005;436:111–8.
7. Calvisi V, Camillieri G, Lupparelli S. Resurfacing versus nonresurfacing the patella in total knee arthroplasty: a critical appraisal of the available evidence. Arch Orthop Trauma Surg. 2009;129(9):1261–70.
8. Bellemans J, Ries MD, Victor J. Total knee arthroplasty: a guide to get better performance. Berlin: Springer-Verlag; 2005.
9. Ranawat CS. Retrieval analysis of porous-coated components for total knee arthroplasty: a report of two cases. Clin Orthop Relat Res. 1986;209:244–8.
10. Verlinden C, Uvin P, Labey L, Luyckx JP, Bellemans J, Vandenneucker H. The influence of malrotation of the femoral component in total knee replacement on the mechanics of patellofemoral contact during gait: an in vitro biomechanical study. J Bone Joint Surg-Br Vol. 2010;92(5):737–42.

11. Brick GW, Scott RD. The patellofemoral component of total knee arthroplasty. Clin Orthop Relat Res. 1988;231:163–78.
12. Boyd AD, Ewald FC, Thomas WH, Poss R, Sledge CB. Long-term complications after total knee arthroplasty with or without resurfacing of the patella. J Bone Joint Surg. 1993;75A(5):674–81.
13. Berry DJ, Rand JA. Isolated patellar component revision of total knee arthroplasty. Clin Orthop Relat Res. 1993;286:110–5.
14. Leopold SS, Silverton CD, Barden RM, Rosenberg AG. Isolated revision of the patellar component in total knee arthroplasty. J Bone Joint Surg. 2003;85A(1):41–7.
15. Doolittle 2nd KH, Turner RH. Patellofemoral problems following total knee arthroplasty. Orthop Rev. 1988;17(7):696–702.
16. Lygre SHL, Espehaug B, Havelin LI, Vollset SE, Furnes O. Failures of total knee arthroplasties with or without patella resurfacing. a study with 0-15 years follow-up from the Norwegian Arthroplasty Register. Acta Orthop. 2011;Accepted.
17. Robertsson O, Bizjajeva S, Fenstad AM, Furnes O, Lidgren L, Mehnert F, et al. Knee arthroplasty in Denmark, Norway and Sweden. Acta Orthop. 2010;81(1):82–9.
18. Clements WJ, Miller L, Whitehouse SL, Graves SE, Ryan P, Crawford RW. Early outcomes of patella resurfacing in total knee arthroplasty. Acta Orthop. 2010;81(1):108–13.
19. National Joint Registry for England and Wales. 7th Annual Report: Surgical data to December 2009. 2010.
20. Amenábar PP, Carrión M, Apablaza D, Paulos J. Artroplastia total de rodilla en pacientes con artritis reumatoide. Rev mé Chile. 2004;132(3):337–45.
21. Andersen HN, Ernst C, Frandsen PA. Polyethylene failure of metal-backed patellar components—111 AGC total knees followed for 7-22 months. Acta Orthop Scand. 1991;62(1):1–3.
22. Bayley JC, Scott RD, Ewald FC, Holmes GB. Failure of the metal backed patellar component after total knee arthroplasty. J Bone Joint Surg Am. 1988;70:668–74.
23. Rosenberg AG, Andriacchi TP, Barden R, Galante JO. Patellar component failure in cementless total knee arthroplasty. Clin Orthop Relat Res. 1988;236:106–14.
24. Stulberg SD, Stulber BN, Hamati Y, Tsao A. Failure mechanisms of metal-backed patellar components. Clin Orthop Relat Res. 1988;236:88–105.
25. Felmet.G, de Nicola U, Springorum HW. Failure of metal-backed uncemented patellar components—report on 3 cases. Acta Orthop Scand. 1989;60(6):715–7.
26. Huang CH, Liau JJ, Ho FY, Lin CY, Young TY, Cheng CK. Polyethylene failure of the patellar component in New Jersey low -contact stress total knee arthroplasties. J Arthroplasty. 2005;20(2):202–8.
27. Collier JP, McNamara JL, Surprenant VA, Jensen RE, Surprenant HP. All-polyethylene patellar components are not the answer. Clin Orthop Relat Res. 1991;273:198–203.
28. Tsao A, Mintz L, McRae CR, Stulberg D, Wright T. Failure of the porous-coated anatomic prosthesis in total knee arthroplasty due to severe polyethylene wear. J Bone Joint Surg. 1993;75A(1):19-26.
29. Cheal EJ, Gerhart TN, Hayes WC, editors. Failure analysis of a porous coated patellar component; New York: American Society of Mechanical Engineers; 1988
30. Sutherland CJ. Patellar Component Dissociation in Total Knee Arthroplasty A Report of Two Cases. Clin Orthop Relat Res. 1988;228:178–81.
31. Lombardi AV, Engh GA, Volz RG, Albrigo JL, Brainard BJ. Fracture/dissociation of the polyethylene in metal backed patellar components in total knee arthroplasty. J Bone Joint Surg Am. 1988;70(5):675–9.
32. Piraino D, Richmond B, Freed H, Belhobek G, Schils J, Stulberg B. Total knee replacement: radiologic findings in failure of porous-coated metal-backed patellar component. Am J Roentgenol. 1990;155(3):555–8.
33. Schwartz O, Aunallah J, Levitin M, Mendes DG. Wear pattern of retrieved patellar implants. Acta Orthop Belgica. 2002;68(4): 362–9.
34. Wright TM, Bartel DL. The problem of surface damage in polyethylene total knee components. Clin Orthop Relat Res. 1986;205:67–74.

35. Hsu HP, Walker PS. Wear and deformation of patellar components in total knee arthroplasty. Clin Orthop Relat Res. 1989;246:260–5.
36. Ellison P, Barton DC, Esler C, Shaw DL, Stone MH, Fisher J. In vitro simulation and quantification of wear within the patellofemoral joint replacement. J Biomech. 2008;41(7):1407–16.
37. Ellison P, Barton DC, Farrar R, Stone M, Fisher J, editors. Simulation of wear within the patellofemoral joint of total knee replacements. 52nd Annual Meeting of the Orthopaedic Research Society; 2006 March 19–22, 2006; Chicago, IL. Orthopaedic Research Society.
38. Burroughs BR, Rubash HE, Estok DM, Jasty M, Krevolin J, Muratoglu OK. Comparison of conventional and highly crosslinked UHMWPE patellae evaluated by a new in vitro patellofemoral joint simulator. J Biomed Mat Res B. 2006;79B:268–74.
39. Korduba LA, Longaray J, Lancin P, Essner A, Wang A, Meneghini RM, editors. Development of an aggressive wear test for patellar implants. 54th Annual Meeting of the Orthopaedic Research Society; San Francisco. Orthopaedic Research Society; 2008.
40. Ellison P, Tipper J, Jennings LM, Fisher J, editors. Resurfacing the patella increases osteolytic potential. 56nd Annual Meeting of Orthopaedic Research Soc; 2010 March 7–10. New Orleans. Orthopaedic Research Society; 2010
41. Dowling JM, Atkinson JR, Dowson D, Charnley J. The characteristics of acetabular cups worn in the human body. J Bone Joint Surg. 1978;60B(3):375–82.
42. Rostoker W, Chao EYS, Galante JO. The appearances of wear on polyethylene - a comparison of in vivo and in vitro wear surfaces. J Biomed Mat Res. 1978;12:317–35.
43. Nusbaum HJ, Rose RM, Paul IL, Crugnola AM. Wear mechanisms for ultrahigh molecular weight polyethylene in the total hip prosthesis. J Appl Polym Sci. 1979;23:777–89.
44. Rose RM, Nusbaum HJ, Schneider H, Ries SB, Paul I, Crugnola A, et al. On the true wear rate of ultra high-molecular-weight polyethylene in the total hip prosthesis. J Bone Joint Surg. 1980;62:537–49.
45. Rose RM, Crugnola A, Ries M, Cimino WR, Radin EL. On the origins of high in vivo wear rates in polyethylene components of total joint prostheses. Clin Orthop Relat Res. 1979;145:277–86.
46. Wroblewski BM. Wear of high-density polyethylene on bone and cartilage. J Bone Joint Surg. 1979;61B(4):498–500.
47. Hood RW, Wright TM, Burstein AH. Retrieval analysis of total knee prostheses: a method and its application to 48 total condylar prostheses. J Biomed Mat Res. 1983;17:829–42.
48. Wright TM, Astion DJ, Bansal M, Rimnac CM, Green T, Insall JN, et al. Failure of carbon fiber-reinforced polyethylene total knee-replacement components—a report of two cases. J Bone Joint SurgAm. 1988;70:926–32.
49. McDonald MD, Bloebaum RD. Distinguishing wear and creep in clinically retrieved polyethylene inserts. J Biomed Mat Res. 1995;29:1–7.
50. Wang A, Stark C, Dumbleton JH. Role of cyclic plastic deformation in the wear of UHMWPE acetabular cups. J Biomed Mat Res. 1995;29:619–26.
51. Bell CJ, Walker PS, Abeysundera MR, Simmons JMH, King PM, Blunn GW. Effect of oxidation on delamination of ultrahigh-molecular-weight polyethylene tibial components. J Arthroplasty. 1998;13(3):280–90.
52. Que L, Topoleski LDT, Parks NL. Surface roughness of retrieved CoCrMo alloy femoral components from PCA artificial total knee joints. J Biomed Mat Res. 2000;53:111–8.
53. Blunn GW, Joshi AB, Lilley PA, Engelbrecht E, Ryd L, Lidgren L, et al. Polyethylene wear in unicondylar knee prostheses. Acta Orthop. 1992;63(3):247–55.
54. Hood RW, Wright TM, Burstein AH, Insall JN, editors. Retrieval analysis of twenty polyethylene patellar buttons. Proc 27th Annual Meeting Orthopaedic; 1981 February 24–26, Las Vegas. Orthopaedic Research Society; 1981.
55. Walker PS, Gold BL. The tribology (friction, lubrication and wear) of all-metal artificial hip joints. Clin Orthop Relat Res. 1996;329S: S4–S10.
56. Blunn GW, Joshi AB, Minns RJ, Lidgren L, Lilley SP, Ryd L, et al. Wear in retrieved condylar knee arthroplasties - a comparison of wear in

different designs of 280 retrieved condylar knee prostheses. J Arthroplasty. 1997;12(3):281–90.
57. Wilcoxon F. Individual comparisons by ranking methods. Biomet Bull. 1945;1(6):80–3.
58. ISO 14242-2 – Implants for surgery—wear of total hip-joint prostheses. Part 2: methods of measurement. ISO; 2000.
59. McGovern TE, Black J, Jacobs JJ, Graham RM, LaBerge M. In vivo wear of Ti6A14V femoral heads—a retrieval study. J Biomed Mat Res. 1996;32:447–57.
60. Nasser S, Campbell PA, Kilgus D, Kossovsky NIR, Amstutz HC. Cementless total joint arthroplasty prostheses with titanium-alloy articular surfaces: a human retrieval analysis. Clin Orthop Relat Res. 1990;261:171–85.
61. Lafortune MA, Cavanagh PR. Three-dimensional kinematics of the patella during walking. In: Johnson B, editor.: Champaign; 1987. p. 337–42.
62. Mann HB, Whitney DR. On a test of whether one or two random variables is stochastically larger than the other. Ann Math Stat. 1947;18(1):50–60.
63. Derbyshire B, Hardaker CS, Fisher J, Brummitt EIK. Assessment of the change in volume of acetabular cups using a coordinate measuring machine. Proc Inst Mech Eng H. 1994;208:151–8.
64. Dowson D, Jobbins B. Design and development of a versatile hip joint simulator and a preliminary assessment of wear and creep in Charnley total replacement hip joints. Eng Med. 1988;17(3):111–7.
65. Barnett PI, McEwen HM, Auger DD, Stone MH, Ingham E, Fisher J. Investigation of wear of knee prostheses in a new displacement/force-controlled simulator. Proc Inst Mech EngH. 2002;216:51–61.
66. Liao YS, McKellop H, Lu Z, Campbell P, Benya P. The effect of frictional heating and forced cooling on the serum lubricant and wear of UHMW polyethylene cups against cobalt-chromium and zirconia balls. Biomaterials. 2003;24(18):3047–59.
67. McEwen HMJ, Barnett PI, Bell CJ, Farrar R, Auger DD, Stone MHFJ. The influence of design, materials and kinematics on the in vitro wear of total knee replacements. J Biomech. 2005;38:357–65.
68. Hall RM, Craig PS, Hardaker C, Siney PD. Measurement of wear in retrieved acetabular sockets. Proc Inst Mech Eng H. 1995(209): 233–42.
69. Dowson D, Jobbins B, Seyed-Harraf A. An evaluation of the penetration of ceramic femoral heads into polyethylene acetabular cups. Wear. 1993;162:880–9.
70. Kurtz SM, Peloza J, Siskey R, Villarraga ML. Analysis of a retrieved polyethylene total disc replacement component. Spine J. 2005;5(3): 344–50.
71. Teeter MG, Naudie DDR, Charron KD, Holdsworth DW. Highly cross-linked polyethylene acetabular liners retrieved four to five years after revision surgery: A report of two cases. J Mech Behav Biomed Mater. 2010;3(6):464–9.

Journal of Long-Term Effects of Medical Implants, 20(1): 73–79 (2010)

Patellar Button Wear Patterns in Well-Functioning Total Knee Arthroplasty Retrievals

Jason A. Lindsey,[2] Devin Conner,[2] Peter Godleski,[1] Brian Perkinson,[1] William M. Mihalko,[1, 3,] & John L. Williams[2, 3]*

[1]University of Tennessee Health Science Center, Campbell Clinic Orthopaedics, Memphis, TN; [2]University of Memphis, Department of Biomedical Engineering, Memphis, TN; [3]InMotion Orthopaedic Research Center, Memphis TN

*Address all correspondence to William M. Mihalko, MD PhD, 1458 W. Poplar Avenue, Suite 100, Memphis, TN 38017; Tel.: 901-759-5512; Fax: 901-759-5571; wmihalko@campbellclinic.com.

ABSTRACT: One of the common reasons for early revision or poor outcome in total knee arthroplasty is due to patellar maltracking, loosening, or pain. The analysis of how the patellofemoral mechanism operates and wears in vivo has not been a focus of many retrieval studies. This paper describes the wear pattern observed on patellar buttons from well-functioning TKA specimens that were harvested as part of a donor program. The attempt was to describe the variations in wear patterns to see if any commonalities existed that may predict a well-functioning patellofemoral mechanism after TKA.

KEY WORDS: knee arthroplasty, patella button, retrieval analysis

I. INTRODUCTION

The exponential increase of the number of total knee arthroplasty cases being performed in the United States is well documented.[1] The current political environment has also put the spotlight on the health care system and the increasing costs that have occurred in the last decade. These two issues have heightened the awareness of outcomes and technology use in medicine. One of the most common reasons for revision surgery after total knee arthroplasty is for issues pertaining to the patellofemoral mechanism.[2–10] Many of these issues include patellar instability, aseptic loosening, and periprosthetic fracture. Studying all the aspects of the current wear issues from patellafemoral designs as well as those pertaining to surgical technique will give helpful information to improving the wear and longevity of TKA patellofemoral mechanism.

Revision surgery is costly to the health care system and the fact that few surgeons are specializing in total joint arthroplasty means that as the demand rises, there will be a larger percentage of primary total knee arthroplasty (TKA) cases being performed by surgeons doing fewer than 25 cases per year.[1] The outcomes of total knee arthroplasty have been linked to the number of cases being performed per year, which means any designs that are susceptible to poor mechanical alignment may see a significant decline in survivorship in the next decade.

Many studies pertaining to the forces, kinematics, and wear observed from the patellar button articulation with the femoral component after total knee arthroplasty have been reported.[11–24] Although these multiple studies have given insight into the forces and kinematics of the joint, there continues to be failures from both design- and surgical technique–related issues after TKA.

By utilizing retrieval analysis studies for failed implants, we can document the issues related to early failures whether they are surgical or design related. But the opposite holds true for the well-functioning

retrieval analysis study. When wear patterns and design/surgical technique parameters are studied, we can also conclude how issues pertaining to wear and surgical technique can optimize outcomes.

This study attempts to describe the common wear patterns from 13 different patellar buttons either retrieved postmortem or at time of removal for infection from well-functioning TKAs. The hypothesis is that similar patterns would be seen with similar areas of wear on the lateral and medial sides of the button.

II. METHODS

The local retrieval program at the Medical Education and Research Institute (Memphis, Tennessee) has been set up though our laboratory and was utilized as the source of the specimens in this study. Each lower extremity was harvested and transported utilizing ASTM standards (ASTM F561-05a). Each knee was harvested through a midline incision and medial parapatellar approach (Fig. 1). A thin osteotome was utilized to remove all patellar buttons with care, making sure not to affect the surface of the button during removal. The lateral edge of the button was marked along with the side of the knee arthroplasty for analysis after removal.

Once removed, the buttons were cleaned and put into a freezer (–20°C) to prevent any further oxidation. The buttons were then removed and the outline of the wear scar was marked under visual guidance by an erasable marker (Dry erase marker, Expo Visa-Vis, Oak Brook, Illinois). The quadrant of the wear scar was documented according to the four quadrants (Fig. 2) described by Hood et al.[25] A solid line was placed to outline the extreme margins of the wear scar and to delineate the total wear area. Within the outlines of each wear scar, a dotted outline was made to mark any areas that showed deeper wear patterns and delineate the total deep wear area (Figs. 3A–3C). Each patellar button was photographed using the macro function of a 7.2 megapixel camera (CyberShot Sony Inc, New York, New York). The orientation of the button was outlined with a ruler for scale and the JPEG images were saved. The JPEG images were then imported into a photo analysis software (Aperio ImageScope, ver 2.1, Aperio Technologies, Inc, Vista, California). The outline of the wear scar and the number of pixels within the outline was calculated and converted to square millimeters for each quadrant (Table 1). The proportional wear area and deep wear area within each patellar quadrant was determined as a ratio to the total patellar wear area and the total patellar deep wear area. ANOVA and Tukey-Kramer HSD post hoc tests were performed to compare the areas within each quadrant. Any patterns that were noted for any of the but-

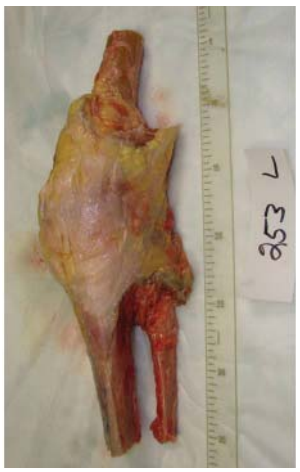

FIGURE 1. Example of one of the en bloc postmortem retrieval specimens utilized for the study.

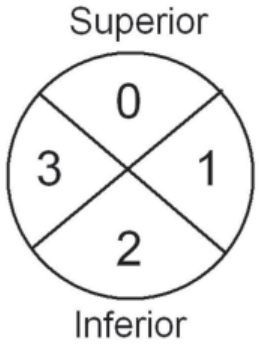

FIGURE 2. Wear quadrants of the polyethylene button utilized for description of the wear scars. The lateral quadrant was always considered quadrant 1.

tons were also recorded and the number of buttons exhibiting this pattern documented.

III. RESULTS

Once the patellar buttons were analyzed, three wear scar patterns were observed (Figs. 3A–3C). These included a stripe wear pattern (Fig. 3A) that was thinner and stretched across the entire button from medial to lateral and mainly in quadrants 1 (lateral) and 3 (medial); a more global or "bow tie"[26] wear pattern (Fig. 3B) that saw substantial wear in all quadrants; and a lateral wear pattern with mainly wear in one quadrant (Fig. 3C). The individual quadrant and overall wear scar areas are listed in Table I. The quadrant with the highest area of wear scar was the lateral quadrant, which showed a significantly greater proportional wear area than the superior or inferior quadrants. The resulting pattern did not seem to follow any correlation with superior-inferior or medial-lateral placement of the patellar buttons as observed at time of harvesting or on fluoroscopic image inspection, except one that exhibited lateral-superior wear (Figs. 3C and 4C). This fluoroscopic lateral view reveals a patellar baha with higher flexion, which resulted in the more superior and lateral wear pattern. One patella saw a superior-to-inferior stripe wear pattern, but was the only button that had a high central peak to the button and a shallow trochlear design, which allowed for the resulting wear scar. One patellar button also revealed a medial quadrant major wear pattern as well. Three asymmetric and 10 round patellar buttons were analyzed in this group, and no wear pattern was specific to the type of patella. The lateral quadrant had more proportional deep wear area (p = 0.005) than any other quadrant (Fig. 5).

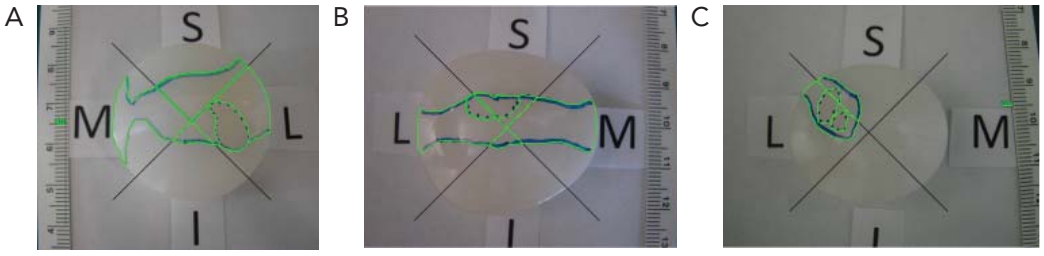

FIGURE 3. (A) Example of a polyethylene button that exhibited a medial-to-lateral stripe type of wear pattern with equal area of the wear scar in quadrants 1 and 3. **(B)** Example of a polytheylene button that exhibited global wear with the wear scar extending into three or more quadrants. **(C)** An example of a polyethylene button that exhibited mostly lateral quadrant wear.

Table 1. Summary of the overall wear scar area and ratio of the wear in each quadrant to the total wear. Means and 95% confidence intervals for each quadrant are descibed.

Knee	Total Wear (mm^2)	Inferior/ Total Wear	Superior/ Total Wear	Lateral/ Total Wear	Medial/ Total Wear
DePuy PFC Sigma FB PS	321.5	0	0.33	0	0
Osteonics Series 700 PS	160.1	0	0.31	1	0
Intermedics Natural Knee System CR	200.5	0.25	0.14	0.38	0.23
Howmedica Duracon CR	502.7	0.04	0.14	0.39	0.44
Richards Genesis CR	335.9	0	0.30	0	0
Zimmer NexGen LPS CR	199.4	0	0.18	0	0
Smith & Nephew Genesis II CR	607.9	0.05	0.25	0.41	0.29
DePuy AMK CR	572.6	0.00	0.25	0.41	0.31
Stryker Scorpio PS	390.2	0.09	0.08	0.40	0.40
DePuy PFC Sigma FB CR	573.2	0.37	0.38	0.08	0.17
Zimmer NexGen LPS CR	280.9	0.00	0.07	0.00	0.98
Zimmer NexGen LPS CR	488.4	0.00	0.32	0.45	0.26
Smith & Nephew Genesis	293.0	0.26	0.01	0.44	0.29
	Mean	0.08	0.21	0.32	0.34
	Lower 95%	-0.010	0.121	0.280	0.245
	Upper 95%	0.174	0.304	0.464	0.429

IV. DISCUSSION

Many variables may affect patellar implant survival in total knee arthroplasty. Biomaterials, patellar geometry, unique patient anatomical characteristics, surgical technique, and implant design all contribute to the long-term outcome of the patella implant. This report has determined that in a consecutive number of well-functioning retrievals obtained at time of necropsy, the lateral quadrant had a significantly greater wear scar area and there were three distinct wear scar patterns in these well-functioning TKAs.

Reports in the literature have shown a variety of wear patterns in the failed patellar prosthesis. Schwartz et al. showed a high incidence of wear in retrieved patellar components from failed arthroplasties.[26] Four modes of damage were seen, specifically cold flow, polishing, delamination, and scratching of the patellar polyethylene surface. It was felt that the high incidence of wear represented a basic deficiency in the patellar implant design, particularly inadequate thickness and nonconforming articulating surfaces, which led to high contact stress and therefore a higher failure rate.

The current study sought to evaluate the patellar wear patterns seen in a variety of implants retrieved from well-functioning knees. Three specific types of wear patterns were identified, namely, stripe, bow tie, and lateral. The striped, bow tie, and

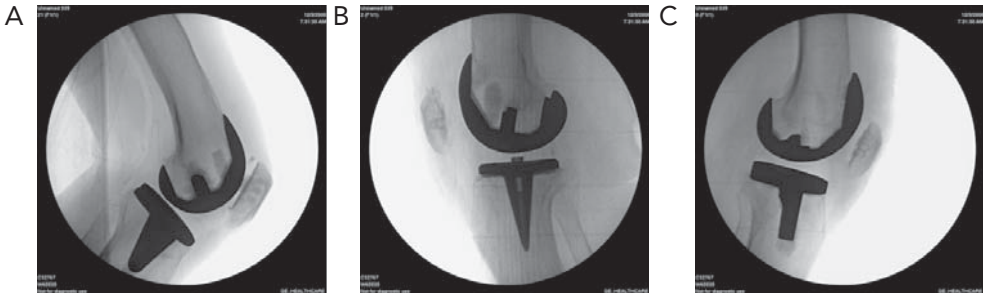

FIGURE 4. (A) Lateral fluoroscopic view of the specimen in Fig. 3A showing the patellar position and height. **(B)** Lateral fluoroscopic view of the specimen in Fig. 3B showing the patellar position and height. **(C)** Lateral fluoroscopic view of the specimen in Fig. 3C that shows a patellar baha position and a flexed patella, which explains the observed superior-lateral wear scar.

predominently lateral wear patterns were identified in well-funtioning knees. These patterns were similar to those seen in implants retrieved for failed components.

Certainly, component position was at times an obvious factor involving the location of wear on the patella (as in the example of the superiorly located wear seen in the case with patella baha in Fig. 4C). Otherwise, wear pattern was not suggestive of implant design.

Nonetheless, no specific difference of patterns was seen in these implants retrieved from well-functioning knee replacements versus those retrieved from implant failures as described in the literature. The "bow tie" pattern seen by Schwartz was similar to the medial-lateral diffuse pattern seen in the current study. Furthermore, it was noted that based on the ANOVA results in this study, the lateral quadrant had significantly more wear on average than any other quadrant, suggesting that in summation of all of a variety of factors, contact forces in the lateral patellar articulation are on the average higher than anywhere else in the patello-femoral implant articulation.

Obviously, there are downfalls to this study since we have small numbers that incorporate many implant designs. The study does however give a comparison of well-functioning patellar buttons to

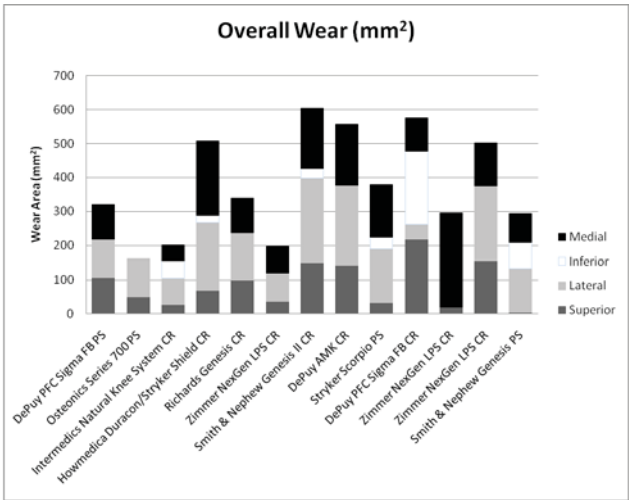

FIGURE 5. Overall wear measured for each patellar button with breakdown by quadrant.

those that were obtained at time of revision surgery and seem to be very comparable. This may simply mean that the failures of the TKA in other studies were simply not due to patellofemoral issues and therefore did not differ.

This study has of course inherent limitations. The relatively small number of samples consisted of a variety of implants types of mobile and fixed bearing total knee replacement designs, and the patella buttons varied in geometry and included round and oval shaped designs and one metal-backed patellar component. Even so, characteristic patterns of wear seen were similar to those reported in the literature for failed patellar implants. This study gives insight into the issues of offset wear and lack of patellar mobility. This lack of patellar mobility can decrease the wear scar area and may increase the contact stresses, thus theoretically increasing wear and the possibility of failure of the patellar button. No difference in these patterns was found in those implants retrieved from well-functioning knees versus those found at the time of revision surgery for failed implants.

REFERENCES

1. Kurtz S, Ong K, Lau E, Mowat F, Halpern M. Projections of primary and revision hip and knee arthroplasty in the US from 2005 to 2030. J Bone Joint Surg. 2007;89A:780–5.
2. Sharkey PF, Hozack WJ, Rothman RH, Shastri S, Jacoby SM. Insall Award paper. Why are total knee arthroplasties failing today? Clin Orthop Relat Res. 2002 Nov;(404):7–13.
3. Anglin C, Brimacombe JM, Wilson DR, Masri BA, Greidanus NV, Tonetti J, Hodgson AJ. Biomechanical consequences of patellar component medialization in total knee arthroplasty. J Arthroplasty. 2010 Aug;25(5):793–802. Epub 2009 Jul 29.
4. Kessler O, Patil S, Colwell CW Jr, D'Lima DD. The effect of femoral component malrotation on patellar biomechanics. J Biomech. 2008 Dec 5;41(16):3332–9.
5. Ma HM, Lu YC, Kwok TG, Ho FY, Huang CY, Huang CH. The effect of the design of the femoral component on the conformity of the patellofemoral joint in total knee replacement. J Bone Joint Surg Br. 2007 Mar;89(3):408–12.
6. Berti L, Benedetti MG, Ensini A, Catani F, Giannini S. Clinical and biomechanical assessment of patella resurfacing in total knee arthroplasty. Clin Biomech (Bristol, Avon). 2006 Jul;21(6):610–6. Epub 2006 Mar 3.
7. Amis AA, Senavongse W, Darcy P. Biomechanics of patellofemoral joint prostheses. Clin Orthop Relat Res. 2005 Jul;436:20–9. Review.
8. Stiehl JB. A clinical overview patellofemoral joint and application to total knee arthroplasty. J Biomech. 2005 Feb;38(2):209–14. Review.
9. Berger RA, Crossett LS, Jacobs JJ, Rubash HE. Malrotation causing patellofemoral complications after total knee arthroplasty. Clin Orthop Relat Res. 1998 Nov;(356):144–53.
10. Fehring TK Rotational malalignment of the femoral component in total knee arthroplasty. Clin Orthop Relat Res. 2000 Nov;(380):72–9.
11. Werner FW, Ayers DC, Maletsky LP, Rullkoetter PJ. The effect of valgus/varus malalignment on load distribution in total knee replacements. J Biomech. 2005 Feb;38(2):349–55.
12. Youm YS, Cho WS, Woo JH, Kim BK. The effect of patellar thickness changes on patellar tilt in total knee arthroplasty. Knee Surg Sports Traumatol Arthrosc. 2010 Jul;18(7):923–7. Epub 2010 Mar 9.
13. Becher C, Heyse TJ, Kron N, Ostermeier S, Hurschler C, Schofer MD, Fuchs-Winkelmann S, Tibesku CO. Posterior stabilized TKA reduce patellofemoral contact pressure compared with cruciate retaining TKA in vitro. Knee Surg Sports Traumatol Arthrosc. 2009 Oct;17(10):1159–65.
14. Leszko F, Sharma A, Komistek RD, Mahfouz MR, Cates HE, Scuderi GR. Comparison of in vivo patellofemoral kinematics for subjects having high-flexion total knee arthroplasty implant with patients having normal knees. J Arthroplasty. 2010 Apr;25(3):398–404. Epub 2009 Feb 20.
15. Carpenter RD, Brilhault J, Majumdar S, Ries MD. Magnetic resonance imaging of in vivo patellofemoral kinematics after total knee arthroplasty. Knee. 2009 Oct;16(5):332–6. Epub 2009 Feb 1.

16. Anglin C, Ho KC, Briard JL, de Lambilly C, Plaskos C, Nodwell E, Stindel E. In vivo patellar kinematics during total knee arthroplasty. Comput Aided Surg. 2008 Nov;13(6):377–91.
17. Anglin C, Brimacombe JM, Hodgson AJ, Masri BA, Greidanus NV, Tonetti J, Wilson DR. Determinants of patellar tracking in total knee arthroplasty. Clin Biomech (Bristol, Avon). 2008 Aug;23(7):900–10. Epub 2008 Jun 5.
18. Sharma A, Leszko F, Komistek RD, Scuderi GR, Cates HE Jr, Liu F. In vivo patellofemoral forces in high flexion total knee arthroplasty. J Biomech. 2008;41(3):642–8.
19. Anglin C, Brimacombe JM, Wilson DR, Masri BA, Greidanus NV, Tonetti J, Hodgson AJ. Intraoperative vs. weightbearing patellar kinematics in total knee arthroplasty: a cadaveric study. Clin Biomech (Bristol, Avon). 2008 Jan;23(1):60–70. Epub 2007 Oct 24.
20. Hollinghurst D, Stoney J, Ward T, Pandit H, Beard D, Murray DW. In vivo sagittal plane kinematics of the Avon patellofemoral arthroplasty. J Arthroplasty. 2007 Jan;22(1):117–21.
21. Ostermeier S, Buhrmester O, Hurschler C, Stukenborg-Colsman C. Dynamic in vitro measurement of patellar movement after total knee arthroplasty: an in vitro study. BMC Musculoskelet Disord. 2005;6:30. Published online 2005 June 15. doi: 10.1186/1471-2474-6-30. Available from: http://www.biomedcentral.com/1471-2474/6/30.
22. Zavatsky AB, Oppold PT, Price AJ. Simultaneous in vitro measurement of patellofemoral kinematics and forces. J Biomech Eng. 2004 Jun;126(3):351–6.
23. Asano T, Akagi M, Koike K, Nakamura T. In vivo three-dimensional patellar tracking on the femur. Clin Orthop Relat Res. 2003 Aug;(413):222–32.
24. Stiehl JB, Komistek RD, Dennis DA, Keblish PA. Kinematics of the patellofemoral joint in total knee arthroplasty. J Arthroplasty. 2001 Sep;16(6):706–14.
25. Hood RW, Wright TM, Burstein AH Retrieval analysis of total knee prosthesis: a method and its application to 48 total condylar prostheses. J Biomed Mater Res. 1983 Sep;17(5);829–4.
26. Schwartz o, Aunallah J, Levitin M, Mendes DG Wear patterns of retrieved patellar implants, Acta Orthop Belg. 2002, 68:4:362–9.

Journal of Long-Term Effects of Medical Implants, 20(1): 81–85 (2010)

Human Postmortem Device Retrieval and Analysis—Orthopaedic, Cardiovascular, and Dental Systems

J. Lemons, B. Brott, & A. Eberhardt*

Departments of Prosthodontics, Medicine and Biomedical Engineering, Schools of Dentistry, Medicine and Engineering, University of Alabama at Birmingham, Birmingham, AL

*Address all correspondence to Dr. Jack Lemons, University of Alabama at Birmingham, Departments of Prosthodontics, Medicine and Biomedical Engineering, Schools of Dentistry, Medicine and Engineering, Box 61 SDB/UAB, Birmingham, AL; Jack.Lemons@ortho.uab.edu

ABSTRACT: On the basis of decades of analyzing implant devices, tissues, and clinical records from revision surgical explants (called device failure), studies now include postmortem donors and in situ conditions (called success). A key issue has been information exchange from an interdisciplinary team where basic physical and biological studies complement details of the clinical conditions for each device. Overall, the summary information has shown that most revisions were based on factors associated with the patient health, disease, and compliance, with few outcomes directly correlated with technology and device-specific factors. However, because of the large numbers of devices implanted annually (millions), any sampling that reveals adverse circumstances could result in a high level of importance and the need for additional studies of this type. Experience from prior retrieval and analysis demonstrates significant value where peer reviewed results from investigations have altered the discipline and have improved the quality and longevity of health care associated with implanted devices. This report summarizes completed and ongoing studies of cardiovascular, dental, and orthopaedic systems. Endovascular stents from autopsies showed damage including fretting and corrosion from overlapping and intersecting conditions, plus some corrosion and element transfers to tissues from individual stents. Studies are proposed to increase numbers to evaluate clinical significance. Dental implants from postmortem donors that functioned more than 10 years provided evaluations of cobalt alloy devices and calcium phosphate bone graft substitutes originally investigated in the 1970s. Tissue integration and stability correlated with data from prior laboratory in vitro and in vivo investigations. Studies of articulation and fixation from orthopaedic total joint arthroplasties showed some limitations related to surface changes of YTZ zirconia, specific damage due to implantation procedures, which led to modified instrumentation and techniques, and several examples of conditions leading to longer-term device-to-bone fixation. These types of multidisciplinary studies are continuing.

KEY WORDS: device, retrieval, orthopaedic, cardiovascular, dental systems

I. INTRODUCTION

Recommendations have been made during national and international consensus conferences for surgical implant device retrieval and analysis (DRA), with these recommendations evolving on a regular basis since the 1970s.[1–5] A significant result from study outcomes have been contributions to the enhancement of clinical outcomes, plus the evolution of published consensus standards for detailed data to be collected.[6,7] A central research theme over past decades has been physical and biological science investigations of devices, tissues, and records associated with devices explanted during revision surgery procedures. An expanded

approach was introduced in 2005 where devices and records were obtained as postmortem samples from human organ-tissue-device donations.[8] This approach permitted comparisons of conditions at revision (called failure) with postmortem en bloc conditions (called success). Overall, the intent of most programs has been to answer the question: What are the relationships of device biomaterial and biodesign to the existing clinical circumstances as related to longer-term in vivo function, plus can improvements be recommended?[8,9]

II. METHODS

Programs conducting human surgical implant DRA must maintain detailed IRB and HIPAA compliance, have facilities for physical and biological studies, have experience for in vitro and in vivo clinical analyses, and have resources for multidisciplinary investigations.[8] The program associated with this report has conducted DRA since the early 1970s and conducted the NIH-sponsored study from 2005 to 2010. The details of protocols and results from recent activities have been published, and the reader is referred to these publications plus the ASTM F04 and ISOTC 150 consensus standards.[6,7,9–29] This report reviews examples from investigations on human postmortem specimens from endovascular stents obtained from autopsies,[20–23] dental implants from patient donations,[24–29] and specimens from en bloc orthopaedic total joint arthroplasty (TJA) revisions and donations.[9–19]

III. RESULTS AND DISCUSSION

Overall, the experience gained over decades leads to a strong opinion supporting the role of human surgical implant DRA as a component of enhancing the treatment of individuals needing a procedure including a device. Clearly, the discipline has been evolving from devices constructed from synthetic origin biomaterials to biologic and synthetic combinations leading eventually to implants for tissue regeneration, i.e., tissue engineered medical products (TEMPs)[30] Many have taken the position that devices constructed from synthetic biomaterials will remain as a part of reconstructive procedures (millions per year) over the next decades. In this regard, most programs conducting DRA include analyses of all types of implants, no matter what the origin.

Considerations of the relative significance of DRA studies for devices utilized in larger numbers per year raises multiple questions about statistical significance, which previously has been called "the issue of the numerator and denominator ratio." Those involved in the profession recognize that examples exist where a few study specimens resulted in a forensic discovery that was applicable to large numbers, e.g., altered alloy metallurgy, altered polyethylene structure/chemistry, inadequate control of manufacturing tolerances, etc. Therefore, investigations based on "forensic discovery" must be considered as a subset of analyses of patient treatment outcomes. For example, consideration of a specific device type application such as a total hip arthroplasty at 200,000 per year and a revision rate of 5% after two to five years results in a total sample size of 10,000 for "possible" DRA studies. Separation of factors from multidisciplinary experience into categories associated with the patient, the technology, and the device leads to further subdivision where changes of the device per se is less than 15% (10% anticipated and 5% unanticipated) or a potential overall number of 1500 per year. About 5%, or 75, of these specimens would represent circumstances where extensive examinations would be needed. Experience over decades also shows that conducting a program of this type represents a significant cost of time and finances (hundreds of thousands of dollars per year).

The central point of this example related to numbers, time, and cost is that DRA sampling should be targeted to conditions identified by clinical performance outcome assessments (unanticipated radiographic, pain, function, or other findings). It is also critical that detailed clinical records would be available so that the sample population for in-depth studies could be reduced for the development of in vitro data to determine device specific cause-effect relationships resulting in the need for a clinical revision.

Studies of postmortem endovascular stents have focused on a theme of conditions possibly influencing vascular restenosis. Overall results showed stent surface damage during in vivo function where stents overlapped or intersected, transfers of metallic elemental debris from pitting, fretting, and galvanic corrosion, and fractures and significantly complex stent-to-tissue interactions based in part on pre-existing disease pathology. Surprisingly, some stents without overlap demonstrated significant corrosion and metallic ion release into surrounding tissues. Interactions with surrounding tissues and local calcifications appear to play a significant role, with evidence of surface abrasions and fracture. Additional studies have included evaluation of fractures of drug-eluting stents with failure analysis, an area of current clinical interest. We have strongly recommended expansion of this program to focus on statistically significant numbers of DRA specimens to provide validated recommendations to the discipline.

Dental implant devices, tissues, and records from three edentulous mandibles treated with one implant design were obtained postmortem from donors. Each of these specimens had functioned successfully for about 11 years. Analyses extended to include bone and soft tissue–to-implant contact percentages, histological analyses of the anatomy after a decade, and multiple high-resolution studies of bone and implant-to-bone interface properties. These studies were quite special in that prior laboratory in vitro and in vivo studies had been conducted on one of the bone grafting biomaterials introduced in the early 1970s. The biomaterials and biodesigns for use were similar for this calcium phosphate–based substance, which provided comparisons of properties and tissue interfaces from laboratory in vivo (animal at 5 years) with human results at 11 years in vivo. Importantly, the human results were as intended with clinical applications exceeding expectations. Multiple examples of orthopaedic device revision DRA studies have been published, and two examples will be summarized. Zirconia ceramic was introduced for total hip arthoplasty (THA) femoral head components to minimize articulating damage to ultrahigh molecular weight polyethylene (UHMWPE). The zirconia was harder and smoother, and initially showed excellent outcomes. Over time and function, the zirconia surface was altered at the atomic level (tetragonal-to-monoclinic atomic transformation), which resulted in increased zirconia surface roughness and increased UHMWPE debris products. Studies based on DRA showed these unanticipated conditions and contributed to a device component recall and recommendations to minimize this clinical outcome. Another example relates to investigations of THA component interfaces with bone and biomaterial, and biomechanical properties associated with in vivo fixation stability. To further evaluate device-to-bone biointegration stability, specimens were obtained for tensile, shear, fatigue, and nanoindentation studies. These investigations remain in progress; however, recent results from postmortem specimens have shown conditions of stable biointegration for various surface biomaterials and biodesigns (porous and cemented with polymethylmethacrylate).

ACKNOWLEDGMENTS

We thank the National Institute of Biomedical Imaging and Bioengineering, NIBIB R01 EB001715 and Histomorphometry and Molecular Analysis Core Laboratory, NIH Grant P30-AR46031.

REFERENCES

1. Weinstein A, Gibbon D, Brown S, Ruff W, editors. Implant retrieval: material and biological analysis, NBS Spec. Pub. No. 601, Washington, DC: U.S. Government Printing Office; 1981.
2. Schnittmann P Shulman L. Dental implants: benefit and risk. National Health Service, Washington, DC. No. 81-1531; 1980.
3. Cochran D, Fritz M. Implant therapy I and II. Ann Periodontol. 1996;1(1):707–821.
4. Conference Statement and Proceedings, NIH Technology Assessment Conference on Improving Implant Performance through Retrieval Information: Challenges and Opportunities, 2000 Jan 10–12; NIH, Washington, DC.

5. Biomaterials and Medical Implant Sciences (BMIS) Workshop on Medical Implant Information, Performance and Policies, 2002 Sept 19–20; Washington, DC.
6. ASTM, Retrieval and analysis of medical devices and associated tissues and fluids, In: ASTM annual book of standards, Vol 13.01, ASTM FO4-561-05, W. Conshohoken, PA: American Society for Testing and Materials, 2005. p. 136–51.
7. ISO, Retrieval and analysis of surgical implants, ISO 12891-1,3, Geneva: International Organization for Standards; 2007.
8. Lemons J. Analysis of in situ and explanted surgical implant devices, PI, NIBIB-BRP 2005-2010.
9. Lemons J, Beck P, Lot, P, Cuckler J, Moore D, Petersen D, Eberhardt A. Evolving implant retrieval program, what's new, Am. Assoc. Ortho. Surg. Scientific Exhibit 41, Annual Meeting; 2008 March; San Francisco.
10. Chowdhury S, Vohra Y, Lemons J, Ueno M, Ikeda J. Accelerating aging of zirconia femoral head implants: change of surface structure and mechanical properties, J Biomed Mater Res B. 2007;81:486–92.
11. Stewart C, Eberhardt AW. Wear testing of zirconia coatings for applications in total hip replacement. Inquiro. 2008;2:71–5.
12. Eberhardt AW, McKee RT, Cuckler JM, Petersen D, Beck PR, Lemons JE. Surface roughness of CoCr and ZrO2 femoral heads with metal transfer: a retrieval and wear simulator study, International J Biomat. 2009. Article ID 185456, 6 pages, 2009.doi10.1155/2009/185456.
13. Santos EM, Vohra S, Catledge SA, McClenny MD, Moore KD. Examination of surface and materials properties of explanted zirconia heads. J Arthroplasty. 2004;19(7S):30–34.
14. Moore KD, Beck PR, Petersen DW, Cuckler JM, Lemons JE, Eberhardt AW. Early failure of a cross-linked polyethylene acetabular liner: a case report, J Bone Joint Surg. 2008;90: 2499–504.
15. Eberhardt AW, Moore KD, Cuckler JM, Beck PR, Lemons JE. Unanticipated failure of a crosslinked acetabular liner. Southern Meeting of the American Society of Biomechanics; 2008 Apr 27–29; Birmingham.
16. Miller MA, Eberhardt AW, Cleary RJ, Verdonschot N, Mann KA. Micro-mechanics of post-mortem retrieved cement-bone interfaces. J Orth Res. 2009; 170–7.
17. Miller MA, Eberhardt AW, Cleary RJ, Verdonschot N, Mann KA. Micro-mechanics of post-mortem retrieved cement-bone interfaces. Orthopedic Research Society; 2009 Feb 22–25; Las Vegas.
18. Miller MA, Eberhardt, AW, Cleary RJ, Verdonschot N, Mann KA. Micro-mechanics of post-mortem retrieved cement-bone interfaces, influence of interface morphology. ASME Summer Bioengineering Conference; 2009 June 25–29; Lake Tahoe.
19. Lemons J. Biological considerations of orthopaedic implants: implant retrieval, In: Lindsey R, editor. Orthopaedic implants, New York: Marcel Dekker; 2009.
20. Brott B, Lemons J, Halwani D, Anderson P, Anayiotos A. The clinical use of endovascular stents and long-term vascular compatibility, Proceedings of Workshop on Metallic Corrosion of Small Implants; 2007 May; Norfolk, VA. W Conshohoken, PA: American Society for Testing and Materials. Paper No. ASTM FO4.
21. Halwani D, Anderson P, Brott B, Anayiotos A, Lemons J. Local release of metallic elements from stents into vascular tissue and associated alterations of stent surfaces, Poster at 19th Annual Vascular Biology and Hypertension Symposium; Sept. 2008; Birmingham, AL.
22. Halwani DO, Anderson PG, Lemons JE, Jordan WD, Anayiotos AS, Brott BC. In vivo corrosion and local release of metallic ions from vascular stents into surrounding tissue. J Invas Cardiol. 2010;22:528–35.
23. Halwani DO, Anderson PG, Brott BC, Anayiotos AS, Lemons JE. Clinical device-related article surface characterization of explanted endovascular stents: evidence of in vivo corrosion. J Biomed Mater Res B. 2010;95(1):225–38.
24. Anabtawi M, Beck P, Bartolucci A, Morgan V, Lemons J. Histological analysis for forty one retrieved dental implants. 2007 Mar 19–23; AADR, New Orleans.
25. Lemons J, Carlson J, Risinger M, Shadix S, Bede P, Martin D. Histomorphometry of ca-

daveric implant hydroxapatite coatings and particulate, International Association of Dental Research; 2008; Toronto. Abstract Poster No. 2533.
26. Carlson J, Wang D, Anabtawi M, Martin D, Lemons J. Histomorphometric observations of bone integration from cadaveric subperiosteal mandibular implants. 2008 April; AADR, Dallas.
27. Beck P, Lemons J. Cadaveric specimen analysis of hydroxyapatite particulates, bone and subperiosteal implants. 2008; AADR, Dallas. Paper No. 1150P.
28. Chopra P, Johnson M, Nagy T, Lemons J. Microcomputed tomographic analysis of bone healing subsequent to graft placement, J Biomed Mater Res B. 2008 Oct. E-pub.
29. Baker MI, Eberhardt AW, Martin DM, McGwin G, Lemons JE. Bone properties surrounding hydroxyapatite-coated custom osseous integrated dental implants, J Biomed Mat Res B. 2010 Oct;95B(1), 218–24.
30. ASTM, Surgical implants. Vol 13.01; 2010; W Conshohoken, PA: American Society for Testing and Materials.

Meetings and Courses Calendar

The following announcements for a conference or a course might be of interest to the readers of this journal. For a new meeting to be listed, sent the information including e-mail addresses or URLs to:

Subrata Saha, Ph.D.
Editor-in-Chief, Journal of Long Term Effects of Medical Implants
Dir., Biomed. Eng. Prog., School of Graduate Studies
Res. Prof. & Dir., Musculoskeletal Res.
Dept. of Orthopaedic Surg. & Rehabilitation Med.
SUNY Downstate Medical Center
450 Clarkson Avenue - Box 30
Brooklyn, New York 11203
E-mail: subrata.saha@downstate.edu

February 2011

February 3-5, 2011
10th Annual Symposium on Current Concepts in Spinal Disorders
Bellagio Hotel
Las Vegas, Nevada
Phone: +1 310 423 5548
Fax: +1 310 423 0309
Web: http://www.csmc.edu/cme

February 12-17, 2011
SPIE Medical Imaging
Disney's Coronado Springs Resort
Lake Buena Vista, FL
Web: http://www.spie.org/micall

February 16-18, 2011
8th International Association of Science & Technology for Development (IASTED)
Conference on Biomedical Engineering (BioMed 2011)
Insbruck, Austria
Phone: +1 403 288 1195
Fax: +1 403 847 6851
E-mail: calgary@iasted.org
Web: http://www.iasted.org

February 16-19, 2011
2011 Annual Meeting AAOS
San Diego, CA
Web: http://www.aaos.org

February 20-22, 2011
AIMBE 20th Annual Event:
Medical & Biological Engineering in the Next 20 years The Promises & the Challenges
Mandarin Oriental Hotel
Washington, DC
Web: http://www.aimbe.org

March 2011

March 3-4, 2011
NYU Hospital for Joint Diseases – Comprehensive Spine Curse
NYU Langone Medical Center - Farkas Auditorium
New York, NY
Web: http://cme.med.nyu.edu/spine

March 5-8, 2011
2011 Philadelphia Meeting Surgery and Rehabilitation of the Hand: With Emphasis on the Elbow and Shoulder
Philadelphia, PA
Phone: +1 610 768 5958
Fax: +1 610 768 8887
E-mail: hrf@handfoundation.org
Web: http://www.handfoundation.org

March 10-11, 2011
Spinal Deformity Live
Eric P. Newman Education Center
Washington University Medical Center
St. Louis, MO
Phone: +1 630 681 1040
Fax: +1 630 682 5811
Web:
http://www.regonline.com/DeformityLive2011

March 24-26, 2011
Global Spine Congress 2011
Catalonia Palace of Congresses
Barcelona, Spain
Web: http://www.globalspinecongress.org

March 30 - April 2, 2011
2011 International Symposium on Biomedical Imaging: *From Micro to Nano* (ISBI '11)
Hyatt Regency McCormick Center
Chicago, IL USA
Web: http://www.biomedicalimaging.org

March 30 – April 2, 2011
Current Solutions in Spine Surgery
Hawks Cay
Duck Key, Florida Keys
Fax: +1 813 558 6114
Web: http://www.foreonline.org

April 2011

April 1-3, 2011
6th International Conference on Ethical Issues in Biomedical Engineering
Polytechnic Institute of NYU
Brooklyn, New York
Phone: +1 212 298 3725
E-mail: nymeetings@nyas.org
Web: http://www.nyas.org/biomed

April 6-9, 2011
Current Solutions in Foot and Ankle Surgery
Sandpearl Resort
Clearwater, FL
Web: http://www.foreonline.org

April 7-10, 2011
American Humanist Association 70th Anniversary Conference
Hyatt Regency Cambridge Hotel
Boston, Mass.
Web:
http://www.americanyhumanist.org/conference

April 9, 2011
The Northeast Undergraduate and Graduate Student Sigma Xi Poster Conference
Stony Brook University
Stony Brook, NY
Web:
http://www.oswego.edu/~bendinsk/sigmaxiconference.html

April 12-14, 2011
University of Minnesota – Design of Medical Devices Conference
Radisson University Hotel
Minneapolis, Minn.
Web: http://www.dmd.umn.edu

April 13-16, 2011
Society for Biomaterials 2011 Annual Meeting & Exposition
Orlando, FL
Web: http://www.2011.biomaterials.org

April 15-16, 2011
AAOS/AAHKS Challenges and Controversies in Total Joint Arthroplasty
Orthopaedic Learning Center
Rosemont, IL
Baltimore, MD
San Francisco, CA
Phone: +1 800 626 6726
+1 847 823 7186
Fax: +1 800 823 8025
Web: http://www.aaos.org/courses

April 25-29, 2011
2011 Material Research Society (MRS) Fall Meeting & Exhibit
Moscone West and San Francisco Marriott
San Francisco, CA
Web: http://www.mrs.org

April 29-30, 2011
Advanced Techniques in Shoulder Arthroscopy, Arthroplasty & Fractures
Mayo Clinic – Surgical Skills Laboratory
Rochester, MN
Web:
http://www.mayo.edu/cme/orthopedic-surgery

April 29 – May 1, 2011
6th World Congress
World Institute of Pain
Seoul, South Korea
Phone: +41 22 908 0488
Fax: +41 22 906 9140
E-mail: wip@kenes.com
Web: http://www.kenes.com/wip

May 2011

May 16-20, 2011
CLAIB V Latin American Congress on Biomedical Engineering
Havana, Cuba
Web:
http://promociondeeventos.sld.cu/claib2011en/

June 2011

June 14-17, 2011
NBC 15th Nordic-Baltic Conference on Biomedical Engineering
Aalborg, Denmark
Website will be launched soon

June 15-18, 2011
Abdominal Wall Reconstruction (AWR) – Georgetown University Hospital Conference
JW Marriott
Washington, DC
Phone: +1 337 235 6606
Fax: +1 337 235 7300
E-mail: info@AWRconference.com
Web: http://www.AWRconference.com

June 16-18, 2011
Abdominal Wall Reconstruction
AWR 2011: Inspiring and AWR Some!
JW Marriott
Washington, DC
Web: http://www.awrconference.com/

June 22-25, 2011
ASME Summer Bioengineering Conference
Farmington, PA
Web:
http://www.asmeconferences.org/SBC2011

June 22-26, 2011

APCMBE 8th Asian-Pacific Conference on Medical & Biological Engineering

Kuala Lumpur, Malaysia

Website will be launched soon

July 2011

July 13-16, 2011
18th Scoliosis Research Society (SRS) International Meeting on Advanced Spine Techniques
Maspalomas, Gran Canaria
Spain
Phone: +1 414 289 9107
Fax: +1 414 276 3349
E-mail: meetings@srs.org

July 25-29, 2011
Sports Medicine Update 2011 – Evaluation and Treatment of the Injured Athlete
The Harbor View Hotel and Kelley House
Edgartown, MA
Phone: +1 800 688 2475
Web: http://www.bu.edu/cme

August 2011

August 30 – September 3, 2011
EMBC 2011 Proposals Special Sessions, Mimisymposia and Conference Workshop
Marriott Copley Hotel
Boston, MA
Web: http://www.embc2011.embs.org

August 30 – September 4, 2011
IEEE EMBC 2011 – Integrating Technology and Medicine for a healthier Tomorrow
Boston, MA
Web: http://www.embc2011.embs.org

September 2011

September 14-17, 2011
European Conference of the International Federation for Medical & Biological Engineering
Budapest, Hungary
Web: http://www.embec2011.com

September 16-20, 2011
ASBMR 33rd Annual Meeting
San Diego, California
Web:
http://www.asbmr.org/meeting/meetingsindex.cfm

September 21-24, 2011
Pain in Europe VII
7th Congress of the European Federation of IASP Chapters (EFIC)
Hamburg, Germany
Phone: +41 22 908 0488
Fax: +41 22 906 9140
E-mail: efic2011@kenes.com

October 2011

October 9-14, 2011
EANS Rome 14th European Congress of Neurosurgery
Rome
Web: http://www.kenes.com/eans

SUNY Downstate Medical Center

NYU·poly
POLYTECHNIC INSTITUTE OF NYU

The New York Academy of Sciences
Building communities, advancing science since 1817

APR 1-3 2011

6th International Conference on Ethical Issues in Biomedical Engineering

For more information visit
www.nyas.org/biomed

Following five successful international conferences, The SUNY Downstate Medical Center, the Polytechnic Institute of New York University, and The New York Academy of Sciences are co-hosting a 3-day conference that aims to examine the ethical issues associated with the **development of new treatment modalities**, many of which pose new **ethical issues** and demand the design and improved knowledge of **ethical guidelines** to be implemented. Biomedical engineers, philosophers, research scientists, lawyers, students, clinicians and representatives from industry and federal agencies will convene to explore ethical guidelines to address the controversial nature of many of the new exciting developments in biomedical engineering.

Call for Abstracts

The Local Program Committee is seeking abstracts submissions of papers relevant to this conference, which will be evaluated for inclusion in the final agenda as oral presentations. The deadline for abstract submission is Wednesday, November 24, 2010. For complete abstract instructions, please send an e-mail to: biomed@nyas.org. Type the words "Abstract Information" in the subject line-there is no need to type a message. Instructions will be forwarded automatically. Any questions, please call 212.298.8681.

Abstracts of all accepted papers from the conference will be published in a special issue of the *Ethics in Biology, Engineering and Medicine, An International Journal* that will be distributed at the conference.

Topical Areas of Interest

- Animal testing for medical devices
- Clinical trials of biomedical devices and implants
- Code of ethics for bioengineers
- Ethical issues in biomedical research
- Ethical issues in clinical engineering
- Ethics issues in dentistry
- Ethical issues in tissue engineering
- Ethics of genetic engineering and cloning
- Ethics of nanobiotechnology
- Ethics of stem cell use and research
- Marketing and regulation of impacts and devices
- Medical liability reform
- Privacy and Bioinformatics

Conference Chair

Subrata Saha, PhD
SUNY Downstate Medical Center

Keynote Speakers

Charles N. Bertolami, D.D.S., D.Med.Sc.
New York University

George Bugliarello, PhD
Polytechnic Institute of NYU

Janice Graham, PhD
Dalhousie University

Invited Speakers

Kenneth R. Foster, PhD
University of Pennsylvania

George Khushf, PhD
University of South Carolina

Daniel Vallero, PhD
Duke University

Registration
(Before March 1, 2011)

Register before March 1, 2011 and save with early bird prices!

Registration Fee*: $150

One-day Registration
(does not include banquet): $100

Student Registration*: $70

Guest Banquet Ticket: $50

**Members of co-sponsoring societies, and faculty and students of cosponsoring universities will receive a 20% reduction in the registration fees*

Conference Location

Polytechnic Institute of NYU
Dibner Building
5 MetroTech Center
Brooklyn, NY, 11201

Special Hotel Discounts with your Registration!

New York Marriott at
the Brooklyn Bridge

Toll Free: 888.436.3759

Website: www.brooklynmarriott.com

Conference attendees may receive a special reduced rate of $189 (plus tax) per day for the duration of the conference. When making reservations mention that you're calling for the "**6th International Ethics Conference**" special rate.

Sponsors

- American Institute of Medical and Biological Engineering (AIMBE)
- International Federation for Medical and Biological Engineering (IFMBE)